

Received March 19, 2023, accepted April 17, 2023, date of current version April 21, 2023.

Digital Object Identifier mm.yyyy/ACCESS.2023.DOI

Making Sense of Meaning: A Survey on Metrics for Semantic and Goal-Oriented Communication

TILAHUN M. GETU^{1,2}, (Member, IEEE), GEORGES KADDOUM^{2,3}, (Senior Member, IEEE), and MEHDI BENNIS⁴, (Fellow, IEEE)

¹Communications Technology Laboratory (CTL), National Institute of Standards and Technology (NIST), Gaithersburg, MD 20899, USA

²Electrical Engineering Department, École de Technologie Supérieure (ETS), Montréal, QC H3C 1K3, Canada

³Cyber Security Systems and Applied AI Research Center, Lebanese American University, Beirut, Lebanon

⁴Centre for Wireless Communications, University of Oulu, 90570 Oulu, Finland

Corresponding author: Tilahun M. Getu (e-mail: tilahun-melkamu.getu.1@ens.etsmtl.ca).

The first author acknowledges the U.S. Department of Commerce and NIST for funding this work, and Dr. Hamid Gharavi (*IEEE Life Fellow* of NIST, MD, USA) for funding and leadership support.

ABSTRACT Semantic communication (SemCom) aims to convey the meaning behind a transmitted message by transmitting only semantically-relevant information. This semantic-centric design helps to minimize power usage, bandwidth consumption, and transmission delay. SemCom and goal-oriented SemCom (or effectiveness-level SemCom) are therefore promising enablers of 6G and developing rapidly. Despite the surge in their swift development, the design, analysis, optimization, and realization of robust and intelligent SemCom as well as goal-oriented SemCom are fraught with many fundamental challenges. One of the challenges is that the lack of unified/universal metrics of SemCom and goal-oriented SemCom can stifle research progress on their respective algorithmic, theoretical, and implementation frontiers. Consequently, this survey paper documents the existing metrics – scattered in many references – of wireless SemCom, optical SemCom, quantum SemCom, and goal-oriented wireless SemCom. By doing so, this paper aims to inspire the design, analysis, and optimization of a wide variety of SemCom and goal-oriented SemCom systems. This article also stimulates the development of unified/universal performance assessment metrics of SemCom and goal-oriented SemCom, as the existing metrics are purely statistical and hardly applicable to reasoning-type tasks that constitute the heart of 6G and beyond.

INDEX TERMS 6G, wireless SemCom, optical SemCom, quantum SemCom, goal-oriented wireless SemCom, metrics of SemCom and goal-oriented SemCom.

I. INTRODUCTION

A. MOTIVATION

Following the global rollout of fifth-generation (5G) wireless communication system applications and services, researchers in academia, industry, and national laboratories have been developing visions [1]–[26] regarding the next generation of wireless communication systems – commonly known as the sixth-generation (6G). 6G is driven – as envisaged in the last four years – by multiple widely envisioned applications as varied as wireless brain-computer interactions, multi-sensory extended reality (XR) applications, blockchain and distributed Ledger technologies, and connected robotic and autonomous systems [1]; haptic communication, massive Internet of things (IoT) [27], integrated smart city, and

automation and manufacturing [28]; the *internet of no things* (metaverse) [29], [30]; industrial IoT [31], internet of robots [25], flying vehicles [17], and wireless data centers [17], [32]; accurate indoor positioning, new communication terminals, high-quality communication services onboard aircraft, worldwide connectivity, integrated networking, communications that support industry verticals [33], holographic communication, tactile communication, and human bond communication [6]; Smart Grid 2.0, Industry 5.0, personalized body area networks, Healthcare 5.0; and the internet of industrial smart things and the internet of healthcare [3].

To make the aforementioned 6G applications a reality, many researchers propose to use a wide variety of 6G enabling technologies [1]–[3], [7], [11], [26] at the infras-

tructure, spectrum, and algorithm/protocol level [34], [35]. Despite the variety of proposals, realizing 6G – as many researchers are presently contemplating – demands not only evolutionary developments but also a revolutionary paradigm shift [1]. The revolutionary paradigm shift – in particular – must tackle the following fundamental challenges of 6G:

- Guaranteeing ultra-high data rate for most users.
- Ensuring an ultra-reliability and low latency for the bulk of users.
- Managing ultra-heterogeneity
- Taming ultra-high complexity in 6G networks.
- Addressing ultra-high mobility
- Accommodating users' needs or perspectives (see [36]).
- Designing with respect to (w.r.t.) various key performance indicators (KPIs).
- Attaining high energy efficiency.
- Realizing energy-efficient artificial intelligence (AI).
- Ensuring security, privacy, and trust across the 6G network.
- Attaining *full intelligence and autonomy*.
- Dealing with the technological uncertainty [37] of 6G technology enablers.

Addressing the itemized fundamental challenges would translate to overcoming numerous interdisciplinary, multidisciplinary, and transdisciplinary (IMT) challenges.

To mitigate the astronomical IMT challenges of 6G, the design of 6G systems and networks must be holistically geared towards minimizing power usage, bandwidth consumption, and transmission delay by minimizing the transmission of semantically irrelevant information. This semantic-centric information transmission calls for the efficient transmission of *semantics* by a semantic transmitter followed by their reliable recovery by a semantic receiver. This type of communication paradigm is now widely regarded as semantic communication (SemCom). SemCom – which was first put forward by Weaver around 1949 [38] – is a communication paradigm aimed at conveying the transmitter's intended meaning. SemCom targets the transmission of only the *semantic information*¹ relevant to the communication goal in order to minimize the divergence between the intended meaning of the transmitted messages and the meaning of the messages ultimately recovered [45], reducing data traffic considerably [46]. SemCom involves the transmission of less data than the traditional communications techniques do [45] because only the semantic information that is pertinent to accurate interpretation at the destination is transmitted. In this respect, SemCom makes it possible to utilize the available network capacity more effectively [47]. A network's capacity can certainly be utilized effectively by avoiding the bit-by-bit

¹Since *semantics* is built upon syntax and studies signs and their relationship to the world [39], the fundamental concept of semantic information relies on the information ecosystem, which is a complete process of *information-knowledge-intelligence conversion* [40], [41]. See [40, Fig.1] for more information. Meanwhile, semantic information can be represented using knowledge graphs (KGs) [42], deep neural networks (DNNs), topologies [43], and *quantum corollas* [44].

reconstruction of the transmitted information at the receiver. Moreover, SemCom aims to incorporate the purpose of transmission when doing so to simplify the data to be transmitted and avoid transmitting redundant information [48].

SemCom epitomizes the “provisioning of the right and significant piece of information to the right point of computation (or actuation) at the right point in time” [49]. This philosophy is of paramount importance for networked control systems in which a system designer has to deal with not only the transmission of relevant semantic information but also the effectiveness of the transmitted semantic information to effectively execute a desired goal/action. As for the desired goal/action, a SemCom in which the efficiency/effectiveness of semantic transmission is explicitly defined and targeted can be qualified as a goal-oriented SemCom [50].² Goal-oriented SemCom is a subset of SemCom that provides a pragmatic view of SemCom wherein the receiver is interested in the significance (semantics) and the effectiveness of the source's transmitted message to accomplish a certain goal [50]. Therefore, goal-oriented SemCom targets the extraction and transmission of only task-relevant information so that the transmitted source signal can be substantially compressed, communication efficiency is improved, and low end-to-end latency can be achieved [52].

The state-of-the-art on SemCom and goal-oriented SemCom features many proposals concerning SemCom [39], [51], [53]–[61] and goal-oriented SemCom [39], [50], [51], [58] techniques. Despite the numerous state-of-the-art techniques that exist for SemCom and goal-oriented SemCom, the design, analysis, optimization, and realization of systems that are based on SemCom and goal-oriented SemCom are fraught with various fundamental challenges. Among the challenges, one important fundamental challenge is the lack of *unified/universal performance assessment metrics* – of SemCom and goal-oriented SemCom – that help facilitate research developments in SemCom and goal-oriented SemCom. To this end, a detailed discussion of the existing performance metrics of SemCom and goal-oriented SemCom – either used or proposed in state-of-the-art works – is therefore required to develop a unified/universal performance assessment metrics. To serve this purpose, this survey paper reports on the existing metrics – from many distinct references – of SemCom and goal-oriented SemCom while aiming to inspire the development of unified/universal performance assessment metrics of SemCom and goal-oriented SemCom. This translates to the following paper contributions.

B. CONTRIBUTIONS

The key contributions of this survey paper – a product of multidisciplinary research – are enumerated below.

²Goal-oriented communication and task-oriented communication – that are based on semantic information – are discussed throughout this paper under the heading “goal-oriented wireless SemCom”. However, the authors of [51] underscore that goal communication is much broader than SemCom. Per Weaver's vision, they classify SemCom as *semantic level-SemCom* and *effectiveness level-SemCom*.

Semantic metrics	Scope of Ref. [51]	Scope of Ref. [54]	Scope of Ref. [55]	Scope of Ref. [58]	Scope of this paper
Semantic metrics for text quality assessment	Partially	Partially	Partially	Partially	Completely
Semantic metrics for speech quality assessment	Partially	Partially	Partially	Partially	Completely
Semantic metrics for image quality assessment	Partially	Partially	Partially	Partially	Completely
Semantic metrics for video quality and 3D human sensing assessment	–	–	–	–	Completely
Age of information- and value of information-based semantic metrics	Partially	–	–	Almost completely	Completely
Resource allocation semantic metrics	–	–	–	–	Completely
Generic semantic metrics of SemCom	–	–	–	–	Completely
Semantic metrics of quantum SemCom	–	–	–	–	Almost completely
Semantic metrics of goal-oriented wireless SemCom	Partially	–	–	Partially	Completely

TABLE 1: Scope of this survey paper w.r.t. related state-of-the-art SemCom survey papers that discuss metrics of SemCom – Ref.: reference; “–” means the particular reference didn’t discuss the semantic metric listed on a given row.

- 1) We discuss existing as well as emerging developments of SemCom in multiple domains including *wireless SemCom*, *optical SemCom*, and *quantum SemCom*.
- 2) We discuss existing as well as emerging developments in goal-oriented wireless SemCom.
- 3) We detail the numerous semantic metrics that are used for text, speech, and image quality assessment.
- 4) We present the semantic metrics that are deployed for video quality and three-dimensional (3D) human sensing assessment.
- 5) We provide an overview of age of information- and value of information-based semantic metrics.
- 6) We outline resource allocation semantic metrics.
- 7) We present generic semantic metrics of SemCom.
- 8) We discuss semantic metrics of quantum SemCom.
- 9) We delineate semantic metrics of goal-oriented wireless SemCom.

The scope of our enumerated contributions w.r.t. the contributions of related state-of-the-art SemCom papers that also discuss semantic metrics are put in perspective by Table 1. Considering the fact that the various metrics of SemCom and goal-oriented SemCom are scattered in different references that disseminate them in different times, we discuss most of the corresponding metrics in this paper with the aim of inspiring the development of unified performance assessment metrics for SemCom and goal-oriented SemCom.

The rest of this paper is organized as follows. Section II presents this paper’s prelude. Sections III, IV, and V detail the semantic metrics that are used for text, speech, and image quality assessment, respectively. Section VI reports on the semantic metrics that are deployed for video quality and 3D human sensing assessment. Section VII provides an overview of age of information- and value of information-based semantic metrics. Section VIII outlines the resource allocation semantic metrics. Sections IX and X present generic semantic metrics of wireless SemCom and semantic metrics of quantum SemCom, respectively. Section XI summarizes the semantic metrics of goal-oriented wireless SemCom. Finally, Section XII contains the concluding summary and research outlook. Meanwhile, the organization and structure of this survey paper are depicted in Fig. 1.

C. NOTATION AND DEFINITIONS

Scalars, vectors, and matrices are represented by italic letters, bold lowercase letters, and bold uppercase letters, respectively. Sets, datasets, skeletons, deep networks, and the Hilbert space are denoted by calligraphic letters. Calligraphic letters that are bold represent tensors. Random variables (RVs) and multivariate RVs (or random vectors) are represented by uppercase letters and bold lowercase letters, respectively. \mathbb{N} , $\mathbb{R}(\mathbb{C})$, \mathbb{R}^+ , $\mathbb{R}^n(\mathbb{C}^n)$, and $\mathbb{R}^{m \times n}$ denote the set of natural numbers, the set of real(complex) numbers, the set of non-negative real numbers, the set of n -dimensional vectors of real(complex) numbers, and the set of $m \times n$ matrices of real numbers, respectively. $:=$ denotes an equality by definition. For $n \in \mathbb{N}$, we let $[n] := \{1, 2, \dots, n\}$. \min , \max , j , $\|\cdot\|_1$, and \mathbf{I}_n denote minimum, maximum, $\sqrt{-1}$, the Schatten-1 norm, and an $n \times n$ identity matrix, respectively. \otimes , $\|\cdot\|$ (or $\|\cdot\|_2$), $(\cdot)^*$, $(\cdot)^T$, and $(\cdot)^H$ stand for tensor product, Euclidean norm, complex conjugate, transpose, and Hermitian, respectively.

$\text{tr}(\cdot)$, $\mathbb{E}\{\cdot\}$, $\mathbb{E}_X\{\cdot\}$, $\mathbb{P}(\cdot)$, and $\mathbb{P}(A|B)$ denote trace (of a matrix), expectation, expectation w.r.t. an RV X , probability, and the probability of event A conditioned on event B , respectively. $\Gamma(\cdot)$, $\Gamma(\cdot, \cdot)$, and $\mathbb{I}\{\cdot\}$ represent the gamma function, the upper incomplete gamma function, and an indicator function that returns 1 if the argument is true and 0 otherwise, respectively. For $z \in \mathbb{C}$ that $z = x + jy$, its magnitude is denoted by $|z|$ and defined as $|z| := \sqrt{x^2 + y^2}$. For a real vector $\mathbf{a} \in \mathbb{R}^n$, its i -th element is denoted by $(\mathbf{a})_i$ for all $i \in [n]$. For two real vectors $\mathbf{a}, \mathbf{b} \in \mathbb{R}^{1 \times n}$, their dot product is denoted by $\mathbf{a} \cdot \mathbf{b}$ and defined as $\mathbf{a} \cdot \mathbf{b} := \sum_{i=1}^n (\mathbf{a})_i (\mathbf{b})_i$. For two vectors $\mathbf{c}, \mathbf{d} \in \mathbb{R}^m$, their element-wise product is denoted by $\mathbf{c} \odot \mathbf{d}$. For a three-way tensor $\mathcal{Y} \in \mathbb{R}^{H \times W \times C}$, its element vector w.r.t. the given h -th and w -th dimension – for $h \in [H]$ and $w \in [W]$ – is denoted by $(\mathcal{Y})_{h,w} \in \mathbb{R}^C$.

$|\psi\rangle$ is the Dirac’s ket notation for a column vector such that $|\psi_A\rangle := [a_0 \ a_1 \ \dots \ a_{N-1}]^T$ [62]. $\langle\psi|$ is the Dirac’s bra notation corresponding to $|\psi\rangle$ and defined as the complex conjugate transpose (Hermitian) of $|\psi\rangle$: i.e., $\langle\psi_A| := (|\psi_A\rangle)^H = [a_0^* \ a_1^* \ \dots \ a_{N-1}^*]$ [62]. For $\langle\psi_A|$ and the quantum state $|\psi_B\rangle := [b_0 \ b_1 \ \dots \ b_{N-1}]^T$, $\langle\psi_A|\psi_B\rangle$ is the *inner product (dot product)* – of the two vectors ψ_A and



FIGURE 1: The organization and structure of this survey paper.

ψ_B – and defined as [62, eq. (2.3)]

$$\langle \psi_A | \psi_B \rangle := \sum_{i=0}^{N-1} a_i^* b_i. \quad (1)$$

For $|\psi_A\rangle$ defined in above and $\langle \psi_B | (\equiv (|\psi_B\rangle)^H)$, $|\psi_A\rangle \langle \psi_B |$ is their *outer product* and defined as [62, eq. (2.4)]

$$|\psi_A\rangle \langle \psi_B| := \begin{bmatrix} a_0 b_0^* & \dots & a_0 b_{N-1}^* \\ \vdots & \ddots & \vdots \\ a_{N-1} b_0^* & \dots & a_{N-1} b_{N-1}^* \end{bmatrix}. \quad (2)$$

In light of this bra-ket notation, a (noiseless) quantum bit (*qubit*) $|\psi\rangle$ – a basic unit of quantum information – is a vector in a two-dimensional complex vector space (two-dimensional Hilbert space) and expressed as [63, eq. (1.1)]

$$|\psi\rangle := \alpha |0\rangle + \beta |1\rangle, \quad (3)$$

where $|0\rangle$ and $|1\rangle$ are the special states known as *computational basis states* that form an orthonormal basis for the vector space, and $\alpha, \beta \in \mathbb{C}$ such that $|\alpha|^2 + |\beta|^2 = 1$ [63]. The complex coefficients α and β are *probability amplitudes*; these amplitudes are not themselves probabilities but allow us to calculate probabilities [64]. Per (3), the qubit $|\psi\rangle$ is a *linear superposition*³ of two quantum states (i.e., $|0\rangle$ and $|1\rangle$), which underscores the fact that a qubit can be in one of the infinitely⁴ many quantum states that are possible [63]. This is explained by the fact that measuring a qubit makes the wave function collapse, pushing the quantum state into just one term of the superposition [62].

A generalized version of qubit – called *qudit*⁵ – is a multi-level computational unit alternative to the conventional 2-level qubit [66]. More specifically, a qudit⁶ is a quantum version of d -ary digits whose state can be characterized by a vector in the d -dimensional Hilbert space \mathcal{H}_d [66]. \mathcal{H}_d is spanned by a set of orthonormal basis vectors

³A quantum mechanical [65] equivalent of a bit, a qubit can be in state of 0, state of 1, and a superposition of state 0 and state 1 [63]. A qubit can be physically materialized as a quantum mechanical system based on *nuclear spin, electron spin, ion trap, quantum dot, optical cavity, and microwave cavity* [63, Ch. 7].

⁴Despite its infinitely many possible quantum states, a qubit cannot be examined, and *quantum mechanics* (see [65]) asserts that we can obtain only very limited information about $|\psi\rangle$ [63]. To this end, when we measure $|\psi\rangle$, its inherent superposition will collapse and we get the result 0 or 1 with probability $|\alpha|^2$ or probability $|\beta|^2$ (under the probability constraint $|\alpha|^2 + |\beta|^2 = 1$), respectively [63].

⁵Compared to qubit, qudit offers a larger state space to store and process information [66], [67]. Hence, qudit can simplify the experimental setup, reduce the circuit complexity, and enhance algorithm efficiency [66]. Generally, qudits offer many advantages over qubits, including higher information and communication capacity, greater noise resilience, enhanced robustness to *quantum cloning* (see [68]), greater violation of local theories, and benefits when it comes to communication complexity problems [67].

⁶As the basic computational element for quantum algorithms, qudit can replace qubit and the state of a qudit is altered by *qudit gates* [66]. Meanwhile, high-dimensional quantum states such as qudits can be generated with *bulk optics and integrated photonics* [67]. The following physical platforms have been used to implement qudit gates or qudit algorithms: the *time and frequency bin of a photon, ion trap, nuclear magnetic resonance (NMR), and molecular magnets* [66].

$\{|0\rangle, |1\rangle, |2\rangle, \dots, |d-1\rangle\}$ [66]. Using these basis vectors, the state of a qudit takes the general form [66, eq. (1)]

$$|\phi\rangle := \alpha_0 |0\rangle + \alpha_1 |1\rangle + \alpha_2 |2\rangle + \dots + \alpha_{d-1} |d-1\rangle \quad (4a)$$

$$= [\alpha_0 \ \alpha_1 \ \alpha_2 \ \dots \ \alpha_{d-1}]^T \in \mathbb{C}^d, \quad (4b)$$

where $\alpha_0, \alpha_1, \alpha_2, \dots, \alpha_{d-1} \in \mathbb{C}$ and $\sum_{i=0}^{d-1} |\alpha_i|^2 = 1$ [66]. The qudit $|\phi\rangle$ can also be expressed as a sum of pure states $|\alpha_d\rangle$ within a density matrix representation given by [69]

$$\rho := \sum_{d=0}^{d-1} p_d |\alpha_d\rangle \langle \alpha_d|, \quad (5)$$

where p_d is the selection probability pertaining to the d -th pure state.

We now proceed to this paper's prelude.

II. PRELUDE

A number of SemCom techniques inspired by the advancements in 6G research [26], [70]; AI [71]–[73], machine learning (ML) [74]–[76], and deep learning (DL) [77]–[79] research; research on quantum computation [63], [80], [81], quantum communication [82]–[84], and quantum networking [62], [85], [86]; and research on optical communications have been proposed in not only the wireless domain – hereinafter referred to *wireless SemCom* – but also in the optical and quantum domains. These latter domains' respective SemCom paradigms are henceforth referred to as *optical SemCom* and *quantum SemCom*. Quantum SemCom, optical SemCom, and wireless SemCom are promising 6G enabling technologies that need much more development and discussion. Stimulating a comprehensive discussion toward rigorous theoretical/algorithmic developments of SemCom, we begin our discussion of the state-of-the-art developments of wireless SemCom.

A. WIRELESS SEMCOM

Aiming to convey a message's desired meaning (rather than supporting symbol-by-symbol reconstruction), wireless SemCom revolves around the extraction of semantic information that is transmitted – by the semantic transmitter – through a wireless communication channel and received by a semantic receiver that has been designed to faithfully recover the transmitted message's intended meaning. Hence, the first step in the wireless SemCom design is the extraction of semantic information to be transmitted from the source data/message to be transmitted. This semantic information extraction is accomplished using a semantic encoder – by employing the source knowledge base (KB) – which is often designed by training deep networks such as *transformers* [87]–[89]. In many the state-of-the-art works, the semantic encoder's function comprises both semantic representation and semantic encoding as schematized in Fig. 2. The output of such a semantic encoder is then fed to a channel encoder, which is usually designed using a trained DNN, that comprises a trained end-to-end semantic transmitter.

Abbreviation	Definition
3D	Three-dimensional
5G	Fifth-generation
6G	Sixth-generation
3-SSIM	Three-component weighted SSIM
AI	Artificial intelligence
ANSI	American National Standards Institute
AN-SNR	Anti-noise SNR
AoI	Age of information
AoII	Age of incorrect information
BER	Bit error rate
BERT	Bidirectional encoder representations from transformers
BLEU	Bilingual evaluation understudy
BS	Base station
CE	cross-entropy
CER	Character error rate
CIDEr	Consensus-based image description evaluation
CLUB	Contrastive log-ratio upper bound
CNN	Convolutional neural network
CVQ	Continuous video quality
CW-SSIM	Complex-wavelet SSIM
DL	Deep learning
DLM	Detail loss metric
DNNs	Deep neural networks
DTMC	Discrete-time Markov chain
Abbreviation	Definition
DVQ	Digital video quality
FDSD	Fréchet deep speech distance
FID	Fréchet inception distance
FR	Full-reference
FR-TV	Full reference television
FSIM	Feature similarity index for image quality assessment
FVQA	Fusion-based video quality assessment
GANs	Generative adversarial networks
HARQ	Hybrid automatic repeat request
HDTV	High Definition TV
HVS	Human visual system
IFC	Information fidelity criterion
IM/DD	Intensity modulation / direct detection
IMT	Interdisciplinary, multidisciplinary, and transdisciplinary
ind	The indicator error
IoT	Internet of things
IQA	Image quality assessment
IS	Inception score
iSemCom	Intelligent SemCom
iSemCom-HetNet	An iSemCom-enabled heterogeneous network
ISS	Image-to-graph semantic similarity
ITU	International Telecommunication Union
IW-SSIM	Information content weighted SSIM
KB	Knowledge base
KDSD	Kernel deep speech distance
KGs	Knowledge graphs
KID	Kernel inception distance
KPIs	Key performance indicators
LPIPS	Learned perceptual image patch similarity
MAD	Most apparent distortion
MCPD	Mean co-located pixel difference
MGA-based IQA	Multi-scale geometric analysis-based IQA
METEOR	Metric for evaluation of translation with explicit ordering
MI	Mutual information
mIoU	Mean intersection over union
ML	Machine learning
MMF	Multi-metric fusion
MODA	Multiple object detection accuracy

TABLE 2: List of abbreviations and acronyms I.

Abbreviation	Definition
MOS	Mean opinion score
MOVIE	Motion-based video integrity evaluation
MPJAE	Mean per joint angle error
MPJLE	Mean per joint localization error
MPJPE	Mean per joint position error
MSE	Mean squared error
MSS	Metric of semantic similarity
MS-SSIM	Multi-scale structural similarity index measure
MSSIM	Mean SSIM
MUs	Mobile users
N-MODA	Normalized MODA
NQM	Noise quality measure
NTIA	National Telecommunications and Information Administration
NR	No-reference
OAM	Orbital angular momentum
OFC	Optical fiber communication
OFDMA	Orthogonal frequency division multiple access
PAM8	Pulse-amplitude modulation 8
PAMS	Perceptual analysis measurement system
PDF	Probability distribution function
PESQ	Perceptual evaluation of speech quality
PSNR	Peak signal-to-noise ratio
PSNR-HVS-M	Peak signal-to-noise ratio-human vision system modified
PSQM	Perceptual speech quality measure
QAoI	Age of information at query
QC	Quantum computing
QCIF	Quarter Common Intermediate Format
QKD	Quantum key distribution
QML	Quantum machine learning
QoE	Quality-of-experience
QRAM	Quantum random access memory
QSC	Quantum semantic communication
rAoI	relative age of information
RR	Reduced-reference
RHS	Right-hand side
RVs	Random variables
SBERT	Sentence-BERT
SemCom	Semantic communication
SDR	Signal-to-distortion ratio
SINR	Signal-to-interference-plus-noise ratio
SMI	Semantic mutual information
SNR	Signal-to-noise ratio
sq	The squared error
S-R	Semantic transmission rate
S-SE	Semantic spectral efficiency
SSIM	Structural similarity index measure
SSM	Semantic similarity metric
ST	Spatio-temporal
STM	System throughput in message
STAQ	Spatial-temporal assessment of quality
ST-MAD	Spatiotemporal MAD
SVM	Support vector machine
TDP	Triplet drop probability
threshold	The threshold error
VFD	Variable frame delay
VIF	Visual information fidelity
VMAF	Video multi-method assessment fusion
VoI	Value of information
VQA	Video quality assessment
VQEG	Video Quality Experts Group
VQM	Video quality metric
VQM_VFD	Video quality model for variable frame delay
VSNR	Visual signal-to-noise ratio
WER	Word error rate
w.r.t.	With respect to
XR	Extended reality

TABLE 3: List of abbreviations and acronyms II.

The semantic transmitter's output is sent through a channel whose output is received by the semantic receiver. As shown in Fig. 2, the semantic receiver is built using a DL-based channel decoder followed by a deep network-based semantic decoder. The DL-based semantic decoder performs semantic decoding followed by semantic inference – using the destination KB as viewed in Fig. 2 – to faithfully recover the transmitted message's intended meaning. While the semantic receiver aims to determine the intended meaning, it can suffer greatly from *semantic noise*⁷ so long as there is a mismatch between the source KB and the destination KB. The destination KB, meanwhile, needs to be shared with the source KB in real-time for effective SemCom akin to productive human conversation, which requires common knowledge of the communicating parties' language and culture [58].

Advancements in DL, in particular, and AI, in general, have spurred a surge in research contributions pertaining to the design and optimization of various DL-enabled wireless SemCom systems. Such SemCom systems constitute the state-of-the-art algorithmic research developments in wireless text SemCom [46], [48], [56], [91]–[99]; wireless audio SemCom [45], [100]–[104]; wireless image SemCom [105]–[115]; wireless video SemCom [116]–[119]; wireless multi-modal SemCom [120]; and wireless cross-modal SemCom [121] pertaining to the efficient wireless transmission of text data, audio data, image data, video data, multimedia data, and multimedia and haptic data, respectively. All these wireless SemCom techniques have been demonstrated to outperform traditional/conventional wireless communication schemes, especially in low signal-to-noise ratio (SNR) regimes.

In addition to the aforementioned wireless SemCom techniques, the rapidly evolving state-of-the-art research landscape of SemCom also encompasses numerous SemCom techniques and trends such as cognitive SemCom [122]; implicit SemCom [123]; adaptive SemCom [124]; context-based SemCom [99], [125]; digital SemCom [126], [127]; SemCom with conceptual spaces [128]; inverse SemCom [129]; one-to-many SemCom [130]; cooperative SemCom [131]; strategic SemCom [132]; and encrypted SemCom [133]. These wireless SemCom techniques have also been corroborated to outperform traditional wireless communication techniques in low SNR regimes. For further details, meanwhile, the reader is referred to the vision papers [89], [91], and [134]–[146] and the tutorial/survey papers [39], [51], and [53]–[61] on state-of-the-art developments in wireless SemCom.

Inspired by some of the aforementioned wireless SemCom techniques, there are also some SemCom proposals and experimental demonstrations in the domain of optical communications. Thus, we continue with the techniques of optical SemCom.

B. OPTICAL SEMCOM

The authors of [147] design and experimentally demonstrate an optical SemCom system in which DL is exploited to extract semantic information from the source and the generated semantic symbols are then directly transmitted through an optical fiber. This optical SemCom system produce higher information compression and achieve more stable performance, particularly in the low received optical power regime, while enhancing the robustness against optical link impairments [147].

As part of their proposed optical SemCom system, the authors of [147] experimentally substantiate the semantic transmission of text and images through an intensity modulation / direct detection (IM/DD)-based optical fiber link. For text transmission, the authors of [147] design the language attention network to restore the meaning of sentences while minimizing semantic errors. For image transmission, on the other hand, they design the dual-attention residual network to extract rich semantic features from images while keeping semantic errors to a minimum. Moreover, to make semantic decoding robust against evident optical link impairments, they deploy a convolutional neural network (CNN) in the semantic decoding network and perform joint optimization.

For the purpose of comparison, the authors of [147] carry out experiments on traditional IM/DD pulse-amplitude modulation 8 (PAM8) and PAM4 optical fiber communication (OFC) systems. For these systems, the results reported by the authors of [147] corroborate that their proposed optical SemCom system achieves higher information compression and is more robust to Gaussian noise as well as optical link impairments [147]. When the optical channel environment is harsh, the performance of traditional OFC systems drops off a “cliff,” whereas the optical SemCom system's performance remains stable [147]. These results attest to the proposed optical SemCom system's considerable advantages over traditional OFC systems, especially in the low received optical power and high optical link impairment regimes [147].

This optical SemCom system's significant advantages demonstrate the viability of SemCom for 6G and beyond in not only the wireless domain but also the optical domain. Apart from optical and wireless domains, SemCom is also proposed in the quantum domain, which we discuss below.

C. QUANTUM SEMCOM

At the crossroads of SemCom [51], [53], [54], [58]; ML [74]–[76]; quantum ML (QML) [148]–[150]; quantum computing [63], [80], [81]; quantum communication [82]–[84]; and quantum networking [62], [85], [86], the authors of [69] propose a SemCom system in the quantum domain dubbed *quantum semantic communication* (QSC) [69, Fig. 1]. QSC is based on the premise that the d -dimensional quantum state – per (4a) – can be viewed as equivalent to the concept of *finite vocabulary* in the information-theoretic domain [69]. Accordingly, the set of d orthonormal basis vectors $\{|0\rangle, |1\rangle, |2\rangle, \dots, |d-1\rangle\}$ spanning the Hilbert space \mathcal{H}_d

⁷Semantic noise causes semantic information to be misunderstood by producing a misleading meaning between the transmitter's intended meaning and the receiver's recovered meaning [90].

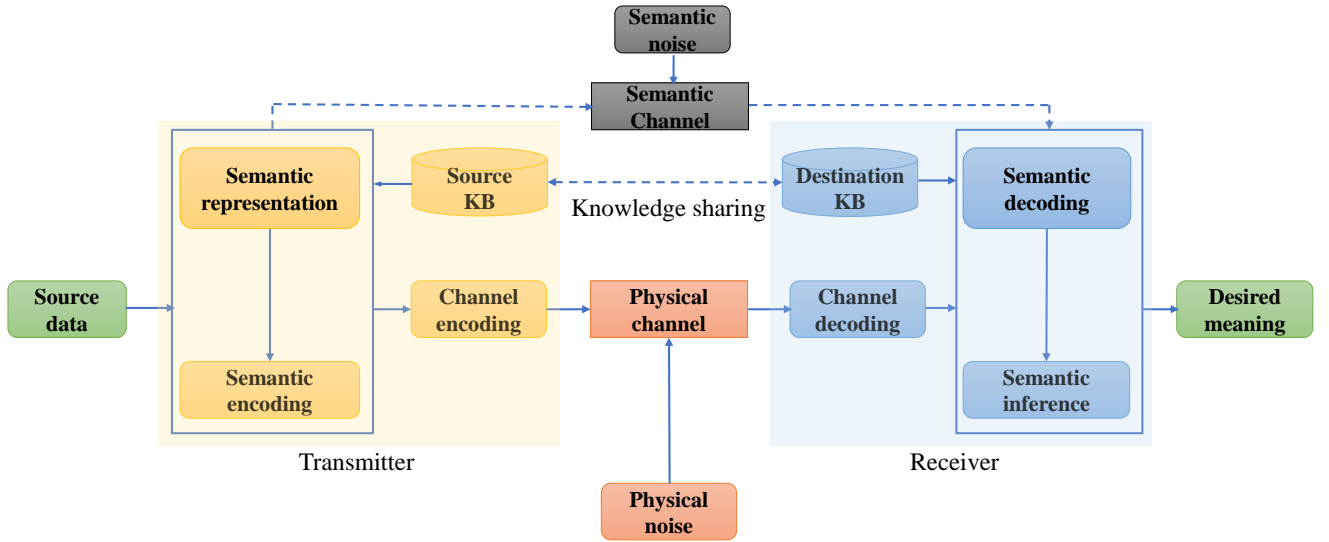


FIGURE 2: System model for SemCom – modified from [58, Fig. 6(b)].

construct a common language⁸ – *vocabulary of contextual meanings* – that can be employed to create a fitting semantic representation of the data [69]. The raw data’s semantic representation can be efficiently achieved by *quantum embedding* using *quantum feature maps* [151].

Using quantum feature maps [151], the authors of [69] propose to encode a classical datum $x \in \mathcal{X}$ into quantum states $|\psi(x)\rangle$ in the d -dimensional⁹ Hilbert space \mathcal{H}_d using a quantum feature map $\psi : \mathcal{X} \rightarrow \mathcal{H}_d$ such that $x \rightarrow |\psi(x)\rangle$. This mapping can be achieved using $U_\psi(x)$ which is known as a *feature-embedding circuit*¹⁰ [151] (or *quantum-embedding circuit* [69]). $U_\psi(x)$ acts¹¹ on the ground or vacuum state $|0 \dots 0\rangle$ of the Hilbert space \mathcal{H}_d as $U_\psi(x)|0 \dots 0\rangle = |\psi(x)\rangle$ [151]. This makes it possible to construct the classical datum’s quantum-embedded semantic representations via *semantic-embedded quantum states* [69]. To transmit these states reliably, the authors of [69] propose to process the semantic-embedded quantum states to be transmitted as follows [69, Fig. 1]:

- 1) The semantically-embedded d -dimensional quantum states are stored in quantum random access memory (QRAM) [69].
- 2) The speaker implements quantum clustering techniques to construct efficient representations of the

⁸Since it is part of a common language, every superposition of the d basis vectors corresponds to a unique contextual meaning [69].

⁹In this particular setting, it is assumed that the Hilbert space dimension d is much greater than the dimension of the classical dataset \mathcal{X} [69].

¹⁰Other than circuit-based (gate-based) quantum computing (QC), which is a very popular approach to QC, various other approaches exist, including measurement-based QC [152], adiabatic QC [153], and topological QC [154].

¹¹From a quantum computing viewpoint, the quantum feature map given by $x \rightarrow |\psi(x)\rangle$ corresponds to a state preparation circuit $U_\psi(x)$ that acts on the ground state $|0 \dots 0\rangle$ [151].

quantum semantics [69].

- 3) The qudits – corresponding to the quantum semantics – are generated using orbital angular momentum (OAM) [155] encoding [69].
- 4) One of the generated *entangled photons*¹² is transmitted to the listener over a quantum channel (optical fiber or free-space optical channel) to initiate the quantum entanglement link [69].
- 5) The listener can then detect the transmitted entangled photon and store it in QRAM. Entanglement purification protocols (e.g. [156]) can be subsequently applied whenever needed.
- 6) The entanglement link between the speaker and the listener is established [69].
- 7) The speaker maps each of the K semantic-representing d -dimensional quantum states to one of its entangled photons [69].
- 8) The quantum teleportation protocol is implemented to deliver the semantics to the listener [69].
- 9) Lastly, the listener conducts quantum measurements (and applies some quantum gates) to retrieve the embedded semantics and recover the context from the raw data using quantum operations [69].

The itemized steps comprise the quantum SemCom technique dubbed QSC [69, Fig. 1]. Apart from QSC, the authors of [157] present a quantum SemCom system that is secured

¹²*Quantum entanglement* – which Albert Einstein famously referred to as “spooky action at a distance” [62] – is the very striking (*counter-intuitive*) quantum mechanical phenomenon that the states of two or more quantum subsystems are correlated in a manner that is not possible in classical systems [62]. Quantum entanglement is a peculiarly quantum mechanical resource that usually plays a prominent role in the applications of quantum computation, quantum information, quantum communication, and quantum networking [62], [63].

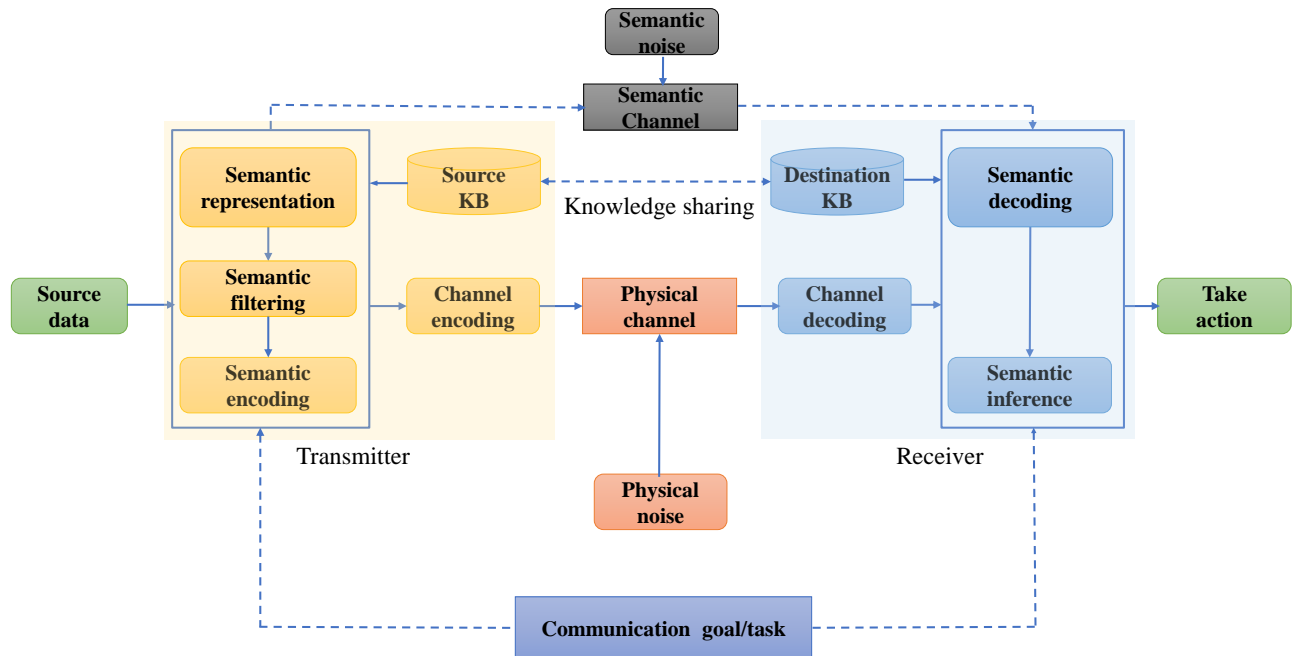


FIGURE 3: System model for goal-oriented SemCom – adapted from [58, Fig. 6(c)].

by quantum key distribution¹³ (QKD). Meanwhile, it is worth mentioning that quantum SemCom – like optical SemCom, wireless SemCom, and other communication paradigms – is not an end but a means to achieve specific goals [159], [160]. This goal-oriented viewpoint justifies the need for goal-oriented wireless SemCom techniques, as discussed below.

D. GOAL-ORIENTED WIRELESS SEMCOM

Revolving around the effectiveness of communication using semantic information, goal-oriented SemCom enables interested communicating parties to achieve a joint communication goal/task [58], [160]. In view of a joint communication goal/task, Fig. 3 shows a generic system model for goal-oriented SemCom, where the goal-oriented SemCom transmitter transforms the source data into semantically encoded information via the cascaded processing – using the source KB w.r.t. a given communication goal/task – of semantic representation, semantic filtering, and semantic encoding. The semantically encoded data is then fed into the channel encoder, whose output is transmitted through a wireless physical channel.

The output of the physical channel is received by the goal-oriented SemCom receiver's channel decoder. Acting on the channel decoder's output, the receiver aims to take a desired action – regarding a communication goal/task and a destination KB (which is shared with the source KB in real-time)

– via a semantic decoding operation followed by semantic inference [58]. The inference module's output – for example, in self-driving cars – can incorporate action execution instructions such as acceleration and braking; responding to pedestrians, roadblocks, traffic signal changes; and the angle for the steering wheel and flashing the headlights [58]. Each of these goals would require application/goal-tailored semantic extraction at the receiver followed by semantic filtering which is, in turn, followed by semantic post-processing prior to the source signal transmission [47], as schematized in [47, Figure 12].

Concerning wireless SemCom and goal-oriented wireless SemCom, the state-of-the-art also comprises many goal-oriented wireless SemCom developments. Major trends in these developments include task-oriented communication with digital modulation [52]; goal-oriented SemCom with AI tasks [161]; intent-based goal-oriented SemCom [162], [163]; and multi-user goal-oriented SemCom [164]. The reader is referred to the vision papers [47], [49], [136], [159], and [165]–[167] and the tutorial/survey papers [39], [50], [51], [58], and [168] on goal-oriented wireless SemCom.

Prior to detailing the metrics of SemCom and goal-oriented SemCom (Sections III through XI), let us first look at the basic *semantic unit* (*sut*) or *semantic base* (*Seb*) [137]. Regarding the latter, the authors of [137] introduce

¹³As a secure communication paradigm, QKD utilizes a cryptographic protocol that incorporates components of quantum mechanics. The reader is referred to [62], [82], and [158] for details about state-of-the-art QKD techniques and developments.

the concept of *Seb*¹⁴ as a basic representation framework for semantic information much like *bit* is the representation and measurement framework for information entropy. According to the authors of [137], Seb provides a modularized and abstractive method to symbolize semantic information, which inspires SemCom to be more efficient [137]. As an alternative definition of the basic unit of semantic information, the authors of [169] advocate that semantic information can be measured by the *sut*, defined to designate the basic unit of semantic information. In light of *sut* and *Seb*, the design, analysis, and optimization of goal-oriented wireless SemCom systems, quantum SemCom systems, optical SemCom systems, and wireless SemCom systems hinge on adequate semantic metrics. Therefore, we continue below with state-of-the-art semantic metrics for text quality assessment.

III. SEMANTIC METRICS FOR TEXT QUALITY ASSESSMENT

To assess the quality of text, several semantic metrics have been developed over the years. Some of these metrics have been exploited since recently in the design, analysis, and optimization of state-of-the-art wireless text SemCom systems [46], [48], [56], [91]–[99] and an optical text SemCom system [147]. Deployed in both optical and wireless text SemCom systems, semantic metrics such as *semantic distance*, *word error rate* (WER), *bilingual evaluation understudy* (BLEU), *consensus-based image description evaluation* (CIDEr), the *semantic similarity metric* (SSM), the *upper tail probability of SSM*, *SSM using sentence-BERT*¹⁵ (SSM using SBERT), the *metric for evaluation of translation with explicit ordering* (METEOR), and *average bit consumption per sentence* are commonly used by designers of wireless and optical text SemCom systems. The mentioned metrics are discussed below, beginning with semantic distance.

A. SEMANTIC DISTANCE

Semantic distance (semantic distortion) measures the semantic dissimilarity between two words [55], [91]. More specifically, semantic distance quantifies the distortion between two words w, \hat{w} on a semantic level and is defined as [91, eq. (5)]

$$d(w, \hat{w}) := 1 - \text{sim}(w, \hat{w}), \quad (6)$$

where $w, \hat{w} \in \mathcal{W} - \mathcal{W}$ being a finite set of all meaningful words – and $\text{sim}(w, \hat{w}) \in [0, 1]$ denotes the semantic similarity between w and \hat{w} . Using (6), we can determine the average semantic error, which is the average semantic distance in probability [55], [91]. To define this probability formally, let the encoder of [91, Fig. 2] observe a word w from a finite set \mathcal{W} with a probability $\mathbb{P}(W = w)$. The encoder maps w into

a channel input $\mathbf{x} = [x_1, \dots, x_n] \in \mathcal{X}^{(n)}$ using an encoding function $g : \mathcal{W} \rightarrow \mathcal{X}^{(n)}$, where $\mathcal{X}^{(n)} \subseteq \mathcal{X}^n$ and \mathcal{X} is a finite alphabet, and $g \in \mathcal{G}$ given \mathcal{G} is the set of all encoding functions. The channel input \mathbf{x} is then transmitted through a noisy channel – which is characterized by the conditional probability $p(\mathbf{Y} = \mathbf{y} | \mathbf{X} = \mathbf{x})$ ¹⁶ – that produces channel output $\mathbf{y} = [y_1, \dots, y_n] \in \mathcal{Y}^{(n)}$, where $\mathcal{Y}^{(n)} \subseteq \mathcal{Y}^n$ and \mathcal{Y} is a finite alphabet. The channel output \mathbf{y} is fed to a decoder that recovers a word $\hat{w} \in \mathcal{W}$ from \mathbf{y} w.r.t. the context q by employing a decoding function $h : \mathcal{Y}^{(n)} \times \mathcal{Q} \rightarrow \mathcal{W}$ given that $h \in \mathcal{H}$ – with \mathcal{H} being the set of all valid decoding functions – and $q \in \mathcal{Q}$, with \mathcal{Q} being the set of all plausible contexts. For this particular setting, the average semantic error (or average semantic distortion) is defined using (6) as [91, eq. (7)]

$$D_\theta((g, h), \mathbb{P}(Q|W, \Theta = \theta)) := \sum_{w \in \mathcal{W}, q \in \mathcal{Q}, \mathbf{y} \in \mathcal{Y}^{(n)}} \sum_{\mathbf{x} \in \mathcal{X}^{(n)}} p(W = w, Q = q, \mathbf{Y} = \mathbf{y}, \mathbf{X} = \mathbf{x} | \Theta = \theta) d(w, h(\mathbf{y}, q)), \quad (7)$$

where $(g, h) \in \mathcal{G} \times \mathcal{H}$ and the RV Θ characterizes a given agent's nature – either helpful or adversarial – via $\mathbb{P}(\Theta = \theta)$ which is defined in [91, eq. (1)]. Because average semantic error – per (7) – determines only the semantic similarity between individual words, it would be difficult to compute for large datasets [51]. This leads us to discuss a computationally easy semantic metric for the assessment of both text and speech quality named WER.

B. WORD ERROR RATE

WER is defined as the edit distance normalized by the length of a sentence [55]. This text SemCom metric is therefore easy to calculate and can reflect semantic similarity to a certain extent [51]. Nevertheless, WER cannot capture the effects of synonyms or semantic similarity [51].

We now proceed with our discussion of a text quality assessment metric that is useful for the design, analysis, and optimization of text SemCom systems – named BLEU.

C. BILINGUAL EVALUATION UNDERSTUDY

To evaluate the quality of a machine translated text, the BLEU score [171] is a metric that is commonly used to assess the effectiveness of text SemCom systems [46], [48], [93]–[95], [98]. SemCom systems' performance can be quantified using the BLEU score – between the transmitted sentence \mathbf{s} and the recovered sentence $\hat{\mathbf{s}}$ – which is defined as [171], [54, eq. (14)]

$$\log \text{BLEU} := \min(1 - l_{\hat{\mathbf{s}}} / l_{\mathbf{s}}, 0) + \sum_{n=1}^N u_n \log P_n, \quad (8)$$

¹⁴The authors of [137] believe that Seb will be an essential building block for a more comprehensive semantic information-processing framework that integrates SemCom and semantic computation. To this end, they recommend studying the Seb representation to enable unified/generalized semantic information extraction and representation for multimodal (syntactic) information [137].

¹⁵SBERT: bidirectional encoder representations from transformers [170].

¹⁶As opposed to our notation, \mathbf{Y} and \mathbf{X} denote multivariate RVs in this particular case.

where $l_{\hat{s}}$ and l_s are, respectively, the length of \hat{s} and s , u_n denotes the weights of the n -grams, and P_n is the n -grams score defined as [54, eq. (15)]

$$P_n := \frac{\sum_k \min(C_k(\hat{s}), C_k(s))}{\sum_k \min(C_k(\hat{s}))}, \quad (9)$$

where $C_k(\cdot)$ represents the frequency count function for the k -th element in the n -th gram [54]. Although BLEU considers linguistic laws given that semantically consistent words often come together in a given corpus, it computes only the differences between the words in two sentences – without providing any insight into the meaning of the sentences [135]. More specifically, the BLUE metric cannot distinguish subtle variations in words such as *polysemy*¹⁷ and synonym [46].

We now continue with our discussion of another text quality assessment metric that is useful for the design, analysis, and optimization of text SemCom systems – named CIDEr.

D. CONSENSUS-BASED IMAGE DESCRIPTION EVALUATION

The authors of [172] propose to use CIDEr as an automatic consensus metric of image description quality. CIDEr was originally used to measure the similarity between a candidate sentence to a collection of human-generated reference sentences (i.e., ground truth sentences) describing a given image [58], [135], [172]. As a result, CIDEr is used as semantic metric for the text SemCom system proposed by the authors of [96]. To define CIDEr which automatically evaluates – for a given image I_i – how well a candidate sentence c_i matches the consensus of a variety of image descriptions $S_i := \{s_{i1}, \dots, s_{im}\}$, let all words of the candidate and reference sentences be mapped to their root forms, each sentence be represented by the set of n -grams present in it (where an n -gram ω_k is a set of one or more ordered words [172]), and $h_k(s_{ij})$ ($h_k(c_i)$) be the number of times an n -gram ω_k occurs in the j -th reference sentence s_{ij} (candidate sentence c_i). For this setting, the term frequency-inverse document frequency weighting $g_k(s_{ij})$ for each n -gram ω_k is computed as [172, eq. (1)]

$$g_k(s_{ij}) := \frac{h_k(s_{ij})}{\sum_{\omega_l \in \Omega} h_l(s_{ij})} \times \log \left(\frac{|\mathcal{I}|}{\sum_{I_p \in \mathcal{I}} \min(1, \sum_q h_k(s_{pq}))} \right), \quad (10)$$

where Ω stands for the vocabulary of all n -grams and \mathcal{I} is the set of all images in the dataset [172]. Employing (10), the CIDEr_n score for n -grams of length n is computed using the *average cosine similarity* [173] between the candidate sentence and the reference sentences as [172, eq. (2)]

$$\text{CIDEr}_n(c_i, S_i) := \frac{1}{m} \sum_{j=1}^m \frac{\mathbf{g}_n(c_i) \cdot \mathbf{g}_n(s_{ij})}{\|\mathbf{g}_n(c_i)\| \|\mathbf{g}_n(s_{ij})\|}, \quad (11)$$

¹⁷Polysemy epitomizes the following phenomenon: when an instance of a word (or phrase) is used in different contexts to convey two or more different meanings [140].

where $\mathbf{g}_n(c_i)$ denotes a vector formed by $g_k(c_i)$ that corresponds to all the n -grams of the candidate sentence c_i , and $\mathbf{g}_n(s_{ij})$ represents a vector formed by $g_k(s_{ij})$ that signifies all the n -grams of the i -th reference sentence s_{ij} [172]. In light of (11), longer n -grams are used to capture grammatical properties and richer semantics [172]. To this end, the CIDEr_n scores from n -grams of varying lengths are combined using (11) as follows [172, eq. (3)]:

$$\text{CIDEr}(c_i, S_i) = \sum_{n=1}^N \text{CIDEr}_n(c_i, S_i), \quad (12)$$

where uniform weights $w_n = 1/N$ work the best [172] and $1 \leq N \leq 4$ (as constrained by the authors of [172]). The advantage of CIDEr – as it is defined in (12) – is that it assesses semantic similarity on the basis of a set of human-generated reference sentences having identical meaning [58], [135] rather than a reference sentence like BLEU. On the other hand, the downside of CIDEr like BLUE is that it is based on the comparison of word groups – CIDEr captures the semantic similarity at the word level [58], [135], rather than the sentence level while considering the various possible contexts of a word.

To address the linguistic fact that a word can have different meanings in various contexts (e.g., “mouse” in biology and “mouse” in computer science), the authors of [46] introduce SSM, which we discuss below.

E. SEMANTIC SIMILARITY METRIC

SSM measures the semantic similarity between the transmitted sentence s and the estimated sentence \hat{s} . For \hat{s} and s , SSM is defined as [46, eq. (13)], [54, eq. (16)]

$$\eta(\hat{s}, s) := \frac{\mathbf{B}_{\Phi}(s) \mathbf{B}_{\Phi}(\hat{s})^T}{\|\mathbf{B}_{\Phi}(s)\| \|\mathbf{B}_{\Phi}(\hat{s})\|}, \quad (13)$$

where $0 \leq \eta(\hat{s}, s) \leq 1$ and $\mathbf{B}_{\Phi}(\cdot)$ denotes the output of BERT, which is an enormous pre-trained model that encompasses billions of parameters used for mining semantic information [46]. As defined in (13), the metric $\eta(s, \hat{s})$ takes values between 0 and 1 (which mirror *semantic irrelevance* and *semantic consistency*, respectively) [174]. Meanwhile, since BERT are sensitive to polysemy, semantic information is quantified by the sentence similarity metric at the sentence level [135]. Meanwhile, the probabilistic aspect of a BERT-based SSM per (13) can be assessed using a probabilistic metric named the *upper tail probability of SSM*.

F. UPPER TAIL PROBABILITY OF SSM

The upper tail probability of SSM $\eta(s, \hat{s})$ w.r.t. $\eta_{\min} \in [0, 1]$ is proposed by the authors of [175] as a suitable metric for assessing the performance of a wireless text SemCom technique and is defined as [175, eq. (8)]

$$p(\eta_{\min}) := \mathbb{P}(\eta(s, \hat{s}) \geq \eta_{\min}), \quad (14)$$

where $\eta(s, \hat{s})$ is defined in (13) and η_{\min} stands for minimum semantic similarity. The upper tail probability of SSM is

useful for quantifying the probabilistic assessment of wireless/optical text SemCom techniques. To this end, the authors of [175] employed it to quantify the asymptotic performance of a DL-enabled semantic communication system (*DeepSC* [46]) subject to single-interferer as well as multi-interferer radio frequency interference. It is worth underscoring, however, that employing the upper tail probability of SSM to assess the performance of a text SemCom technique can lead to mathematical intractability – especially when analyzing the non-asymptotic performance of a DL-based text SemCom technique – due to DL models’ fundamental *lack of interpretability* [176], [177] and the lack of a commonly agreed-upon (unified) definition of semantics / semantic information.

The probabilistic metric set out in (14) is inspired by the SSM metric defined in (13). The metric in (13) is a cosine similarity metric using BERT. Nevertheless, the sentence embeddings that result from using a pre-trained BERT model without fine-tuning on semantic textual similarity task inadequately capture the sentences’ semantic meaning due to anisotropic embedding space [178], [179]. We therefore discuss below another text SemCom metric termed *SSM using SBERT*¹⁸ [180].

G. SSM USING SBERT

To begin with, “child” and “children” are semantically associated even though their lexical similarity computed using BLEU is zero [179]. Despite the input and output having such a low BLEU score for lexical similarity, their semantic similarity can be high [179]. To capture this notion of high semantic similarity, the authors of [179] represent sentences as embeddings using an embedding model M and compute the cosine similarity between the input sentence s and the recovered sentence \hat{s} as follows [179, eq. (4)]:

$$\text{match}(\hat{s}, s) := \frac{M(s)M(\hat{s})^T}{\|M(s)\|\|M(\hat{s})\|}. \quad (15)$$

Rather than using BERT without fine-tuning on semantic textual similarity task (which will poorly capture the semantic meaning of the sentences [178], [179]), the authors of [179] use SBERT [180] – fine-tuned on semantic textual similarity tasks – as an embedding model M . To this end, the definition in (15) represents the metric SSM using SBERT provided that the SBERT model is fine-tuned on semantic textual similarity tasks to encode the sentence embedding [179].

We now move on to our discussion of another text quality assessment metric that is useful for the design, analysis, and optimization of text SemCom systems – termed METEOR.

H. METRIC FOR EVALUATION OF TRANSLATION WITH EXPLICIT ORDERING

METEOR is an automatic metric for the assessment of machine translation that is based on a generalized concept of *unigram matching* – based on their surface forms, stemmed forms, and meanings – between a translation produced by a

machine and a set of reference translations produced by a human [181]. It therefore expands the synonym set by introducing external knowledge sources [174], such as *WordNet* (see [182]). In addition, METEOR employs precision P_m and recall R_m to evaluate the similarity between transmitted and received texts as follows [174, eq. (3)]:

$$\text{METEOR} := (1 - \text{Pen})\bar{F}, \quad (16)$$

where Pen is the penalty coefficient and \bar{F} is the harmonic mean that combines P_m and R_m as given by [174, eq. (2)]

$$\bar{F} := \frac{P_m R_m}{\alpha P_m + (1 - \alpha) R_m}, \quad (17)$$

where α is the hyperparameter according to WordNet [174]. To summarize, the authors of [181] substantiate that METEOR considerably improves correlation with human judgment. Despite this notable advantage, it is restricted to unigram matches, which makes it a strictly word-level metric [183]. This leads us to the discussion of our last text SemCom metric, called average bit consumption per sentence.

I. AVERAGE BIT CONSUMPTION PER SENTENCE

The authors of [98] introduce *average bit consumption per sentence* as a wireless text SemCom metric. This metric measures a system’s performance from a communication perspective [54]. More specifically, the authors of [98] deploy this text semantic metric to evaluate the performance of their proposed text semantic transmission techniques with hybrid automatic repeat request (HARQ).

The reader is referred to [184] for a survey on the evolution of semantic similarity and to [185] for a survey on the methods, tools, and applications of semantic textual similarity for additional information on the possibly useful metrics applicable for text SemCom. Wrapping up, the existing semantic metrics for text quality assessment that are applicable in both wireless text SemCom and optical text SemCom are summarized along with their pros and cons in Table 4.

We now continue with our discussion on state-of-the-art semantic metrics for speech quality assessment.

IV. SEMANTIC METRICS FOR SPEECH QUALITY ASSESSMENT

For speech quality assessment, the following metrics are commonly used: *signal-to-distortion ratio* (SDR), *perceptual evaluation of speech quality* (PESQ), *(unconditional) Fréchet deep speech distance* (FDSD), and *(unconditional) kernel deep speech distance* (KDSD) [54], [58]. Recently, WER and *character error rate* (CER) have been employed to assess the quality of speech recovered by the semantic receiver in a wireless audio SemCom system [45], [100]–[104]. In what follows, we discuss the following semantic metrics applicable to audio SemCom: WER, CER, SDR, PESQ, FDSD, and KDSD. We begin with a brief discussion of WER.

¹⁸SBERT: sentence-BERT.

Metrics	Pros	Cons
(Average) semantic distance/distortion	This metric uses semantic distance based on lexical taxonomies as a distortion measure [51].	Since this metric only calculates the semantic similarity between individual words, it would be difficult to compute for large data sets [51].
WER	WER is easy to calculate and can reflect the semantic similarity to a some extent [51].	WER can hardly capture the effects of synonyms or semantic similarity [51].
BLEU	BLEU observes the fundamental linguistic law that semantically similar sentences are invariable in the semantic space [51].	1) Rather than the semantic meaning of words in sentences, BLEU can only compare the differences between words in two sentences [51]. 2) BLUE cannot distinguish more subtle variation in words such as polysemy and synonym [46].
CIDEr	Unlike BLEU, CIDEr does not assess semantic similarity based on a reference sentence, but a group of sentences with the same meaning [51].	1) CIDEr focuses more on the middle part of a sentence (the middle part possessing more n -gram weight) [51]. 2) CIDEr captures the respective semantic similarity at the word level [58], [135], rather than at a sentence level while considering the several contexts of a word.
SSM (with BERT)	Pertaining to BERT's sensitivity to polysemy, SSM (with BERT) can explain semantics at the sentence level [51].	1) As a cause of limitation to this metric, it is not easy to generalize the pre-trained BERT model on others [51]. 2) The sentence embeddings from a pre-trained BERT model without fine-tuning on semantic textual similarity task inadequately capture the sentences' semantic meaning because of anisotropic embedding space [178], [179].
The upper tail probability of SSM	This metric captures all the probabilistic aspects of the SSM w.r.t. the minimum semantic similarity $\eta_{\min} \in [0, 1]$.	This metric can lead to mathematical intractability due to the DL models' fundamental lack of interpretability and the lack of commonly agreed upon (unified) definition of semantics as well as semantic information.
SSM using SBERT	This text SemCom metric can capture a high semantic similarity even when the respective BLEU score is low	The SBERT model is fine-tuned on semantic textual similarity tasks in order to encode the sentence embedding [179].
METEOR	1) METEOR expands the synonym set by introducing external knowledge sources [174], such as WordNet (see [182]). 2) METEOR can considerably improve correlation with human judgments [181].	METEOR is restricted to unigram matches [183]: 1) By emphasizing on only one match type per stage, the aligner misses a considerable part of the likely alignment space [183]. 2) Choosing partial alignments grounded only on the least number of per-stage crossing alignment links can practically give rise to missing full alignments [183].

TABLE 4: Main semantic metrics for text quality assessment along with their pros and cons – WER: word error rate; BLEU: bilingual evaluation understudy; SSM: semantic similarity metric; BERT: bidirectional encoder representations from transformers; SBERT: sentence-BERT; METEOR: metric for evaluation of translation with the explicit ordering.

A. WORD ERROR RATE

Since audio data and text data are very similar, WER has also been applied to assess the accuracy of speech signal transmission [51]. To this end, it is defined in terms of the number of word substitutions (S_W), word deletions (D_W), and word insertions (I_W) as [102, eq. (10)]

$$\text{WER} := \frac{S_W + D_W + I_W}{N_W}, \quad (18)$$

where N_W stands for the number of words in the original speech transcription. As defined in (18), WER has been applied in the design of various audio SemCom techniques including the one used in [186].

We now continue with our discussion of a speech quality assessment metric that is useful for the design, analysis, and optimization of audio SemCom systems – termed CER.

B. CHARACTER ERROR RATE

Unlike WER for the evaluation of text similarity, the CER metric operates at the character level rather than the word level to assess the accuracy of speech recognition [51], [102]. Accordingly, similar to WER, CER is defined in terms of the number of character substitutions (S_C), character deletions (D_C), and character insertions (I_C) as [102, eq. (9)]

$$\text{CER} := \frac{S_C + D_C + I_C}{N_C}, \quad (19)$$

where N_C denotes the number of characters in the original speech transcription.

We now proceed with our discussion of another speech quality assessment metric that is useful for the design, analysis, and optimization of audio SemCom systems – named SDR.

C. SIGNAL-TO-DISTORTION RATIO

SDR is a commonly used metric for speech transmission [100], [101], [187]. For a given speech sample sequence $\mathbf{s} = [s_1, s_2, \dots, s_W] \in \mathbb{R}^{1 \times W}$ and a decoded speech sequence $\hat{\mathbf{s}} = [\hat{s}_1, \hat{s}_2, \dots, \hat{s}_W] \in \mathbb{R}^{1 \times W}$, SDR is defined as [100, eq. (6)], [187, eq. (13)]

$$\text{SDR} := 10 \log_{10} \left(\frac{\|\mathbf{s}\|^2}{\|\mathbf{s} - \hat{\mathbf{s}}\|^2} \right). \quad (20)$$

As can be inferred from (20), SDR and mean squared error (MSE) are related [51] such that one can be inferred from the other. Accordingly, (20) asserts that a lower MSE value leads to higher SDR value, and vice versa. In addition, because a difference in SDR produces a visible performance difference, it can be used to optimize DNNs [51].

We now continue with our discussion of yet another speech quality assessment metric that is useful for the design, analysis, and optimization of audio SemCom systems – termed PESQ.

D. PERCEPTUAL EVALUATION OF SPEECH QUALITY

PESQ [188] is an International Telecommunication Union (ITU)-standardized¹⁹ metric for evaluating the subjective quality of speech signals under various conditions – such as background noise, analog filtering, and variable delay – by scoring their quality on a scale from -0.5 to 4.5 [100], [188]. This metric is the result of merging the perceptual analysis measurement system (PAMS) and an enhanced version of the perceptual speech quality measure (PSQM) named PSQM99 [188]. Meanwhile, the basic diagram of PESQ and its philosophy is shown in Fig. 4.

PESQ is deployed in [100] and [101] to evaluate the performance of SemCom systems for speech transmission. PESQ presumes that humans' perceptual memory is short, which makes it a realistic metric w.r.t. human behavior [58]. Nonetheless, PESQ quantifies the accuracy of speech transmission rather than its semantic content [58].

We now continue with our discussion of one more speech quality assessment metric that is important for the design, analysis, and optimization of audio SemCom systems – dubbed FDSD.

E. FRÉCHET DEEP SPEECH DISTANCE

FDSD is used to quantify the quality of synthesized speech signals [54], [190]. If we let the original speech samples $\mathbf{D} \in \mathbb{R}^{K \times L}$ and the synthesized speech samples $\hat{\mathbf{D}} \in \mathbb{R}^{\hat{K} \times L}$ have means $\boldsymbol{\mu}_{\mathbf{D}}$ and $\boldsymbol{\mu}_{\hat{\mathbf{D}}}$, respectively, FDSD can be defined mathematically as [54, eq. (21)]

$$\Gamma^2 := \|\boldsymbol{\mu}_{\mathbf{D}} - \boldsymbol{\mu}_{\hat{\mathbf{D}}}\|^2 + \text{tr}(\boldsymbol{\Sigma}_{\mathbf{D}} + \boldsymbol{\Sigma}_{\hat{\mathbf{D}}} - \sqrt{\boldsymbol{\Sigma}_{\mathbf{D}}\boldsymbol{\Sigma}_{\hat{\mathbf{D}}}}), \quad (21)$$

where $\boldsymbol{\Sigma}_{\mathbf{D}}$ and $\boldsymbol{\Sigma}_{\hat{\mathbf{D}}}$ denote the covariance matrices of \mathbf{D} and $\hat{\mathbf{D}}$, respectively. In light of (21), the smaller the value of FDSD, the more similar the real and synthesized speech signals are [54]. FDSD is employed in the design and optimization of an audio SemCom system in [104].

This leads us to the discussion of our last speech quality assessment metric that is important for the design, analysis, and optimization of audio SemCom systems – named KDSD.

F. KERNEL DEEP SPEECH DISTANCE

Like FDSD, KDSD is also utilized to assess the quality of synthesized speech signals [54], [190]. Using the definitions set out in Section IV-E, KDSD can be defined mathematically w.r.t. kernel $q(\cdot, \cdot)$ as [54, eq. (22)]

$$\begin{aligned} \Delta^2 := & \frac{1}{K(K-1)} \sum_{1 \leq i, j \leq K: i \neq j} q(\mathbf{D}_i, \hat{\mathbf{D}}_j) + \frac{1}{\hat{K}(\hat{K}-1)} \\ & \times \sum_{1 \leq i, j \leq \hat{K}: i \neq j} q(\mathbf{D}_i, \hat{\mathbf{D}}_j) + \sum_{i=1}^K \sum_{j=1}^{\hat{K}} q(\mathbf{D}_i, \hat{\mathbf{D}}_j). \end{aligned} \quad (22)$$

When it comes to the definition in (22), the smaller the KDSD values are, the more similar the real and synthesized

speech signals are [54]. KDSD is exploited in the design and optimization of an audio SemCom system in [104].

The aforementioned metrics for speech quality assessment hardly quantify performance at the level of semantic understanding [58]. Thus, the audio SemCom research field lacks semantic assessment metrics that incorporate semantic understanding, like BERT and BLEU [58]. At last, the existing metrics for speech quality assessment that are applicable to wireless audio SemCom are summarized along with their pros and cons in Table 5.

We now continue with our discussion on the state-of-the-art semantic metrics for image quality assessment.

V. SEMANTIC METRICS FOR IMAGE QUALITY ASSESSMENT

Numerous semantic metrics have been proposed to date for image quality assessment (IQA) [191]. Some of these IQA metrics have been exploited in the design, analysis, or optimization of state-of-the-art wireless image SemCom systems [105]–[115] and an optical image SemCom system [147]. Applicable to these systems, image SemCom metrics such as *image semantic similarity*, *peak signal-to-noise ratio* (PSNR), *structural similarity index measure* (SSIM), *multi-scale structural similarity index measure* (MS-SSIM), *learned perceptual image patch similarity* (LPIPS), *mean intersection over union* (mIoU), *image-to-graph semantic similarity* (ISS), and *recognition accuracy* are widely used by designers of wireless as well as optical image SemCom systems. These metrics are detailed henceforward, beginning with image semantic similarity.

A. IMAGE SEMANTIC SIMILARITY

The image semantic similarity of two images A and B is computed as [54, eq. (18)]

$$\Theta(f(A), f(B)) := \|f(A) - f(B)\|_2^2, \quad (23)$$

where $f(\cdot)$ denotes an image embedding function that maps an image to a point in the Euclidean space [54]. However, the metric defined by (23) depends on the higher-order image structure, which is often context-dependent [54].

We now move on to our discussion of a computationally simple IQA metric that is important for designing, analyzing, and optimizing image SemCom systems – known as PSNR.

B. PEAK SIGNAL-TO-NOISE RATIO

PSNR quantifies the ratio between the maximum possible power of the desired signal and the power of the noise that has contaminated the desired signal [105]. Accordingly, PSNR is defined in a logarithmic-scale as [105, eq. (4)]

$$\text{PSNR} := 10 \log_{10} \frac{\text{MAX}^2}{\text{MSE}} \quad [\text{dB}], \quad (24)$$

where MAX denotes the maximum possible number of image pixels and MSE represents the mean squared error between a reference image and a reconstructed image. The following conclusion can be drawn from the definition in (24): as the

¹⁹ITU standardized PESQ as the *ITU-T Recommendation P.862* [189].

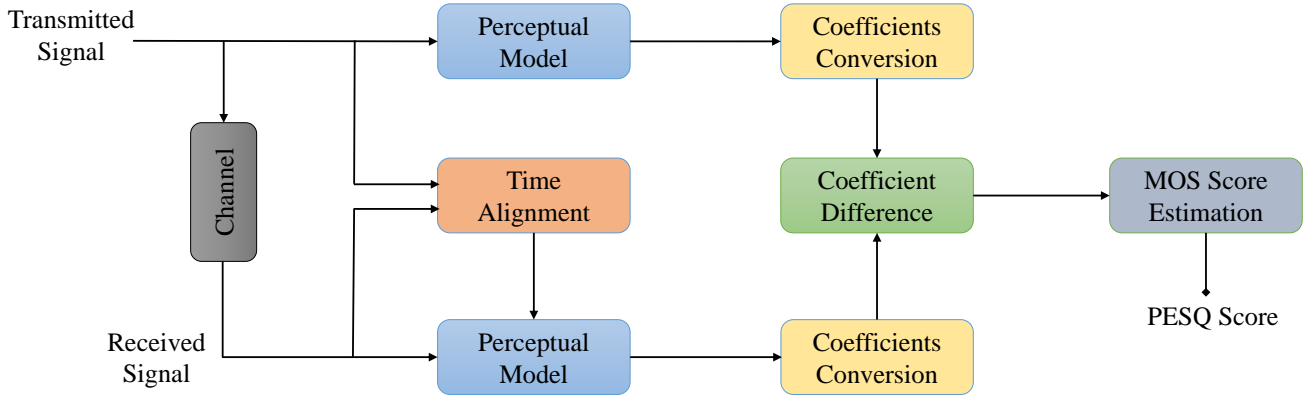


FIGURE 4: Basic diagram of PESQ [58, Fig. 13] and its philosophy [189, Figure 1/P.862] – MOS: mean opinion score.

Metrics	Pros	Cons
WER	WER is a computationally easy audio SemCom metric.	WER's quantification may not be consistent with human perception.
CER	CER is also a computationally simple audio SemCom metric.	CER's evaluation may not be consistent with human perception.
SDR	1) SDR is easy to calculate [51]. 2) SDR can reflect the quality of voice to a certain degree [51].	The evaluation results of SDR are sensitive to the volume of audios [51].
PESQ	1) PESQ's evaluation is objective [51]. 2) PESQ's assessment is close to human perception [51].	PESQ exhibits an intrinsically high computational complexity [51].
FDSD	FDSD is demonstrated experimentally that it ranks models consistent with MOSes obtained through human evaluation [190].	FDSD manifests an inherent computational complexity.
KDSD	KDSD is also corroborated experimentally that it ranks models in accordance with MOSes obtained via human evaluation [190].	KDSD exhibits an intrinsic computational complexity.

TABLE 5: Main semantic metrics for speech quality assessment along with their pros and cons – WER: word error rate; CER: character error rate; SDR: signal-to-distortion ratio; PESQ: perceptual evaluation of speech quality; FDSD: unconditional Fréchet deep speech distance; KDSD: unconditional kernel deep speech distance; MOSes: mean opinion scores.

MSE between the transmitted image and the reconstructed image becomes smaller, the PSNR²⁰ gets larger, meaning a better-quality of reconstructed image [55].

We now move on to our discussion of a widely known IQA metric that is also important for designing, analyzing, and optimizing image SemCom systems – termed SSIM.

C. STRUCTURAL SIMILARITY INDEX MEASURE

To formally define the metric SSIM, let us first define an overall similarity measure for two non-negative image signals x and y as [192, eq. (5)]

$$S(x, y) := f(l(x, y), c(x, y), s(x, y)), \quad (25)$$

²⁰PSNR can also be employed to assess the quality of video transmission since a video is made of several image frames [55].

where $S(x, y)$ denotes the overall measure of similarity between x and y ; $l(\cdot, \cdot)$, $c(\cdot, \cdot)$, and $s(\cdot, \cdot)$ represent the luminance comparison function, the contrast comparison function, and the structure comparison function, respectively; and $f(\cdot, \cdot, \cdot)$ is the similarity measure function whose arguments are the outputs of $l(\cdot, \cdot)$, $c(\cdot, \cdot)$, and $s(\cdot, \cdot)$. In light of (25) and the functions $l(\cdot, \cdot)$, $c(\cdot, \cdot)$, and $s(\cdot, \cdot)$ as defined in [192, eq. (6)], [192, eq. (9)], and [192, eq. (10)], respectively, the SSIM between x and y is defined as [192, eq. (12)]

$$\text{SSIM}(x, y) := [l(x, y)]^\alpha [c(x, y)]^\beta [s(x, y)]^\gamma, \quad (26)$$

where $\alpha, \beta, \gamma > 0$ are parameters used to adjust the relative importance of the three functions' outputs [192]. In view of (26), one may require a single overall quality measure – for the entire image in question – which can be captured by the

metric *mean SSIM* (MSSIM) that is defined via (26) as [192, eq. (17)]

$$\text{MSSIM}(\mathbf{X}, \mathbf{Y}) := \frac{1}{M} \sum_{j=1}^M \text{SSIM}(\mathbf{x}_j, \mathbf{y}_j), \quad (27)$$

where \mathbf{X} and \mathbf{Y} are the reference and distorted images, respectively; M is the number of local windows of the image; and \mathbf{x}_j and \mathbf{y}_j are the images' content at the j -th local window [192].

It is worth mentioning that SSIM is less effective when assessing blurred and noisy images [51]. To overcome this limitation, SSIM variants such as *three-component weighted SSIM* (3-SSIM) [193] and *feature similarity index for image quality assessment* (FSIM) [194] are proposed.

We now continue with our discussion of another IQA metric that is used for designing, analyzing, and optimizing image SemCom systems – named MS-SSIM.

D. MULTI-SCALE STRUCTURAL SIMILARITY INDEX MEASURE

Practically speaking, the subjective evaluation of an image varies when the following factors change: the distance from the image plane to the observer, the sampling density of the image signal, and the perceptual capability of the observer's visual system [195]. Multi-scale method is therefore convenient to incorporate the details of images captured at various resolutions [195]. To this end, the authors of [195] put forward the metric MS-SSIM for image quality assessment, whose system diagram is schematized in Fig. 5. As is shown in Fig. 5, the MS-SSIM system uses the reference and distorted image signals as the input, which are fed into the system that iteratively applies a low-pass filter and downsamples the filtered image by a factor of 2 [195]. When the original image is indexed as scale 1 and the highest scale as scale M (obtained after $M - 1$ iterations), the MS-SSIM metric between signals \mathbf{x} and \mathbf{y} can be defined by combining the measurements taken at different scales as follows [195, eq. (7)]:

$$\text{MS-SSIM}(\mathbf{x}, \mathbf{y}) := [l_M(\mathbf{x}, \mathbf{y})]^{\alpha_M} \prod_{j=1}^M [c_j(\mathbf{x}, \mathbf{y})]^{\beta_j} [s_j(\mathbf{x}, \mathbf{y})]^{\gamma_j}, \quad (28)$$

where $c_j(\mathbf{x}, \mathbf{y})$ and $s_j(\mathbf{x}, \mathbf{y})$ are the contrast comparison and the structure comparison at the j -th scale, respectively; $l_M(\mathbf{x}, \mathbf{y})$ denotes the luminance comparison, which is computed only at scale M ; and the constants α_M , β_j , and γ_j are used to adjust the relative importance of the components mentioned [195]. It is worth noting that the MS-SSIM definition in (28) encompasses SSIM as a special case.

In light of (MS-)SSIM, the LPIPS model [196], [197], which we discuss below, is another crucial metric for image SemCom.

E. LEARNED PERCEPTUAL IMAGE PATCH SIMILARITY

The authors of [198] introduce the metric LPIPS, whose key idea is to use *deep features* to construct a loss function.

This approach comprises two steps: calculating the distance from a given network – (pre-trained) network \mathcal{F} – and then predicting perceptual judgment, to wind up with a loss function [198, Figure 3]. The following are three possible LPIPS configurations – namely *lin*, *tune*, and *scratch* [198], [199] – depending on how the loss function was constructed:

- In the *lin* configuration, the pre-trained network weights \mathcal{F} are fixed, and the linear weights w are learned on top.²¹
- In the *tune* configuration, a pre-trained classification model is employed for initialization, and all the weights for network \mathcal{F} are tweaked/fine-tuned.
- In the *scratch* configuration, a network is initialized from random normal weights and trained entirely using judgment from related studies [198].

For the first step of LPIPS (i.e., distance calculation), the distance between a reference patch x and a distorted patch x_0 is calculated using network \mathcal{F} as follows [198, eq. (1)]:

$$d(x, x_0) := \sum_l \frac{1}{H_l W_l} \sum_{h,w} \|w_l \odot [(\hat{\mathbf{y}}_l)_{h,w} - (\hat{\mathbf{y}}_{l,0})_{h,w}]\|_2^2, \quad (29)$$

where $H_l, W_l \in \mathbb{N}$ are the spatial components of the l -th layer; $(\hat{\mathbf{y}}_l)_{h,w}$ and $(\hat{\mathbf{y}}_{l,0})_{h,w}$ are the comprising vectors of tensors $\hat{\mathbf{y}}_l \in \mathbb{R}^{H_l \times W_l \times C_l}$ and $\hat{\mathbf{y}}_{l,0} \in \mathbb{R}^{H_l \times W_l \times C_l}$, respectively, the latter of which are extracted deep feature embeddings from the l -th layer that have been unit-normalized in the channel dimension; and w_l is a scaling vector deployed for channel-wise *activation* scaling [198]. Following the distance calculation per (29), the second step of LPIPS is to predict perceptual judgment through a small network \mathcal{G} that has been trained – using cross-entropy (CE) loss – to predict perceptual judgment h from distance pair (d_0, d_1) [198]. Consequently, the loss function is ultimately expressed as [199, eq. (2.11)]

$$\mathcal{L}(x, x_0, x_1, h) = -h \log \mathcal{G}(d(x, x_0), d(x, x_1)) - (1-h) \times \log(1 - \mathcal{G}(d(x, x_0), d(x, x_1))), \quad (30)$$

where d_0 and d_1 denote the distance between patches $\{x, x_0\}$ and $\{x, x_1\}$, respectively; and h is the predicted perceptual judgment [198]. Furthermore, to try and cover as many properties as possible [199], the authors of [200] present a weighted version of LPIPS with two other loss functions (adversarial loss and optical flow loss for temporal dynamics).

When a system designer requires accurate semantic-level recovery, an image SemCom system can be designed/analyzed using the metric mIoU [110], which we discuss below.

F. MEAN INTERSECTION OVER UNION

The metric mIoU is defined as [110, eq. (4)]

$$\text{mIoU} := \frac{1}{N_{cls}} \sum_{i=1}^{N_{cls}} \frac{P_i \cap G_i}{P_i \cup G_i}, \quad (31)$$

²¹In an existing feature space, this comprises the perceptual calibration of a few parameters [198].

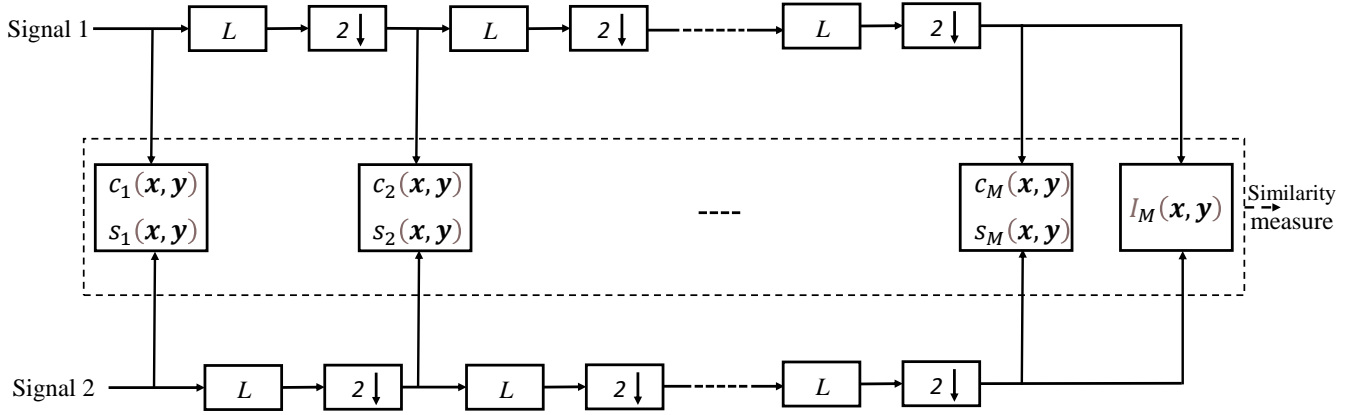


FIGURE 5: Basic diagram of the MS-SSIM system – L : low-pass filtering; $2 \downarrow$: downsampling by 2 [195, Fig. 1].

where P_i represents the set of pixel regions predicted by the decoder for the i -th object category, G_i stands for the actual set of pixel regions pertaining to the i -th object category, and N_{cls} denotes the number of object categories (e.g., pedestrians, vehicles, and trucks) in the input image [110]. For the definition in (31), the higher the mIoU value, the better the image SemCom performance [110].

We now continue with our discussion of another IQA metric that is used for designing, analyzing, and optimizing image SemCom systems – called ISS.

G. IMAGE-TO-GRAPH SEMANTIC SIMILARITY

ISS [201] is an important image SemCom metric for assessing the performance of cooperative image SemCom networks in which a set of servers cooperatively transmit images to a set of users using SemCom schemes (vis-à-vis the transmission of semantic information that captures the meaning of images). To formally define the metric ISS in the context of cooperative semantic communication networks, let us define the semantic information about an image G_k extracted by a server v and transmitted to a user k as [201, eq. (1)]

$$\Psi_{vk} := \{\psi_{vk}^1, \psi_{vk}^2, \dots, \psi_{vk}^n, \dots, \psi_{vk}^{N_{vk}}\}, \quad (32)$$

where N_{vk} is the number of semantic triples in image G_k ; $\psi_{vk}^n := (e_{vk,i}^n, l_{vk,ij}^n, e_{vk,j}^n)$ is a semantic triple given that $e_{vk,i}^n$ is the category of object i in image G_k ; and $l_{vk,ij}^n$ denotes the relationship between objects $e_{vk,i}^n$ and $e_{vk,j}^n$ [201]. Note that $l_{vk,ij}^n \neq l_{vk,ji}^n$ since $l_{vk,ij}^n$ is directional [201].

Some semantic triplets in Ψ_{vk} may contain irrelevant information. Thus, to enhance the efficiency of the SemCom model considered by the authors of [201], each server v transmits the semantic triples that incorporate a significant image meaning [201]. Thus, the partial semantic information

that server v transmits to a user k can be equated to [201, eq. (3)]

$$\hat{\Psi}_{vk} := \{\hat{\psi}_{vk}^1, \hat{\psi}_{vk}^2, \dots, \hat{\psi}_{vk}^n, \dots, \hat{\psi}_{vk}^{\hat{N}_{vk}}\} \subset \Psi_{vk}, \quad (33)$$

where \hat{N}_{vk} denotes the number of selected semantic triples in $\hat{\Psi}_{vk}$.

The authors of [201] employ ISS to evaluate the performance of cooperative image SemCom networks per the aforementioned scenario. Furthermore, whereas SSIM measures the differences in a set of pixels, ISS captures the correlation between the meaning of the image and that of its corresponding semantic information [201]. Meanwhile, the authors of [201] deploy a DNN-based encoder to *vectorize* the original image G_k and the semantic information Ψ_{vk} which are, respectively, defined as [201]

$$C(G_k) := \{C(\psi_{vk}^1), \dots, C(\psi_{vk}^n), \dots, C(\psi_{vk}^{N_{vk}})\} \quad (34a)$$

$$O_{vk} := \{C(\hat{\psi}_{vk}^1), \dots, C(\hat{\psi}_{vk}^n), \dots, C(\hat{\psi}_{vk}^{\hat{N}_{vk}})\}, \quad (34b)$$

where $C(\cdot)$ represents a *vectorization* function that forms the relationship between the image and the input semantic information by matching text-image pairs with similar meanings [201].

ISS is defined as the cosine angle between an image vector and its corresponding normalized semantic triple vectors [201]. Accordingly, for the formulations in (32)-(34b), the ISS of $\hat{\Psi}_{vk}$ that is transmitted from server v to user k is

defined as [201, eq. (6)]

$$E(\hat{\psi}_{vk}, a_{vk}) := \sum_{q=1}^Q a_{vk}^q \times \frac{\left\| \sum_{n=1}^{\hat{N}_{vk}} \overline{C(\hat{\psi}_{vk}^n)} \cdot C(G_k)^T \overline{C(\hat{\psi}_{vk}^n)} \right\|}{\|C(G_k)\|}, \quad (35)$$

where Q denotes the number of downlink orthogonal resource blocks (RBs), $a_{vk} := [a_{vk}^1, \dots, a_{vk}^Q]$ represents an RB allocation vector for user k of server v given that $a_{vk}^q \in \{0, 1\}$ is the user-server connection index, and $\overline{O_{vk}} := \{\overline{C(\hat{\psi}_{vk}^1)}, \dots, \overline{C(\hat{\psi}_{vk}^n)}, \dots, \overline{C(\hat{\psi}_{vk}^{\hat{N}_{vk}})}\}$ is the Gram-Schmidt orthogonalized version of O_{vk} per (34b). It is evident from (35) that the value of ISS increases with the number of transmitted semantic triples, in line with the objectives of human cognition [201].

We now proceed with a discussion on our last IQA metric that is used for designing, analyzing, and optimizing image SemCom systems – called recognition accuracy.

H. RECOGNITION ACCURACY

Recognition accuracy is a metric for assessing the quality of reconstructed images that is proposed by the authors of [113] for a joint transmission-recognition scheme for an image SemCom system also proposed by them.

Other major IQA metrics are *complex-wavelet SSIM* (CW-SSIM) [202], *fast SSIM* and *fast MS-SSIM* [203], *information content weighted SSIM* (IW-SSIM) [204], *information fidelity criterion* (IFC) [205], *visual information fidelity* (VIF) [206], *multi-scale geometric analysis-based IQA* (MGA-based IQA) [207], the *detail loss metric* (DLM) [208], *multi-metric fusion* (MMF) [209], *most apparent distortion* (MAD) [210], *peak signal-to-noise ratio-human vision system modified* (PSNR-HVS-M) [211], the *noise quality measure* (NQM) [212], and *visual signal-to-noise ratio* (VSNR) [213]. These metrics are also crucial for the design, analysis, and optimization of image SemCom systems. The image SemCom metrics defined in Sections V-A through V-H are often employed to evaluate the semantic similarity between the natural images transmitted and those received. Generative adversarial networks (GANs) [214]–[216], on the other hand, are being exploited to produce natural-looking synthetic images whose similarity is also assessed in comparison with natural images. To this end, metrics such as *adversarial loss* [214], *inception score* (IS) [217], *Fréchet inception distance* (FID) [218], and *kernel inception distance* (KID) [219]²² have been proposed to measure the similarity between natural and GAN-generated images. At last, the existing semantic

metrics that are used for image quality assessment and applicable to both wireless image SemCom and optical image SemCom are summarized along with their pros and cons in Table 6.

We now proceed with our discussion on the state-of-the-art semantic metrics for video quality and 3D human sensing assessment.

VI. SEMANTIC METRICS FOR VIDEO QUALITY AND 3D HUMAN SENSING ASSESSMENT

Video quality assessment (VQA) metrics can be classified based on the availability of reference [191]. When no reference signal is available to compare the distorted/test signal with, the VQA metric is termed a *no-reference* (NR) metric [191]. On the other hand, if information is available for part of the reference medium (for instance, a group of extracted features), the VQA metric is called a *reduced-reference* (RR) metric [191]. Contrary to RR metric, the *full-reference* (FR) VQA metric requires the entire reference medium to assess the distorted/test medium [191]. The FR VQA metric is expected to have the best video quality prediction performance since it has complete information about the original medium [191].

VQA metrics can also be categorized into five types based on their assessment methodology [191]:

- 1) *Image/video fidelity metrics*: these metrics operate based only on the direct accumulation of errors and thus are often FR [191]. Even though these VQA metrics are the simplest ones that are still widely used, they are usually not a good reflection of perceived visual quality when the distortion is not additive [191].
- 2) *Human visual system (HVS) model-based metrics*: these VQA metrics typically deploy frequency-based decomposition and take into consideration various aspects of the HVS, such as contrast and orientation sensitivity, spatial and temporal masking effects, frequency selectivity, and color perception [191]. They can therefore can become very complex and computationally expensive [191].
- 3) *Signal structure (information or other feature)-based metrics*: some of these metrics quantify visual fidelity on the basis of the assumption that a high-quality image/video is one whose structural content – such as object boundaries or regions of high entropy – parallels that of the original image/video [191]. The other metrics of this type are contingent on the assumption that the HVS understands an image mainly through its low-level features [191]. Consequently, image deterioration can be perceived by comparing the low-level features of the reference and distorted images [191].
- 4) *Packet analysis-based metrics*: these metrics center upon evaluating the impact of network impairments on visual quality [191]. To do so and measure quality loss, they often exploit the parameters extracted from the transport stream [191]. Meanwhile, these metrics have the advantage of being able to measure the quality

²²Because FID and KID aim to compare the distribution of generated images with the distribution of real images, they cannot fully utilize the spatial relationship between features [51]. On the other hand, it is worth underscoring the following assessment-related concepts: 1) a lower FID value is demonstrated to correlate well with higher-quality images; 2) a lower KID score indicates better sampling quality, as KID quantifies the *maximum mean discrepancy* in a classifier's feature space [51].

Metrics	Pros	Cons
PSNR	1) PSNR is a simple and computationally inexpensive IQA metric [191]. 2) PSNR can roughly reflect the image similarity [51].	1) PSNR is a shallow function that fails to count the many nuances of human perception [54]. 2) PSNR usually correlates poorly with subjective visual quality [191], [220]. 3) PSNR is not continually consistent with human perception [51].
SSIM	1) SSIM is an easy metric to implement [191]. 2) SSIM exhibits good correlation with subjective scores [191]. 3) SSIM is more consistent – compared with PSNR – with human perception in IQA [51].	1) SSIM is also a shallow function that fails to count the many nuances of human perception [54]. 2) SSIM is sensitive to relative translations, rotations, and scalings of image [191], [220]. 3) SSIM is less effective when it is employed to assess among blurred and noisy images [51]. 4) SSIM reflects a higher evaluation than the actual scale [51].
MS-SSIM	1) MS-SSIM is a convenient approach to incorporate image details at various resolutions [195]. 2) MS-SSIM manifests better correlation with subjective scores than SSIM [191].	MS-SSIM exhibits considerable computational complexity as M gets large.
LPIPS	LPIPS is based on the feature maps of different DNN architectures that have sound effectiveness in accounting for human perception of image quality [197].	LPIPS has an inherent computational complexity which can also be aggravated by a significant training cost of a deep network.
Image semantic similarity	This metric is a computationally easy semantic metric.	This metric depends on the higher-order image structure, which is often context-dependent [54].
ISS	In comparison with SSIM, the ISS metric can capture the correlation of the meaning between the image and its corresponding semantic information [201].	The ISS metric is computationally complex.
FID	FID manifests distinctive robustness to noise [51].	Since FID aims to compare the distribution of generated images with the distribution of real images, it can not entirely utilize the spatial relationship between features [51].
KID	KID exhibits peculiar robustness to noise [51].	Because KID revolves around comparing the distribution of generated images with the distribution of real images, it can not completely utilize the spatial relationship between features [51].

TABLE 6: Main semantic metrics for IQA along with their pros and cons – PSNR: peak signal-to-noise ratio; SSIM: structural similarity index measure; MS-SSIM: multi-scale structural similarity index measure; LPIPS: learned perceptual image patch similarity; ISS: image-to-graph semantic similarity; FID: Fréchet inception distance; KID: kernel inception distance.

of several image/video streams in parallel and are becoming more prevalent because of the increasing popularity of network-based video delivery service, such as Internet streaming [191].

- 5) *Learning-oriented metrics*: these metrics extract particular features from the image/video and then employ ML techniques to obtain a trained model [191]. The perceived quality of images/videos is then predicted using the trained model [191].

In light of the aforementioned classifications of VQA metrics, we discuss below *traditional VQA metrics*, the *motion-based video integrity evaluation* (MOVIE) index [221], *fusion-based video quality assessment* (FVQA) [222], the *video quality metric* (VQM) [223], the *video quality model for variable frame delay* (VQM_VFD) [224], and *video multi-method assessment fusion* (VMAF) [225], [226], which are applicable for designing wireless video SemCom systems [116]–[119]. We begin with traditional VQA metrics.

A. TRADITIONAL VQA METRICS

Two techniques have traditionally been employed in *video codec* research and development to assess video quality: 1) subjective visual testing, and 2) calculating simple (and computationally inexpensive) objective metrics such as PSNR, or more recently, SSIM [226]. Subjective VQA metrics such as the *mean opinion score* (MOS) can be useful for obtaining human judgment on video quality [225]. However, many

researchers' findings echo the fact that MOS is a time-consuming and (financially) expensive metric that requires specialized expertise [225]. Besides, MOS cannot produce real-time quality ratings across a distribution network [225]. Objective IQA metrics such as MSE, PSNR, and SSIM are usually utilized within codecs to optimize coding decisions and report the final quality of an encoded video [226]. In this respect, PSNR remains the *de facto* standard for codec comparison and standardization, though researchers and practitioners are cognizant that it does not consistently reflect human perception [226].

IQA metrics such as fast MS-SSIM [203] have been adapted for streamed video and commercialized as *SSIMWAVE* [225]. *Video Quality Monitor*, on the other hand, is a commercial tool that measures video quality in relation to format and protocol specifications while requiring no reference [225]. This NR VQA metric can objectively evaluate blockiness, blurriness, and frame rate [225].

We now proceed with our brief discussion of the VQA metric dubbed the MOVIE index [223].

B. THE MOTION-BASED VIDEO INTEGRITY EVALUATION INDEX

The MOVIE index is an FR, HVS model-based VQA metric that is proposed by the authors of [221] and uses optical flow estimation to adaptively guide spatial-temporal filtering by exploiting three-dimensional Gabor filter banks [191],

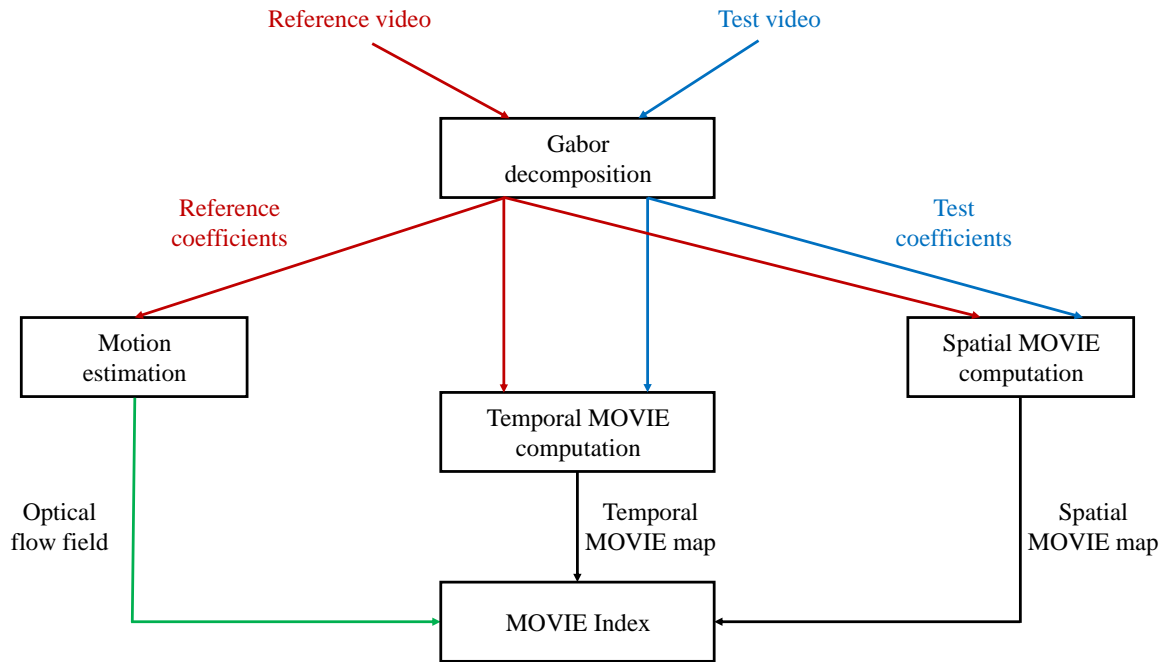


FIGURE 6: Block diagram of the MOVIE index [221, Fig. 1].

[221]. A subset of Gabor filters is selected adaptively at each location based on the direction and speed of motion [191], [221]. To this end, the principal axis of the filter set is oriented in the frequency domain along the direction of motion [191], [221].

As can be seen in Fig. 6, the MOVIE index computation begins with the Gabor decomposition of the reference and test videos. These videos undergo linear decomposition using a Gabor filter family [221]. Following decomposition, three major computations are carried out – as schematized in Fig. 6 – to compute the MOVIE index:

- 1) *Motion estimation* uses the output of the 3D Gabor decomposition of the reference video to determine its *optical flow field*; see Fig. 6.
- 2) *Temporal MOVIE computation* captures temporal degradation in the video following 3D Gabor decomposition by using motion information from the reference video and assesses the quality of the test video along the reference video's motion trajectories [191], [221]. This produces the *temporal MOVIE map*; see Fig. 6.
- 3) *Spatial MOVIE computation* employs the output of the multi-scale Gabor decomposition of the reference and test videos to gauge spatial distortions in the video and produce the *spatial MOVIE map* [191], [221].

The above-computed spatial MOVIE map, temporal MOVIE map, and optical flow field must be combined per Fig. 6 to obtain the VQA metric MOVIE index [191], [221].

We now detail another crucial VQA metric – FVQA [222].

C. FUSION-BASED VIDEO QUALITY ASSESSMENT

FVQA is an FR, fusion-based, and learning-oriented VQA metric that is used to predict the visual quality of a streaming video [222]. To this end, FVQA is composed of two main steps [222] as depicted in Fig. 7:

- First, video sequences are grouped based on their content complexity while minimizing content diversity within each group according to their content complexity [222].
- Second, various existing VQA techniques – particularly, FR VQA methods – are applied to the reference and distorted videos, and their scores are fused to produce the final video quality score [222]. The corresponding fusion coefficients are learned from training video samples that belong to the same group as the videos assessed [222].

Once the two steps have been completed, the FVQA index's performance is assessed by cross validation [222].

Video grouping – by classifying videos of similar content into a group – makes it possible to build a more accurate quality prediction model within each group [222]. To this end and for the purpose of VQA, the authors of [222] opt for considering the spatial and the temporal information defined in the *ITU-T Recommendation P.910* [227] to portray the spatio-temporal characteristics of source videos and apply them to grouped video content. This leads to there being

two groups, named *Group I* and *Group II* [222, Fig. 3]. In addition to this grouping, compression and resizing are two types of distortion that exist in the *MCL-V* [228] video quality database [222]. Consequently, there ends up being four groups, as shown in Fig. 7 below. For each group, the authors of [222] consider the FVQA technique that fuses the scores of five VQA indices by employing a support vector machine (SVM) as a supervised learning algorithm to determine their weight coefficients. After that, a fused decision is obtained for each video group – as can be seen in Fig. 7.

Finally, the authors of [222] corroborate FVQA's superior performance compared to other VQA methods using the *MCL-V* [228] (video) database.

We now move on to our discussion of the nationally and internationally standardized VQA metric known as VQM.

D. VIDEO QUALITY METRIC

VQM is an RR, HVS model-based VQA metric that was developed by the National Telecommunications and Information Administration (NTIA) to deliver an objective measurement of perceived video quality [191], [223]. VQM supports the following quality models depending on the video sequence considered, with various calibration options available prior to feature extraction: 1) the television model, 2) the video conferencing model [191], and 3) the general model. As for the general model, it comprises seven independent parameters [191], [223]:

- four of which (*si_loss*, *hv_loss*, *hv_gain*, and *si_gain*) reflect the features extracted from the spatial gradients of the *Y* luminance component [191], [223];
- two of which (*chroma_spread*, *chroma_extreme*) are based on the features extracted from the vector formed by the two chrominance components (*Cb*, *Cr*) [191], [223]; and
- the last of which (*ct_ati_gain*) is contingent on the product of the features that evaluate contrast and motion, both of which are extracted from the *Y* luminance component [191], [223].

VQM exploits the linear combination of the seven parameters and uses the original video and the processed video as inputs for computation [191], [223]. VQM and its associated calibration techniques were adopted by the American National Standards Institute (ANSI) as a North American Standard in 2003 because it produced the best results for the Video Quality Experts Group (VQEG) Phase II full reference television (FR-TV) test [223]. VQM has also been considered a normative method in two draft recommendations made by the ITU [223].

We now move on to discuss a VQA metric – called VQM_VFD – that was developed by NTIA, inspired by VQM, and appropriately accounts for the perceptual impact of variable frame delay (VFD) [224].

E. VIDEO QUALITY MODEL FOR VARIABLE FRAME DELAY

VQM_VFD is an RR, HVS model-based, and learning-oriented VQA metric [224]. It also employs perceptual features distilled from the spatio-temporal (ST) blocks of a fixed angular extent [224]. These features enable it to track subjective quality over a wide range of image sizes and viewing distances [224]. To this end, VQM_VFD relies on eight objective video quality parameters [224]:

- The *HV_Loss* parameter, which is derived from the one used in VQM, but incorporates four differences [224].
- The *HV_Gain*, *SI_Loss*, and *SI_Gain* parameters, which are similar to the ones used in VQM [224].
- The *TI_Gain* parameter, which is used to compute an ST block's root mean square (rms) motion energy or temporal information [224].
- The *RMSE_Gain* parameter, which is calculated as the rms error between the VFD-matched original clip and the ST blocks in the processed clip [224].
- The *VFD_Par1* parameter, which captures the perceptual impact of repeated or dropped frames and variable video delays [224].
- The *VFD_Par1*·*PSNR_VFD* parameter captures the perceptual attributes of both PSNR and VFD (computed as the product of *VFD_Par1* and *PSNR_VFD*²³) [224].

The eight parameters are mapped to subjective quality estimates by training a two-layer neural network [224]. The authors of [224] corroborated that VQM_VFD can attain 0.9 correlation to subjective quality using subjective datasets at image sizes ranging from Quarter Common Intermediate Format (QCIF) to High Definition TV (HDTV) by testing it on a trained two-layer neural network [224]. VQM_VFD is therefore recognized by many as the state-of-the-art in the field of VQA.

We note that the traditional as well as one or more other VQA metrics discussed above do not work well with Netflix content [226]. To address this limitation, Netflix researchers adopted an ML-based model to design the metric VMAF [225], [226], which seeks to reflect the HVS in terms of video quality [226]. VMAF is similar²⁴ to VQM_VFD in spirit [226] and therefore discussed next.

F. VIDEO MULTI-METHOD ASSESSMENT FUSION

VMAF is an FR, HVS model-based, and learning-oriented VQA metric that predicts subjective quality by merging multiple elementary quality metrics [225], [226]. This metrics merging is inspired by the basic rationale that each constituent elementary metric can have its own strengths and weaknesses w.r.t. the source content's characteristics, type of artifacts, and degree of distortion [226]. VMAF can preserve all the strengths of the individual metrics and produce a more

²³*PSNR_VFD* is the PSNR calculated after the original clip has been VFD-matched to the processed clip [224].

²⁴The main difference between VQM_VFD and VMAF is that the former extracts features at lower levels than the latter does, such as spatial and temporal gradients [226].

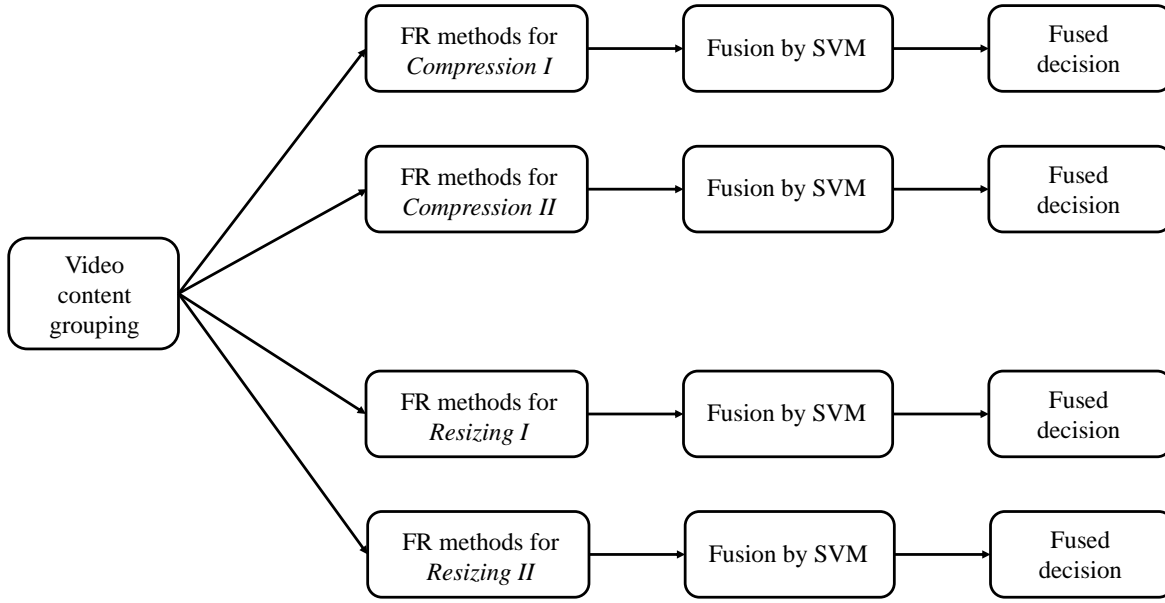


FIGURE 7: Block diagram of the FVQA metric – FR: full-reference; SVM: support vector machine [222, Fig. 2].

accurate final score by combining the elementary metrics using an ML algorithm [226].

A huge sample of MOS scores are used as the ground truth to train a quality estimation model using an ML algorithm known as an SVM regressor in view of the fact that VMAF was formulated by Netflix to correlate strongly with subjective MOS scores [225]. To this end, the current version of VMAF employs three image fidelity metrics – DLM [208], VIF [206], and anti-noise SNR (AN-SNR) – and one temporal signal – mean co-located pixel difference (MCPD) – as elementary metrics that have been fused together by an SVM regression [225], [226]. As for MCPD, the MCPD (the temporal component) of a frame w.r.t. the previous frame is a crucial parameter that is usually lacking metrics that compare only the reference image and the decoded image [225].

The authors of [226] thoroughly assess VMAF's performance and demonstrate – using a Netflix dataset and three popular public datasets – that VMAF outperforms a number of VQA metrics, including VQM_VFD [224]. In addition, the authors of [225] corroborate the following results:

- There exists a strong correlation (0.948) between subjective MOS and the VMAF score computed [225].
- While VMAF is a robust predictor of a collective subjective opinion of video quality, the results reported in [225] confirm that the value computed often (85% of the time) overestimates the subjective quality.
- If a video service provider were to encode a video to attain a VMAF score of approximately 93, the service

provider could then be confident that it is optimally serving the vast majority of its subscribers [225].²⁵

Apart from the afore-discussed VQA metrics, there exist a number of other VQA metrics: *Speed-SSIM* (an FR, signal structure-based metric) [229], *digital video quality* (DVQ) (an FR, HVS model-based metric) [230], *continuous video quality* (CVQ) (an NR, learning-oriented metric) [231], *TetraVQM* (an FR, HVS model-based metric) [232], *V-Factor* (an NR, packet-analysis-based metric) [233], *spatial-temporal assessment of quality* (STAQ) (an RR, HVS model-based metric) [234], and *spatiotemporal MAD* (ST-MAD) (an FR, HVS model-based metric) [235]. These VQA metrics are also useful for the design, analysis, and optimization of 6G systems based on video SemCom.

We now move on to our brief discussion of a 3D human sensing metric dubbed mean per joint position error (MPJPE).

G. MEAN PER JOINT POSITION ERROR

Since MPJPE is a semantic metric that is applicable to 3D human pose estimation, it is defined for a frame f and a skeleton \mathcal{S} as [236, eq. (8)]

$$E_{MPJPE}(f, \mathcal{S}) := \frac{1}{N_S} \sum_{i=1}^{N_S} \|m_{f, \mathcal{S}}^{(f)}(i) - m_{\text{gt}, \mathcal{S}}^{(f)}(i)\|_2, \quad (36)$$

²⁵Content is indistinguishable from the original or includes noticeable (but not annoying) distortion [225].

where N_S denotes the number of joints in skeleton S ; \mathbf{f} is the pose estimator; \mathbf{gt} denotes the ground truth; $m_{\mathbf{f},S}^{(f)}(i)$ is a function that returns the coordinates of the i -th joint of skeleton S at frame f from \mathbf{f} ; and $m_{\mathbf{gt},S}^{(f)}(i)$ is the i -th joint of the ground truth frame f . MPJPE is employed as an evaluation metric in goal-oriented SemCom and a sensing technique proposed by the authors of [237] for a 3D human mesh construction task. The authors of [236] also propose the metrics *mean per joint angle error* (MPJAE) [236, eq. (9)] and *mean per joint localization error* (MPJLE) [236, eq. (10)] to assess the quality of 3D human sensing.

The design, analysis, and optimization of video SemCom systems can be guided by not only the video SemCom metrics that are presented and discussed in Sections VI-A through VI-G above, but also age of information- and value of information-based semantic metrics, which we discuss next.

VII. AGE OF INFORMATION- AND VALUE OF INFORMATION-BASED SEMANTIC METRICS

Semantic metrics that are based on the age of information (AoI) and the value of information (VoI) – also known as *effectiveness-level metrics* [51] – can be used in the design, analysis, and optimization of many classical SemCom systems (in both the wireless and optical domains) [58]. Classical SemCom systems can involve text SemCom [46], [48], [56], [91]–[99]; audio SemCom [45], [100]–[104]; image SemCom [105]–[115]; video SemCom [116]–[119]; multimodal SemCom [120]; or cross-modal SemCom [121]. AoI- and VoI-based semantic metrics also have several applications in goal-oriented SemCom [51]. Consequently, we discuss below *AoI-based semantic metrics*, *VoI-based semantic metrics*, and *combined semantic metrics*. We begin with AoI-based semantic metrics.

A. AOI-BASED SEMANTIC METRICS

Let us start by formally defining AoI²⁶ [238]–[247].

Definition 1 (AoI [238, Definition 2.1.1]): Consider a system involving a communication duo of a source and a destination. Regarding this duo of source and destination, suppose t'_k be the times at which the status updates are received at the destination. The index of the most recently received update at time ξ is given by [238, eq. (2.1)]

$$N(\xi) := \max\{k | t'_k \leq \xi\}. \quad (37)$$

Using (37), the timestamp of the most recently received update is defined as [238, eq. (2.2)]

$$u(\xi) := t_{N(\xi)}. \quad (38)$$

Employing (38) and (37), the AoI of the source s at the destination d is a random process defined as [238, eq. (2.3)]

$$\Delta(t) := t - u(t). \quad (39)$$

²⁶In the literature, the phrases *age of information* (AoI), *status age*, or *plain age* are used interchangeably [238].

In light of (39), the age of the most recently received packet is defined as the difference between the current time and the timestamp of the packet [244]. Using (39), meanwhile, the *time average AoI* (*time average age of a status update*) [238], [244] is defined below.

Definition 2 (Time average AoI [238, Definition 2.1.2]): For an interval of observation $(0, T)$ and $\Delta(t)$ being the AoI per Definition 1, the time average age of a status update system is expressed as [238, eq. (2.7)], [244, eq. (1)]

$$\Delta_T := \frac{1}{T} \int_0^T \Delta(t) dt. \quad (40)$$

Note that the integral in (40) amounts to the area under $\Delta(t)$. Inspired by AoI and time average AoI, the authors of [248] and [249] propose the metric *peak age of information* (PAoI), which is defined below.

Definition 3 (PAoI [249, Definition 3]): Let the RVs T_{k-1} and Y_k be the time in the system for the previously transmitted packet and the interdeparture time (or the time elapsed between service completion of the $(k-1)$ -th packet and service completion of the k -th packet), respectively. The value of age attained immediately before receiving the k -th update is termed peak AoI (*peak age*) and defined as [249, eq. (10)]

$$A_k := T_{k-1} + Y_k. \quad (41)$$

Regarding its advantage of a simpler formulation, PAoI can be used instead of AoI [238]. To this end, PAoI can be employed in applications in which there is interest in knowing/infering the worst-case age or a need to apply a threshold restriction on age [238].

AoI and the aforementioned AoI-related²⁷ metrics have numerous applications in monitoring systems – where only the most recent state generated by the source is of interest to the destination – such as vehicular monitoring systems, industrial sensor networks, unmanned aerial vehicle path planning, and surveillance videos [58], [239]. AoI also has applications in caching and data analytics [238], remote estimation, multi-server scenarios, and multi-hop networks [242]. Despite such broad applicability, AoI has inherent limitations due to the fact that its definition does not consider the current VoI process and its estimate at the monitor [241], [242], [251]. Consequently, age-optimal sampling policies have been found to be sub-optimal²⁸ in several remote estimation applications [241], [252]. Meanwhile, AoI and AoI-related metrics ignore the validity of the recovered data, and in some cases the monitor is concerned with only abnormal and abrupt states at a source [58], [252]. Furthermore, because AoI does not consider the value of current states, some pointless updates are transmitted to the monitor, which

²⁷Another AoI-related metric that also has many applications in status update systems is the metric *relative age of information* (rAoI) [250]. The rAoI metric is defined as the AoI observed at the receiver *relative to the AoI at the transmitter* [250]. Thus, rAoI is also an important semantic metric.

²⁸Should the service times follow a heavy-tail distribution, age-optimal sampling, periodic sampling, and zero-wait sampling policies are hardly optimal [252].

results in resources being wasted [58]. This justifies the need for VoI-based semantic metrics.

B. VOI-BASED SEMANTIC METRICS

Before VoI was introduced to communication systems – especially networked control systems [49], [253] – as a new metric [49], the concept of VoI was well-known in the information analysis community, which defined it as the price a decision maker is willing to pay to take the information into account [58], [254]. In the context of conventional communications, on the other hand, VoI can be viewed as a measure of uncertainty reduction from the source's information set with successful transmission [58], [255]. However, when it comes to communications with specific tasks, VoI needs to be redefined yet again and is employed to assess the relevance of a piece of information to a given communication task – whereas AoI and AoI-related metrics focus on freshness and ignore content [58]. To underscore this VoI-guided design strategy, in the context of a remote temperature control system as discussed in [241], the overarching design goal is to guarantee that the controller reacts promptly to any abnormal increase in temperature compared to the real-time temperature variation of the sources [58]. Accordingly, the data concerning any abnormal temperature increase should be assigned high VoI [58]. In this respect, the image classification task studied in [161] is assessed by the (metric) VoI pertaining to the importance of the extracted features for the accurate classification of the images. Furthermore, VoI can be employed as part of a prioritizing scheduler [51], [256].

Despite being a crucial semantic metric for both SemCom and goal-oriented SemCom, the definition of VoI is largely task-dependent, which makes the derivation of an explicit function for VoI challenging [58]. In this vein, deriving a definite function of VoI is a cumbersome task for complex systems and the research that has been diving into VoI-based metrics is relatively insufficient, to date [58]. Moreover, even though the value of data is usually decided by not only the content but also the communication context, the state-of-the-art VoI calculations do not take into consideration the factors mentioned [58]. On the other hand, factors such as context and content have inspired the following combined semantic metrics.

C. COMBINED SEMANTIC METRICS

The discussed error-based, AoI-based, and VoI-based semantics metrics focus merely on one attribute of the information conveyed by the recovered data [58]. To address this limitation, combined metrics – applicable as combined SemCom metrics – have been proposed. The authors of [243] integrate VoI into AoI-based metrics and propose the *age of information at query* (QAoI); and the authors of [241] and [251] integrate AoI into error-based metrics and put forward *age of incorrect information* (AoII).

The definition of AoI and the afore-discussed AoI-related metrics implicitly assume that new information is used at any time [243]. Nonetheless, the instants – at which information

is collected and used – are not always contingent on a certain query process [243]. To address this issue w.r.t. the fact that discrete-time systems involve queries wherein the monitoring process samples available information [243], the authors of [243] put forward a model that accounts for the discrete-time nature of many monitoring processes and formally define QAoI as follows.

Definition 4 (QAoI [243]): Consider a time-slotted system indexed by $t = 1, 2, \dots$, and let $t_{q,1}, t_{q,2}, \dots$, be the query arrival times at the edge node. For this setting, the long-term expected QAoI is defined as [243, eq. (3)]

$$\tau_{\infty} := \lim_{t \rightarrow \infty} \mathbb{E} \left\{ \sum_{i: t_{q,i} \leq t} \Delta(t_{q,i}) \right\}, \quad (42)$$

where $\Delta(t)$ is the AoI per Definition 1.

QAoI generalizes AoI by sampling $\Delta(t)$ per an arbitrary querying process while considering only the instants at which a query arrives [243]. Accordingly, the QAoI-based scheme is likely to produce fresh updates when a query arrives, though its average AoI can be worse than that of an AoI-based scheme [243]. On the other hand, age-optimal sampling policies have been found to be sub-optimal – as noted above – in various remote estimation applications [241], [252]. For remote estimation applications in the context of SemCom and goal-oriented SemCom, the authors of [241] and [251] put forward the AoII metric, which is defined below.

Definition 5 (AoII [241], [251]): Consider a basic transmitter-receiver system subjected to a process that can possibly change at any time instant t . Let a process X_t be observed by the transmitter at time t and \hat{X}_t be the estimate created by the monitor (receiver). For this setup, the AoII metric is defined as [241]

$$\Delta_{\text{AoII}}(X_t, \hat{X}_t, t) := f(t) \times g(X_t, \hat{X}_t), \quad (43)$$

where $f : [0, \infty) \mapsto [0, \infty)$ is a non-decreasing function whose role is penalizing the system increasingly the more prolonged the mismatch between X_t and \hat{X}_t is and $g : \mathcal{D} \times \mathcal{D} \mapsto [0, \infty)$ – for \mathcal{D} being the state space of X_t – is a function that mirrors the gap between X_t and \hat{X}_t .

As for the function g on the right-hand side (RHS) of (43), one can adopt the standard error-based metrics such as the indicator error (ind) function, the squared error (sq) function, and the threshold error (threshold) function, which are defined in (44a), (44b), and (44c), respectively, as follows [241, eqs. (5)-(7)]:

$$g_{\text{ind}}(X_t, \hat{X}_t) := \mathbb{I}\{X_t \neq \hat{X}_t\} \quad (44a)$$

$$g_{\text{sq}}(X_t, \hat{X}_t) := (X_t - \hat{X}_t)^2, \text{ and} \quad (44b)$$

$$g_{\text{threshold}}(X_t, \hat{X}_t) := \mathbb{I}\{|X_t - \hat{X}_t| \geq c\}, \quad (44c)$$

where $c \in \mathbb{R}^+$ stands for a predefined threshold. Per (44a)-(44c), the functions g_{ind} , g_{sq} , and $g_{\text{threshold}}$ are chosen when any mismatch between X_t and \hat{X}_t (regardless of its value) harms the system's performance, when the system's performance is impacted more significantly the larger the gap

between X_t and \hat{X}_t is, and when the system's performance is unsusceptible to small mismatches between X_t and \hat{X}_t , respectively [241]. Meanwhile, the function f on the RHS of (43) can take the form of the linear time-dissatisfaction (linear) function, the degree m monomial (monomial) function, and the time-threshold dissatisfaction (threshold) function. These functions are defined in (45a), (45b), and (45c), respectively, w.r.t. V_t – the last time instant whereupon $g(X_t, \hat{X}_t)$ was equal to 0 (or the last time instant wherein the monitor had sufficiently accurate information regarding X_t) [241] – as follows [241, eqs. (8)–(10)]:

$$f_{\text{linear}}(t) := t - V_t \quad (45a)$$

$$f_{\text{monomial}}(t) := (t - V_t)^m, \text{ and} \quad (45b)$$

$$f_{\text{threshold}}(t) := \mathbb{I}\{t - V_t \geq c\}, \quad (45c)$$

where $m > 1$ is a positive integer and $c \in \mathbb{R}^+$ is a fixed threshold. According to (45a)–(45c), the functions f_{linear} , f_{monomial} , and $f_{\text{threshold}}$ are chosen when the system's impact due to the mismatch between X_t and \hat{X}_t grows steadily with time, when the system's performance deteriorates quickly as a result of the mismatch between X_t and \hat{X}_t , and when the system's performance is resistant to the mismatch between X_t and \hat{X}_t for a certain time duration c , respectively [241].

At last, the existing AoI- and VoI-based metrics that are applicable to both SemCom and goal-oriented SemCom are summarized along with their pros and cons in Table 7.

Combined semantic metrics such as QAOI and AOII are useful in the design, analysis, and optimization of communications systems based on (goal-oriented) SemCom. Apart from inspiring the design, analysis, and optimization of several systems based on (goal-oriented) SemCom, AoI- and VoI-based semantic metrics have also inspired resource allocation-oriented optimization across multiple classical SemCom networks and semantic-aware networks. To optimize SemCom for semantic-aware networking, a system designer needs resource allocation semantic metrics, which are discussed below.

VIII. RESOURCE ALLOCATION SEMANTIC METRICS

The optimization of usually scarce resources – for optimality and efficiency across one or more networks – across wireless or optical SemCom networks is one of the key problems facing classical SemCom systems. Resource allocation semantic metrics are therefore crucial to optimize several types of classical SemCom systems – in either the wireless or optical domain – such as text SemCom [46], [48], [56], [91]–[99]; audio SemCom [45], [100]–[104]; image SemCom [105]–[115]; video SemCom [116]–[119]; multimodal SemCom [120]; and cross-modal SemCom [121]. The following resource allocation semantic metrics are largely relevant to optimize the mentioned SemCom systems in either a wireless or an optical network setting: the *metric of semantic similarity* (MSS), *semantic transmission rate* (S-R), *semantic spectral efficiency* (S-SE), *quality-of-experience* (QoE), and *system*

throughput in message (STM). We present these semantic metrics below, beginning with MSS.

A. METRIC OF SEMANTIC SIMILARITY

The authors of [257] and [258] define MSS for a semantic-driven network transmitting semantic information on its downlink using orthogonal frequency division multiple access (OFDMA) technology over Q downlink orthogonal RBs. W.r.t. the Q RBs, let $\alpha_i := [\alpha_{i,1}, \dots, \alpha_{i,q}, \dots, \alpha_{i,Q}]$ be the resource allocation vector of user i , \mathcal{G}'_i be the partial semantic information (modeled by a KG) that the base station (BS) transmits to user i , and $L'_i(\alpha_i, \mathcal{G}'_i)$ be the recovered text. For this setting, the MSS of $L'_i(\alpha_i, \mathcal{G}'_i)$ is defined as follows [258, eq. (11)]:

$$E_i(\alpha_i, \mathcal{G}'_i) := \xi_i \frac{A_i(\alpha_i, \mathcal{G}'_i) R_i(\alpha_i, \mathcal{G}'_i)}{\varphi A_i(\alpha_i, \mathcal{G}'_i) + (1 - \varphi) R_i(\alpha_i, \mathcal{G}'_i)}, \quad (46)$$

where ξ_i is a penalty (regarding a short text) that is defined in [258, eq. (12)], $\varphi \in (0, 1)$ is the weight parameter employed to adjust the semantic accuracy $A_i(\alpha_i, \mathcal{G}'_i)$ and the semantic completeness $R_i(\alpha_i, \mathcal{G}'_i)$ of $L'_i(\alpha_i, \mathcal{G}'_i)$, which are defined in [258, eq. (9)] and [258, eq. (10)], respectively.

We now proceed to discuss another resource allocation semantic metric – named S-R.

B. SEMANTIC TRANSMISSION RATE

S-R is defined as the amount of semantic information effectively transmitted per second and measured in *suts/s* [169]. For a text SemCom system, the S-R $\Gamma_{n,m}$ of the n -th user over the m -th channel is defined as [169, eq. (4)]

$$\Gamma_{n,m} := \frac{WI}{k_n L} \xi_{n,m}, \quad (47)$$

where W , I , and $k_n L$ are the channel bandwidth, the amount of semantic information, and the average number of semantic symbols at the n -th user, respectively, and $\xi_{n,m}$ is the semantic similarity – per [46, eq. (13)] – of the n -th user over the m -th channel [169].

We now continue with our discussion of another resource allocation semantic metric – termed S-SE.

C. SEMANTIC SPECTRAL EFFICIENCY

S-SE is defined as the rate at which semantic information can be successfully transmitted over a unit of bandwidth and is measured in *suts/s/Hz* [169]. For a text SemCom system, the S-SE of the n -th user over the m -th channel is defined via (47) as [169, eq. (5)]

$$\Phi := \frac{\Gamma_{n,m}}{W} = \frac{I}{k_n L} \xi_{n,m}. \quad (48)$$

We now move on to discuss another resource allocation semantic metric – dubbed QoE.

D. QUALITY-OF-EXPERIENCE

In the context of semantic-aware resource allocation in a multi-cell multi-task network, the QoE of the q -th user group

Metrics	Pros	Cons
AoI-based semantic metrics	1) AoI can reflect the freshness of information [51]. 2) PAoI can reflect the freshness of information [51]. 3) With the advantage of a simpler formulation, PAoI can be used instead of AoI [238]. 4) PAoI can be employed in applications where there is interest in the worst case age or the need to apply a threshold restriction on age [238].	1) AoI may misjudge the value of information [51]. 2) PAoI may misconstrue the value of information [51]. 3) The definition of AoI does not consider the current value of the information process and its estimate at the monitor [241], [242], [251]. 4) AoI and AoI-related metrics ignore the validity of the recovered data and, in some cases, the monitor is only concerned with the abnormal and abrupt states at the source [58], [252]. 5) Since AoI does not consider the value of current states, some pointless updates are transmitted to the monitor – yielding resource wastage [58].
VoI-based semantic metrics	1) These semantic metrics capture the value of information [51]. 2) VoI is a crucial semantic metric for design, analysis, and optimization of both SemCom and goal-oriented SemCom systems.	1) For some complicated systems, it is not definitely easy to design the VoI function [51]. 2) As the definition of VoI is largely task-dependent, the derivation of an explicit function for VoI is certainly challenging [58]. 3) Although the value of data is usually decided not only by the content but also by the communication context, the state-of-the-art VoI calculations have not taken into consideration these relevant factors [58].
Combined semantic metrics	1) Combined semantic metrics rightfully consider crucial factors such as context and content. 2) AoII blends the age and value of information to reflect the significance of updates [51].	1) Concerning AoII, the optimal estimation of the penalty function ought to be further investigated [51]. 2) The discussed combined semantic metrics (i.e., QAOI and AoII) can be computationally demanding.

TABLE 7: AoI- and VoI-Based semantic metrics for image quality assessment along with their pros and cons – AoI: age of information; QAOI: the age of information at query; PAoI: peak age of information; AoII: age of incorrect information; VoI: value of information.

in the b -th cell – which is denoted by QoE_q^b – is defined as [259, eq. (8)]

$$QoE_q^b := \sum_{u \in \mathcal{G}_q^b} w_u G_u^R + (1 - w_u) G_u^A \quad (49a)$$

$$= \sum_{u \in \mathcal{G}_q^b} \frac{w_u}{1 + e^{\beta_u(\varphi_u^{\text{req}} - \varphi_u)}} + \frac{(1 - w_u)}{1 + e^{\lambda_u(\xi_u^{\text{req}} - \xi_u^b)}}, \quad (49b)$$

where u denotes the user index, \mathcal{G}_q^b is the user group of the q -th user in the b -th cell, w_u and $1 - w_u$ are the weights of the semantic rate and the semantic accuracy of the u -th user, respectively, G_u^R and G_u^A are the scores of the semantic rate and the semantic accuracy of the u -th user, respectively, β_u and λ_u denote the growth rates of G_u^R and G_u^A , respectively, and φ_u^{req} and ξ_u^{req} symbolize the minimum semantic rate and semantic accuracy required to attain 50% of the scores, respectively [259].

We now continue to our discussion of another resource allocation semantic metric – termed STM.

E. SYSTEM THROUGHPUT IN MESSAGE

STM represents network performance from a semantic perspective and is proposed by the authors of [260] in the broader context of intelligent SemCom (iSemCom) and an iSemCom-enabled heterogeneous network (iSemCom-HetNet). For an iSemCom-HetNet, let $\mathcal{B} := \{BS_1, BS_2, \dots, BS_L\}$ be a set of BSs for BS_j – the j -th BS in a network served by L BSs, $\mathcal{U} := \{MU_1, MU_2, \dots, MU_M\}$ be the set of all mobile users

(MUs) for MU_i – the i -th MU, and $x_{ij} \in \{0, 1\}$ be an association indicator, where $x_{ij} = 1$ if MU_i is associated with BS_j , and $x_{ij} = 0$ otherwise. For this setting, the STM – denoted by T_M – is defined as [260, eq. (7)]

$$T_M := \sum_{i \in \mathcal{U}} \sum_{j \in \mathcal{B}} x_{ij} S_i(b_{ij}), \quad (50)$$

where $S_i(\cdot)$ represents a universal bit-to-message transformation function pertaining to MU_i under a given channel condition [260], and b_{ij} stands for the downlink bit rate of MU_i (served by BS_j with n_{ij} bandwidth) defined as follows [260, eq. (3)]:

$$b_{ij} := n_{ij} \log_2(1 + \gamma_{ij}), \quad (51)$$

where γ_{ij} is the signal-to-interference-plus-noise ratio (SINR) experienced by MU_i from BS_j [260].

While the semantic metrics discussed above in Sections VIII-A through VIII-E are chiefly applicable for resource allocation optimization in many types of SemCom systems, the design, analysis, and optimization of several types of SemCom systems have been inspired by the generic semantic metrics of SemCom, which we discuss below.

IX. GENERIC SEMANTIC METRICS OF SEMCOM

The generic semantic metrics of SemCom that we discuss in this section are metrics that are applicable to the design, analysis, and optimization of a wide variety of classical SemCom systems – in either the wireless or optical domain – including text SemCom [46], [48], [56], [91]–[99];

audio SemCom [45], [100]–[104]; image SemCom [105]–[115]; video SemCom [116]–[119]; multimodal SemCom [120]; and cross-modal SemCom [121]. We present below the following generic semantic metrics of SemCom that have inspired the materialization of the mentioned SemCom systems: the *general quality index of semantic service*, *triplet drop probability* (TDP), *semantic mutual information* (SMI), the *semantic impact*, the *communication symmetry index*, and *reasoning capacity*. We start with the general quality index of semantic service.

A. GENERAL QUALITY INDEX OF SEMANTIC SERVICE

The authors of [261] propose the general quality index of semantic service which is defined as [261, eq. (1)]

$$SS := \frac{ST(\hat{S})}{ST(S)}, \quad (52)$$

where the function $ST(\cdot)$ captures how well the source performs a given task, and S and \hat{S} denote the unprocessed information at the transmitter and the information recovered through semantics at the receiver, respectively. For the definition in (52), the authors of [261] suggest to convert the output of $ST(\cdot)$ to a range $[0, 1]$ using *sigmoid* and other similar functions.

We now move on to our discussion of another generic semantic metric of SemCom – dubbed TDP.

B. TRIPLET DROP PROBABILITY

The TDP P_k is an important semantic metric for both SemCom and goal-oriented SemCom [262] and is defined as [262, eq. (17)]

$$P_k := \sum_{j=D_E+1}^{D_T} E_k^j (1 - E_k)^{D_T-j}, \quad (53)$$

where D_T denotes the bit length, D_E represents the maximum number of bits in error, and E_k is the k -th user's average bit error rate (BER) and defined as [262, eq. (15)], [263, eq. (13)]

$$E_k := \int_0^\infty \frac{\Gamma(\lambda_2, \lambda_1 \gamma)}{2\Gamma(\lambda_2)} f_{\gamma_k}(\gamma) d\gamma, \quad (54)$$

where (54) is valid under a variety of modulation formats, $\frac{\Gamma(\lambda_2, \lambda_1 \gamma)}{2\Gamma(\lambda_2)}$ equates to the conditional bit error probability, λ_1 and λ_2 are modulation-specific parameters that take different values under different modulation schemes, γ_k is the SINR of the k -th user, and $f_{\gamma_k}(\cdot)$ symbolizes the probability distribution function (PDF) of γ_k .

We now discuss another generic semantic metric of SemCom – named SMI.

C. SEMANTIC MUTUAL INFORMATION

SMI is proposed by the authors of [264] and aims to quantify the semantic-level distortion present during the compression process for specific downstream AI task. When a downstream AI task processes the pixel-level information of the input

images, the feature-level information and then semantic-level information can be acquired [264]. Semantic-level information is the meaning that is eventually understood by the downstream AI task and contained in perceptual results [264].

SMI quantifies the mutual information (MI) of all the perceptual results, which comprise all the semantic-level information of the downstream AI task [264]. To define this metric formally (using the notation of [264]), let \mathbf{y}_b be the perceptual results of the original image \mathbf{x}_b and \mathbf{y}'_b be the perceptual results of the compressed image \mathbf{x}'_b . Estimating the SMI of the perceptual results \mathbf{y}_b and \mathbf{y}'_b is challenging because the *entropy* of the original image dataset is mathematically intractable [264]. To overcome this intractability and estimate their respective SMI, the authors of [264] exploit contrastive log-ratio upper bound (CLUB) [265]²⁹ – an MI estimator – due to its ability to produce reliable estimates. To this end, the authors of [264] employ \mathbf{y}_b and \mathbf{y}'_b as inputs to train an SMI estimation network from which they can obtain the mean and variance of \mathbf{y}'_b [264]. Using this computed mean and variance values, the authors of [264] compute the conditional PDF $p(\mathbf{y}'_b|\mathbf{y}_b)$. With the $p(\mathbf{y}'_b|\mathbf{y}_b)$ computed, the SMI is defined – through the MI CLUB [265, eq. (10)]; see also (55) – as [264, eq. (11)]

$$I_{\text{CLUB}}(\mathbf{y}_b; \mathbf{y}'_b) := \mathbb{E}_{p(\mathbf{y}_b, \mathbf{y}'_b)} \{\log p(\mathbf{y}'_b|\mathbf{y}_b)\} - \mathbb{E}_{p(\mathbf{y}_b)} \mathbb{E}_{p(\mathbf{y}'_b)} \{\log p(\mathbf{y}'_b|\mathbf{y}_b)\}, \quad (57)$$

where $p(\mathbf{y}_b, \mathbf{y}'_b)$ is a joint PDF. Underscoring its advantage as defined in (57), SMI can reflect/capture the semantic-level distortion [51]. However, SMI needs to be estimated by an additional module [51].

The previously discussed generic SemCom metrics do not necessarily take into account the fact that the apprentice can leverage reasoning and causality to generate the originally transmitted message [53]. In such a scenario, which is at the heart of reasoning-driven SemCom systems [53], the overall situation can change drastically, and there is a need for a suite of novel and generic SemCom metrics that can qualify the level of symmetry between a teacher and an apprentice [53]. Such metrics are proposed by the authors of [53] and named as the *semantic impact*, the *communication symmetry index*, and *reasoning capacity*. These metrics are presented below, beginning with semantic impact.

²⁹When the conditional PDF $p(\mathbf{y}|\mathbf{x})$ is known, the MI CLUB is defined for two random multivariate RVs \mathbf{x} and \mathbf{y} as [265, eq. (10)]:

$$I_{\text{CLUB}}(\mathbf{x}; \mathbf{y}) := \mathbb{E}_{p(\mathbf{x}, \mathbf{y})} \{\log p(\mathbf{y}|\mathbf{x})\} - \mathbb{E}_{p(\mathbf{x})} \mathbb{E}_{p(\mathbf{y})} \{\log p(\mathbf{y}|\mathbf{x})\}, \quad (55)$$

where $p(\mathbf{x}, \mathbf{y})$ is the joint PDF. The simplification of (55) leads to a theorem [265, Theorem 3.1] on an important inequality that is given by [265, eq. (12)]

$$I(\mathbf{x}; \mathbf{y}) \leq I_{\text{CLUB}}(\mathbf{x}; \mathbf{y}), \quad (56)$$

where $I(\mathbf{x}; \mathbf{y})$ is the MI and equality is attained if and only if (iff) \mathbf{x} and \mathbf{y} are independent RVs [265]. Hence, $I_{\text{CLUB}}(\mathbf{x}; \mathbf{y})$ is an upper bound of $I(\mathbf{x}; \mathbf{y})$.

D. SEMANTIC IMPACT

If we consider a particular semantic representation³⁰ Z_i and its semantic content element Y_i , the significance of Z_i is equivalent to the number of data packets one would have needed to convey the exact same message [53]. To this end, semantic impact is formally defined as follows.

Definition 6 (Semantic impact [53, Definition 12]): Let Z_i be a particular semantic representation and its semantic content element be Y_i . The semantic impact ι_τ generated by Z_i during a time duration τ is defined as the number of packets that would have been needed to be transmitted to regenerate Y_i .

Per Definition 6, semantic impact is part of another generic metric of SemCom dubbed the communication symmetry index [53], which is presented below.

E. COMMUNICATION SYMMETRY INDEX

The communication symmetry index is proposed by the authors of [53] and formally defined below.

Proposition 1 (Communication symmetry index [53, Proposition 2]): For a transmission session τ , the communication symmetry index $\eta_{b,d,\tau}$ between a teacher b and an apprentice d is given by [53, eq. (13)]

$$\eta_{b,d,\tau} := \frac{\zeta_{d,\tau}}{\nu_{b,\tau}} \times \iota_{\tau,Y_i}, \quad (58)$$

where $\zeta_{d,\tau}$ is the number of query packets demanded by the apprentice to reason over the transmitted message, $\nu_{b,\tau}$ is the number of raw data packets transmitted by the teacher to accompany the transmitted semantic representation, and ι_{τ,Y_i} is the semantic impact w.r.t. the generation of the semantic content element Y_i . Note that one can find $\zeta_{d,\tau}$ by applying the concept of semantic impact on the employed representation provided that the queries are communicated via a semantic representation to the teacher.

As defined in Proposition 1, the communication symmetry index makes it possible to characterize the reasoning state of the teacher and apprentice as well as the equilibrium they attain [53]. Accordingly, the following five settings are in order.

- If $\eta_{b,d,\tau} \leq 1$ and $\iota_\tau > 1$: in this setting, the apprentice has little to no knowledge base [53]. Thus, this SemCom setting asymptotically mirrors the classical communication scenario, wherein most of the data is sent in its raw form to complement the semantic representation [53].
- If $\eta_{b,d,\tau} \rightarrow \iota_\tau$ and $\iota_\tau > 1$: in this setting, the apprentice has considerable knowledge/reasoning faculties, and the teacher complements their transmitted information with raw data [53]. Nonetheless, the apprentice intervenes regularly to understand the data's causal structure (and progressively counts on semantic representations) [53].
- If $\eta_{b,d,\tau} = \iota_\tau$ and $\iota_\tau > 1$: in this setting, the apprentice intervenes in the same way as current receivers transmit

an acknowledgment, and the teacher depends on the transmission of raw data only to describe the *unlearnable* part of the data [53].

- If $\eta_{b,d,\tau} > \iota_\tau$ and $\iota_\tau > 1$: in this setting, the datastream is mostly learnable (i.e., not *memorizable*) [53]. Consequently, the teacher depends mainly on semantic representations, and the apprentice actively intervenes to produce the transmitted message from the set of received semantic representations [53].
- If $\eta_{b,d,\tau} > \iota_\tau$ and $\iota_\tau \leq 1$: in this challenging setting, the apprentice demands a greater number of queries than the number of raw data transmissions the teacher sends [53]. As a result, the teacher is unable to extract a fitting semantic representation to be communicated to the apprentice [53].

It is worth mentioning that unless a defect in reasoning is observed, $\eta_{b,d,\tau}$ does not go considerably below 1 [53].

Should the receiver become an apprentice that counts on learning the data content rather than simply recovering it in a bit-by-bit fashion, the apprentice's understanding and impact on the reconstruction process are fittingly KPIs of a reliable communication link (between teacher and apprentice) [53]. This leads us to the generic metric of SemCom dubbed reasoning capacity, which we explain below.

F. REASONING CAPACITY

The following factors are essential to characterize the apprentice's understanding: 1) reasoning as evaluated by the number of queries made by the apprentice; 2) efficiency and minimalism (as assessed by the number of raw messages sent to supplement the semantic representation), as well as the semantic representation's impact [53]. To this end, the formal definition of reasoning capacity is provided below.

Proposition 2 (Reasoning capacity [53, Proposition 3]): The reasoning capacity between a teacher b and an apprentice d is expressed as [53, eq. (15)]

$$C_R := \Omega \log_2(1 + \eta_{b,d}), \quad (59)$$

where Ω is the maximum computing capability of the server deployed to represent/generate the semantic representation and $\eta_{b,d}$ is the communication symmetry index per second.

Reasoning capacity is universal in the sense that it is independent of the type of semantic representation employed [53]. When the datastream includes both a learnable component and a memorizable component, the total achievable capacity C_T can be expressed as [53, eq. (16)]

$$C_T := C_C + C_R = W \log_2(1 + \gamma) + \Omega \log_2(1 + \eta_{b,d}), \quad (60)$$

where C_C and C_R are the Shannon capacity and reasoning capacity, respectively, W is the bandwidth, and γ is the SINR [53].

The generic semantic metrics presented above in Sections IX-A through IX-F are important semantic metrics for the design, analysis, and optimization of classical (wireless and optical) SemCom systems. In addition to classical SemCom

³⁰According to the authors of [53], semantic content embodies the "meaningful" part of the data and the semantic representation is the "minimal way to represent this meaning."

systems, there also exist quantum SemCom systems whose design, analysis, and optimization are informed (or guided) by the following semantic metrics of quantum SemCom.

X. SEMANTIC METRICS OF QUANTUM SEMCOM

The authors of [69] propose to assess the performance of their quantum SemCom system (named QSC) using the metric *fidelity* [64], [266], [267], which is widely known in the quantum research community. Fidelity is a measure of the closeness of two quantum states [267]. Hence, it is a useful semantic metric for the design, analysis, and optimization of quantum SemCom systems. We therefore discuss below three of its well-known variations, namely *pure-state fidelity*, *expected fidelity*, and *Uhlmann fidelity* [267, Ch. 9], beginning with pure-state fidelity.

A. PURE-STATE FIDELITY

Pure-state fidelity is formally defined as follows.

Definition 7 (Pure-state fidelity [267, Definition 9.2.1]): Let \mathcal{H} be a Hilbert space and $|\psi\rangle, |\phi\rangle \in \mathcal{H}$ be pure states. The pure state fidelity is the squared overlap of $|\psi\rangle$ and $|\phi\rangle$ defined as [267, eq. (9.85)]

$$F(\psi, \phi) := |\langle\psi|\phi\rangle|^2. \quad (61)$$

As defined in (61), $F(\psi, \phi)$ (i.e., pure-state fidelity) can be operationally interpreted as the probability that the output state $|\phi\rangle$ would pass a test – carried out by someone who knows the input state – for being the same as the input state $|\psi\rangle$ [267]. As for the commutativity of the inner product, it follows directly from (61) that $F(\psi, \phi) = F(\phi, \psi)$. This metric fulfills the following bounds [267, eq. (9.86)]:

$$0 \leq F(\psi, \phi) \leq 1, \quad (62)$$

where $F(\psi, \phi) = 0$ iff the two corresponding states are orthogonal to each other [267] and $F(\psi, \phi) = 1$ iff the two respective states are the same. Regarding the latter case being contradictory to a distance measure that should be equal to zero when the two states are equal, the fidelity measure is not a distance measure in the strict mathematical sense [267]. This brings us to our discussion on a quantum SemCom metric that measures the closeness between a pure state and a mixed state – named expected fidelity.

B. EXPECTED FIDELITY

Generally, a quantum information-processing protocol is noisy and can map the pure input state $|\psi\rangle$ to a mixed state ρ [267]. These two states' closeness can be quantified by the metric expected fidelity [267], which is defined as follows.

Definition 8 (Expected fidelity [267, Definition 9.2.2]): Let $|\psi\rangle \in \mathcal{H}$ be a pure state and $\rho \in \mathcal{D}(\mathcal{H})$ be a mixed state. The expected fidelity $F(\psi, \rho)$ between these two states is given by [267, eq. (9.89)]

$$F(\psi, \rho) := \langle\psi|\rho|\psi\rangle. \quad (63)$$

The definition in (63) follows directly from decomposing ρ per the spectral decomposition³¹ $\rho = \sum_x p_X(x) |\phi_x\rangle\langle\phi_x|$ and applying expectation w.r.t. X to (61). In contrast to (61), (63) characterizes fidelity when the input state is pure and the output state is mixed [267]. Note that $F(\psi, \rho)$ per (63) is a generalization of the pure-state fidelity definition given in (61) and obeys the same bounds [267, eq. (9.95)]:

$$0 \leq F(\psi, \rho) \leq 1, \quad (64)$$

where $F(\psi, \rho) = 1$ iff the mixed state ρ is equal to $|\psi\rangle\langle\psi|$ and $F(\psi, \rho) = 0$ iff the support of ρ is orthogonal to $|\psi\rangle\langle\psi|$ [267]. This measure, however, cannot be applied when both states are mixed. The closeness between two mixed states can be quantified using the metric Uhlmann fidelity, which we discuss below.

C. UHLMANN FIDELITY

To formalize Uhlmann fidelity, we borrow an idea from pure-state fidelity (per Definition 7) to determine the fidelity between two mixed states ρ_A and σ_A that represent different states of a quantum system A [267]. To do so, let $|\phi^\rho\rangle_{RA}$ and $|\phi^\sigma\rangle_{RA}$ stand for certain *purifications* of the mixed states ρ_A and σ_A , respectively, to some reference system R [267].³² The Uhlmann fidelity $F(\rho_A, \sigma_A)$ between ρ_A and σ_A (mixed states) can now be defined as the maximum overlap between their respective purifications and given by [267, eq. (9.97)]

$$F(\rho_A, \sigma_A) := \max_{|\phi^\rho\rangle_{RA}, |\phi^\sigma\rangle_{RA}} |\langle\phi^\rho|\phi^\sigma\rangle_{RA}|^2, \quad (65)$$

where the maximization is w.r.t. all purifications $|\phi^\rho\rangle_{RA}$ and $|\phi^\sigma\rangle_{RA}$ of the corresponding mixed states ρ_A and σ_A [267]. The RHS of (65) can instead be maximized over *unitaries* pursuant to the theorem that all purifications are equivalent up to unitaries on the reference system [267]. This leads us to the following formal definition of Uhlmann fidelity.

Definition 9 (Uhlmann fidelity [267, Definition 9.2.3]): For two mixed states ρ_A and σ_A , the Uhlmann fidelity $F(\rho_A, \sigma_A)$ is the maximum overlap between their respective purifications and is given by [267, eq. (9.100)]

$$F(\rho_A, \sigma_A) := \max_U |\langle\phi^\rho|_{RA} U_R \otimes I_A |\phi^\sigma\rangle_{RA}|^2, \quad (66)$$

where the maximization is w.r.t. all unitaries U acting on the purification system R [267].

The Uhlmann fidelity definition in (66) then leads us to the following important theorem.

Theorem 1 (Uhlmann's Theorem [267, Theorem 9.2.1]): The underneath two expressions for fidelity are equal [267, eq. (9.102)]:

$$F(\rho_A, \sigma_A) = \max_U |\langle\phi^\rho|_{RA} U_R \otimes I_A |\phi^\sigma\rangle_{RA}|^2 = \|\sqrt{\rho_A}\sqrt{\sigma_A}\|_1^2. \quad (67)$$

³¹In this case, $p_X(x) = \mathbb{P}(X = x)$ is the *probability mass function* (PMF) of a discrete RV X .

³²For this specific scenario, it is assumed that the reference system has the same dimensions as system A [267].

For Theorem 1 and (67), it is worth remarking that Uhlmann fidelity generalizes both the pure-state fidelity defined in (61) and the expected fidelity defined in (63) [267]. The reader is referred to [267, Ch. 9] for many more important properties of fidelity. The reader is also referred to [268] for definitions and computations of fidelity pertaining to high-dimensional quantum states such as qudits.

The aforementioned semantic metrics have inspired the design, analysis, and optimization of quantum SemCom networks as well as various quantum systems that are based on quantum SemCom. Quantum SemCom like any other type of communication system – such as wireless SemCom and optical SemCom – is not an end but a means to achieve specific goals [159]. This goal-centric standpoint rationalizes the need for goal-oriented wireless SemCom techniques and hence the following semantic metrics of goal-oriented wireless SemCom.

XI. SEMANTIC METRICS OF GOAL-ORIENTED WIRELESS SEMCOM

To capture the role of data in achieving the goal of communication, a number of semantic metrics have been developed to date for goal-oriented wireless SemCom. These goal-oriented semantic metrics are chiefly crucial for the design, analysis, and optimization of goal-oriented wireless SemCom systems. Accordingly, we discuss below the following semantic metrics of goal-oriented wireless SemCom³³: the τ metric, the *real-time reconstruction error*, the *cost of actuation error*, *multiple object detection accuracy* (MODA), *value of information* (VoI), *mean per joint position error* (MPJPE), *triplet drop probability* (TDP), *age of incorrect information* (AoII), *semantic impact*, *communication symmetry index*, and *reasoning capacity*. We commence our discussion with the τ metric.

A. THE τ METRIC

The authors of [167] introduce τ as a generic goal-oriented wireless SemCom metric that can quantify the effectiveness of multiple transmission tasks and equates to [167, eq. (14)], [54, eq. (17)]

$$\tau := \frac{1 - \psi(s, \hat{s})}{\mathbb{E}\{n\}}, \quad (68)$$

where $\mathbb{E}\{n\}$ designates the average number of symbols per transmitted message and $\psi(s, \hat{s})$ quantifies the semantic error between s and \hat{s} , which can take different context-dependent forms (e.g., BLEU score, MSE, or CE) [167].

We now proceed to discuss another goal-oriented wireless SemCom metric – named the *real-time reconstruction error*.

B. REAL-TIME RECONSTRUCTION ERROR

Real-time reconstruction error is proposed by the authors of [159] and evaluates the divergence – in real-time as time evolves – of values between the original source and the

reconstructed source [159]. This error specifically reflects the discrepancy in real-time data exchange [51].

To formally define real-time reconstruction error and time-averaged real-time reconstruction error, let the original source and the reconstructed source – at time-slot t – be denoted by X_t and \hat{X}_t , respectively. Using these parameters, real-time reconstruction error is given by [269]

$$E_t := \mathbb{I}\{X_t \neq \hat{X}_t\}, \quad (69)$$

where E_t has a value of 0 or 1 for a two-state discrete-time Markov chain (DTMC). Accordingly, the system can be in either an erroneous state ($E_t = 1$) or a synced state ($E_t = 0$), and the time-averaged real-time reconstruction error is given by [269, eq. (1)]

$$\bar{E} := \lim_{T \rightarrow \infty} \frac{\sum_{t=1}^T E_t}{T}. \quad (70)$$

In many analytical and numerical studies, the evolution of the state of the system (i.e., E_t) is described by a Markov Chain; see [269, Fig. 2]. This brings us to another relevant goal-oriented wireless SemCom metric known as the *cost of actuation error*.

C. COST OF ACTUATION ERROR

The cost of actuation error was put forward by the authors of [159] and captures the significance of the error at the actuation point considering the fact that some errors may be non-commutative and have a higher impact than others [159]. There are three possible cases in which this type of error occurs in a time-slotted system [159]:

- *The original source is in the first state, but the reconstructed source believes that it is in the second state:* in this case, the cost of actuation error is low [159].
- *The original source is in the second state, but the reconstructed source believes that it is in the first state:* this pertains to a scenario in which the penalty/loss from taking a wrong action upon a misconceived system's state is high [159]. Accordingly, in this case, the cost of actuation error is presumed to be relatively high [159].
- *Both the original source and the reconstructed source are in the same (first/second) state:* in this case, the states match and there is no cost of actuation error [159].

In the itemized cases, some errors can have larger impact than others [269]. To quantify the average impact, let $C_{i,j}$ be the cost – at time-slot t – of being in state i at the original source and in state $j \neq i$ at the reconstructed source (i.e., $E_t = 1$) [269]. It is assumed that $C_{i,j}$ doesn't change over time and that $C_{0,1} \neq C_{1,0}$ [269]. The authors of [269], on the other hand, calculate the average cost of actuation error using a two-dimensional Markov chain that can characterize the joint status of the system for the current state at the original source whether or not the reconstructed source is synced. The average cost of actuation error is therefore given by [269, eq. (6)]

$$\bar{C}_A := \pi_{(0,1)} C_{0,1} + \pi_{(1,0)} C_{1,0}, \quad (71)$$

³³The authors of [51] present some metrics of goal-oriented SemCom under the heading “effectiveness-level metrics.”

where $\pi_{(0,1)}$ and $\pi_{(1,0)}$ are obtained from the stationary distribution of the two-dimensional DTMC [269]. This formulation offers a general view of the system, which can be deployed to derive optimal online policies using Markov decision processes or deep reinforcement learning [269].

We now move on to discuss another goal-oriented wireless SemCom metric – termed MODA.

D. MULTIPLE OBJECT DETECTION ACCURACY

The authors of [270] assess the performance of their proposed goal-oriented wireless SemCom scheme by employing the metric MODA [271]. It is defined w.r.t. each frame t as [271, eq. (7)]

$$MODA(t) := 1 - \frac{c_m(m_t) + c_f(fp_t)}{N_G^{(t)}}, \quad (72)$$

where m_t and fp_t are the number of misses and the number of false positives, respectively, for every frame t , $c_m(\cdot)$ and $c_f(\cdot)$ are the cost functions of the missed detects and false positives, respectively, and $N_G^{(t)}$ denotes the number of ground truth objects in the t -th frame [271]. Normalized MODA (N-MODA) is another important goal-oriented wireless SemCom metric and is defined in [271, eq. (8)].

We now move on to discuss another goal-oriented wireless SemCom metric – called VoI.

E. VALUE OF INFORMATION

VoI, as it is defined in Section VII-B, specifically gauges the advantage of transmitting data packets for a communication goal, and considers not only the packets' content, but also their respective cost of transmission [49], [58]. Accordingly, the VoI metric can be quantified as the difference between the benefit a given sample affords and how much it costs to transmit it [49]. VoI-based transmission policies, thus, have the potential to considerably reduce data traffic to achieve a given level of control performance, especially in networked control systems [49], [253]. Apart from in those systems, VoI is of more interest than accuracy in resource-constrained communications, where the relevance of data packets awaiting transmission is evaluated w.r.t. the system objective [58]. VoI-based metrics are a better fit for goal-oriented wireless SemCom systems than error-based metrics [58].

Apart from VoI, MODA, the cost of actuation error, real-time reconstruction error, and the τ metric, which are highlighted above in Sections XI-A through XI-E, there are also generic SemCom metrics such as MPJPE, TDP, AoII, semantic impact, communication symmetry index, and reasoning capacity that are applicable to the design, analysis, and optimization of goal-oriented wireless SemCom systems. These metrics and their applications are highlighted below as miscellaneous metrics of goal-oriented SemCom.

F. MISCELLANEOUS METRICS OF GOAL-ORIENTED SEMCOM

1) Mean Per Joint Position Error

MPJPE is an important metric for evaluating the performance of goal-oriented wireless SemCom schemes such as goal-oriented SemCom for 3D human mesh construction tasks [237]. It is defined in (36).

2) Triplet Drop Probability

TDP is a generic semantic metric that is also a crucial performance analysis/optimization metric for wireless systems that are based on goal-oriented wireless SemCom [262]. It is defined in (53).

3) Age of Incorrect Information

AoII [241], [242], [251] is an age-based metric that facilitates goal-oriented wireless SemCom. When it comes to goal-oriented SemCom, the authors of [241] demonstrate that AoII is able to capture the data's role in achieving the communication goal. It is defined in Definition 5.

4) Semantic Impact

Semantic impact is a generic semantic metric that is applicable to the design, analysis, and optimization of systems that are based on goal-oriented wireless SemCom. It is defined in Definition 6.

5) Communication Symmetry Index

Communication symmetry index is a generic semantic metric that is applicable to the design, analysis, and optimization of goal-oriented wireless SemCom systems. It is defined in Proposition 1.

6) Reasoning Capacity

Reasoning capacity is a generic semantic metric that is also applicable to the design, analysis, and optimization of systems that are based on goal-oriented wireless SemCom. It is defined in Proposition 2.

We now conclude this work below with our concluding summary and research outlook.

XII. CONCLUDING SUMMARY AND RESEARCH OUTLOOK

The semantic-centric design in SemCom and goal-oriented SemCom helps to minimize power usage, bandwidth consumption, and transmission delay. These crucial advantages of SemCom and goal-oriented SemCom can mitigate some of the fundamental challenges of 6G. Consequently, SemCom and goal-oriented SemCom have been widely advocated as promising enablers of 6G and developing rapidly. Despite the upsurge in their rapid development, the design, analysis, optimization, and realization of robust and intelligent SemCom as well as goal-oriented SemCom face many fundamental challenges. Amongst these challenges, the important one is the lack of unified/universal performance assessment metrics for SemCom and goal-oriented SemCom. To put this specific challenge in perspective and stimulate fundamental research, this survey paper offered a detailed discussion on the

existing metrics for SemCom and goal-oriented SemCom. More specifically, it presented semantic metrics used for text, speech, and image quality assessment; semantic metrics used for video quality and 3D human sensing assessment; AoI- and VoI-based semantic metrics; resource allocation semantic metrics; generic semantic metrics of SemCom; semantic metrics of quantum SemCom; and semantic metrics of goal-oriented wireless SemCom. By presenting all these metrics used for designing SemCom and goal-oriented SemCom systems, this paper intends to inspire the design, analysis, and optimization of many types of SemCom and goal-oriented SemCom systems. This article also invigorates the development of unified/universal performance assessment metrics of SemCom and goal-oriented SemCom, as the existing metrics are purely statistical and hardly applicable to reasoning-type tasks that constitute the heart of 6G and beyond.

DISCLAIMER

The identification of any commercial product or trade name does not imply endorsement or recommendation by the National Institute of Standards and Technology, nor is it intended to imply that the materials or equipment identified are necessarily the best available for the purpose.

REFERENCES

- [1] W. Saad, M. Bennis, and M. Chen, "A vision of 6G wireless systems: Applications, trends, technologies, and open research problems," *IEEE Netw.*, vol. 34, no. 3, pp. 134–142, 2020.
- [2] K. B. Letaief, Y. Shi, J. Lu, and J. Lu, "Edge artificial intelligence for 6G: Vision, enabling technologies, and applications," *IEEE J. Sel. Areas Commun.*, vol. 40, no. 1, pp. 5–36, 2022.
- [3] C. D. Alwis, A. Kalla, Q.-V. Pham, P. Kumar, K. Dev, W.-J. Hwang, and M. Liyanage, "Survey on 6G frontiers: Trends, applications, requirements, technologies and future research," *IEEE Open J. Commun. Soc.*, vol. 2, pp. 836–886, 2021.
- [4] I. F. Akyildiz, A. Kak, and S. Nie, "6G and beyond: The future of wireless communications systems," *IEEE Access*, vol. 8, pp. 133 995–134 030, 2020.
- [5] M. Alsabah, M. A. Naser, B. M. Mahmmod, S. H. Abdhussain, M. R. Eissa, A. Al-Baidhani, N. K. Noordin, S. M. Sait, K. A. Al-Utaibi, and F. Hashim, "6G wireless communications networks: A comprehensive survey," *IEEE Access*, vol. 9, pp. 148 191–148 243, 2021.
- [6] S. Dang et al., "What should 6G be?" *Nat. Electron.*, vol. 3, pp. 20–29, 2020.
- [7] X. You et al., "Towards 6G wireless communication networks: vision, enabling technologies, and new paradigm shifts," *Sci. China Inf. Sci.*, vol. 64, 2021.
- [8] W. Jiang, B. Han, M. A. Habibi, and H. D. Schotten, "The road towards 6G: A comprehensive survey," *IEEE Open J. Commun. Soc.*, vol. 2, pp. 334–366, 2021.
- [9] P. Porambage, G. Gür, D. P. M. Osorio, M. Liyanage, A. Gurtov, and M. Ylianttila, "The roadmap to 6G security and privacy," *IEEE Open J. Commun. Soc.*, vol. 2, pp. 1094–1122, 2021.
- [10] J. R. Bhat and S. A. Alqahtani, "6G ecosystem: Current status and future perspective," *IEEE Access*, vol. 9, pp. 43 134–43 167, 2021.
- [11] A. Shahraki, M. Abbasi, M. J. Piran, and A. Taherkordi, "A comprehensive survey on 6G networks: Applications, core services, enabling technologies, and future challenges," 2021. [Online]. Available: <https://arxiv.org/pdf/2101.12475.pdf>
- [12] Y. Lu and X. Zheng, "6G: A survey on technologies, scenarios, challenges, and the related issues," *J. Ind. Inf. Integr.*, vol. 19, p. 100158, 2020.
- [13] E. Yaacoub and M. Alouini, "A key 6G challenge and opportunity—connecting the base of the pyramid: A survey on rural connectivity," *Proc. IEEE*, vol. 108, no. 4, pp. 533–582, 2020.
- [14] J. Zhao and Y. Liu, "A survey of intelligent reflecting surfaces (IRSs): Towards 6G wireless communication networks," 2019. [Online]. Available: <https://arxiv.org/pdf/1907.04789.pdf>
- [15] M. Z. Chowdhury, M. Shahjalal, S. Ahmed, and Y. M. Jang, "6G wireless communication systems: Applications, requirements, technologies, challenges, and research directions," *IEEE Open J. Commun. Soc.*, vol. 1, pp. 957–975, 2020.
- [16] H. Viswanathan and P. E. Mogensen, "Communications in the 6G era," *IEEE Access*, vol. 8, pp. 57 063–57 074, 2020.
- [17] L. Bariah, L. Mohjazi, S. Muhaidat, P. C. Sofotasios, G. K. Kurt, H. Yanikomeroglu, and O. A. Dobre, "A prospective look: Key enabling technologies, applications and open research topics in 6G networks," *IEEE Access*, 2020.
- [18] H. Tataria, M. Shafi, A. F. Molisch, M. Dohler, H. Sjöland, and F. Tufveson, "6G wireless systems: Vision, requirements, challenges, insights, and opportunities," *Proc. IEEE*, vol. 109, no. 7, pp. 1166–1199, 2021.
- [19] G. P. Fettweis and H. Boche, "6G: The personal tactile internet - and open questions for information theory," *IEEE BITS the Information Theory Magazine*, pp. 1–1, 2021.
- [20] M. A. Uusitalo et al., "6G vision, value, use cases and technologies from european 6G flagship project Hexa-X," *IEEE Access*, vol. 9, pp. 160 004–160 020, 2021.
- [21] C. De Lima et al., "Convergent communication, sensing and localization in 6G systems: An overview of technologies, opportunities and challenges," *IEEE Access*, vol. 9, pp. 26 902–26 925, 2021.
- [22] L. U. Khan, I. Yaqoob, M. Imran, Z. Han, and C. S. Hong, "6G wireless systems: A vision, architectural elements, and future directions," *IEEE Access*, vol. 8, pp. 147 029–147 044, 2020.
- [23] T. S. Rappaport, Y. Xing, O. Kanhere, S. Ju, A. Madanayake, S. Mandal, A. Alkhatieb, and G. C. Trichopoulos, "Wireless communications and applications above 100 GHz: Opportunities and challenges for 6G and beyond," *IEEE Access*, vol. 7, pp. 78 729–78 757, 2019.
- [24] Y. Hao, Y. Miao, M. Chen, H. Gharavi, and V. C. M. Leung, "6G cognitive information theory: A mailbox perspective," *Big Data Cogn. Comput.*, vol. 5, no. 4, 2021.
- [25] S. Chen, Y. Liang, S. Sun, S. Kang, W. Cheng, and M. Peng, "Vision, requirements, and technology trend of 6G: How to tackle the challenges of system coverage, capacity, user data-rate and movement speed," *IEEE Wireless Commun.*, vol. 27, no. 2, pp. 218–228, Apr. 2020.
- [26] E. Bertin, N. Crespi, and T. Magedanz (Eds.), *Shaping Future 6G Networks: Needs, Impacts, and Technologies*. Hoboken, NJ, USA: Wiley, 2022.
- [27] P. Popovski, F. Chiariotti, V. Croisfelt, A. E. Kalør, I. Leyva-Mayorga, L. Marchegiani, S. R. Pandey, and B. Soret, "Internet of things (IoT) connectivity in 6G: An interplay of time, space, intelligence, and value," 2021. [Online]. Available: <https://arxiv.org/pdf/2111.05811.pdf>
- [28] F. Tariq, M. R. A. Khandaker, K. Wong, M. A. Imran, M. Bennis, and M. Debbah, "A speculative study on 6G," 18 Feb. 2019. [Online]. Available: <https://arxiv.org/pdf/1902.06700.pdf>
- [29] M. Maier, A. Ebrahimzadeh, S. Rostami, and A. Beniiiche, "The internet of no things: Making the internet disappear and "see the invisible"," *IEEE Commun. Mag.*, vol. 58, no. 11, pp. 76–82, 2020.
- [30] M. Xu, W. C. Ng, W. Y. B. Lim, J. Kang, Z. Xiong, D. Niyato, Q. Yang, X. S. Shen, and C. Miao, "A full dive into realizing the edge-enabled metaverse: Visions, enabling technologies, and challenges," 2022. [Online]. Available: <https://arxiv.org/pdf/2203.05471.pdf>
- [31] G. Gui, M. Liu, F. Tang, N. Kato, and F. Adachi, "6G: Opening new horizons for integration of comfort, security and intelligence," *IEEE Wireless Commun.*, pp. 1–7, 2020.
- [32] A. Celik, B. Shihadah, and M.-S. Alouini, "Wireless data center networks: Advances, challenges, and opportunities," 28 Nov. 2018. [Online]. Available: <https://arxiv.org/pdf/1811.11717.pdf>
- [33] R. W. Heath, "Going toward 6G," *IEEE Signal Process. Mag.*, pp. 3–4, May 2019.
- [34] N. Rajatheva et al., "Scoring the terabit/s goal:broadband connectivity in 6G," 2020. [Online]. Available: <https://arxiv.org/pdf/2008.07220.pdf>
- [35] N. Rajatheva et al., "White paper on broadband connectivity in 6G," 2020. [Online]. Available: <https://arxiv.org/pdf/2004.14247.pdf>
- [36] K. David and H. Berndt, "6G vision and requirements: Is there any need for beyond 5G?" *IEEE Veh. Technol. Mag.*, vol. 13, no. 3, pp. 72–80, Sep. 2018.
- [37] M. Latva-aho and K. L. (eds.), "Key drivers and research challenges for 6G ubiquitous wireless intelligence," Sep. 2019. [Online]. Available: <http://jultika.oulu.fi/Record/isbn978-952-62-2354-4>

- [38] C. E. Shannon and W. Weaver, *The Mathematical Theory of Communication*. Urbana, IL, USA: Univ. Illinois Press, 1949.
- [39] D. Gunduz, Z. Qin, I. E. Aguerri, H. S. Dhillon, Z. Yang, A. Yener, K. K. Wong, and C.-B. Chae, "Beyond transmitting bits: Context, semantics, and task-oriented communications," 2022. [Online]. Available: <https://arxiv.org/pdf/2207.09353.pdf>
- [40] Y. Zhong, "A theory of semantic information," *China Commun.*, vol. 14, no. 1, pp. 1–17, 2017.
- [41] Y. Zhong and G. Dodig-Crnković, *A Theory of Semantic Information in the Context of its Ecology*, 2020, ch. Chapter 5, pp. 81–112.
- [42] S. Ji, S. Pan, E. Cambria, P. Marttinen, and P. S. Yu, "A survey on knowledge graphs: Representation, acquisition, and applications," *IEEE Trans. Neural Netw. Learn. Syst.*, vol. 33, pp. 494–514, 2022.
- [43] J.-C. Belfiore and D. Bennequin, "Topos and stacks of deep neural networks," 2021. [Online]. Available: <https://arxiv.org/pdf/2106.14587.pdf>
- [44] P. Tetlow, D. Garg, L. Chase, M. Mattingley-Scott, N. Bronn, K. Naidoo, and E. Reinert, "Towards a semantic information theory (introducing quantum corollas)," 2022. [Online]. Available: <https://arxiv.org/pdf/2201.05478.pdf>
- [45] H. Tong, Z. Yang, S. Wang, Y. Hu, O. Semiari, W. Saad, and C. Yin, "Federated learning for audio semantic communication," *Front. Comms. Net.*, vol. 2, 2021.
- [46] H. Xie, Z. Qin, G. Li, and B.-H. Juang, "Deep learning enabled semantic communication systems," *IEEE Trans. Signal Process.*, vol. 69, pp. 2663–2675, Apr. 2021.
- [47] M. Kalfa, M. Gok, A. Atalik, B. Tegin, T. M. Duman, and O. Arikan, "Towards goal-oriented semantic signal processing: Applications and future challenges," *Digit. Signal Process.*, vol. 119, pp. 103–134, Dec. 2021.
- [48] Q. Zhou, R. Li, Z. Zhao, C. Peng, and H. Zhang, "Semantic communication with adaptive universal transformer," *IEEE Wirel. Commun. Lett.*, vol. 11, no. 3, pp. 453–457, 2022.
- [49] E. Uysal, O. Kaya, A. Ephremides, J. Gross, M. Codreanu, P. Popovski, M. Assaad, G. Liva, A. Munari, T. Soleymani, B. Soret, and K. H. Johansson, "Semantic communications in networked systems: A data significance perspective," 2021. [Online]. Available: <https://arxiv.org/pdf/2103.05391>
- [50] C. Zhang, H. Zou, S. Lasaulce, W. Saad, M. Kountouris, and M. Bennis, "Goal-oriented communications for the IoT and application to data compression," 2022. [Online]. Available: <https://arxiv.org/pdf/2211.05378.pdf>
- [51] Z. Lu, R. Li, K. Lu, X. Chen, E. Hossain, Z. Zhao, and H. Zhang, "Semantics-empowered communication: A tutorial-cum-survey," 2022. [Online]. Available: <https://arxiv.org/pdf/2212.08487.pdf>
- [52] S. Xie, Y. Wu, S. Ma, M. Ding, Y. Shi, and M. Tang, "Robust information bottleneck for task-oriented communication with digital modulation," 2022. [Online]. Available: <https://arxiv.org/pdf/2209.10382.pdf>
- [53] C. Chaccour, W. Saad, M. Debbah, Z. Han, and H. V. Poor, "Less data, more knowledge: Building next generation semantic communication networks," 2022. [Online]. Available: <https://arxiv.org/pdf/2211.14343.pdf>
- [54] Z. Qin, X. Tao, J. Lu, W. Tong, and G. Y. Li, "Semantic communications: Principles and challenges," 2022. [Online]. Available: <https://arxiv.org/pdf/2201.01389v5.pdf>
- [55] X. Luo, H.-H. Chen, and Q. Guo, "Semantic communications: Overview, open issues, and future research directions," *IEEE Wirel. Commun.*, vol. 29, no. 1, pp. 210–219, 2022.
- [56] K. Lu, Q. Zhou, R. Li, Z. Zhao, X. Chen, J. Wu, and H. Zhang, "Rethinking modern communication from semantic coding to semantic communication," *IEEE Wirel. Commun.*, pp. 1–13, 2022.
- [57] K. Niu, J. Dai, S. Yao, S. Wang, Z. Si, X. Qin, and P. Zhang, "Towards semantic communications: A paradigm shift," 2022. [Online]. Available: <https://arxiv.org/pdf/2203.06692.pdf>
- [58] W. Yang, H. Du, Z. Liew, W. Y. B. Lim, Z. Xiong, D. Niyato, X. Chi, X. S. Shen, and C. Miao, "Semantic communications for 6G future internet: Fundamentals, applications, and challenges," 2022. [Online]. Available: <https://arxiv.org/pdf/2207.00427.pdf>
- [59] D. Wheeler and B. Natarajan, "Engineering semantic communication: A survey," 2022. [Online]. Available: <https://arxiv.org/pdf/2208.06314.pdf>
- [60] Y. Zhang, F. Wang, W. Xu, and C. Liu, "Semantic communications: A new paradigm for networked intelligence," in *Proc. MLSP*, 2022, pp. 1–6.
- [61] P. Jiang, C.-K. Wen, S. Jin, and G. Y. Li, "Wireless semantic transmission via revising modules in conventional communications," 2022. [Online]. Available: <https://arxiv.org/pdf/2210.00473.pdf>
- [62] R. Van Meter, *Quantum Networking*. Hoboken, NJ, USA: Wiley, 2014.
- [63] M. A. Nielsen and I. L. Chuang, *Quantum Computation and Quantum Information*, 10th Anniversary ed. New York, NY, USA: Cambridge Univ. Press, 2010.
- [64] M. M. Wilde, *Quantum Information Theory*, 2nd ed. Cambridge, UK: Cambridge Univ. Press, 2017.
- [65] D. A. B. Miller, *Quantum Mechanics for Scientists and Engineers*. New York, NY, USA: Cambridge Univ. Press, 2008.
- [66] Y. Wang, Z. Hu, B. C. Sanders, and S. Kais, "Qudits and high-dimensional quantum computing," *Front. Phys.*, vol. 8, Nov. 2020.
- [67] D. Cozzolino, B. D. Lio, D. Bacco, and L. K. Oxenl we, "High-dimensional quantum communication: Benefits, progress, and future challenges," *Adv. Quantum Technol.*, vol. 2, no. 12, p. 1900038, Oct. 2019.
- [68] W. K. Wootters and W. H. Zurek, "A single quantum cannot be cloned," *Nature*, vol. 299, pp. 802–803, 1982.
- [69] M. Chehimi, C. Chaccour, and W. Saad, "Quantum semantic communications: An unexplored avenue for contextual networking," 2022. [Online]. Available: <https://arxiv.org/pdf/2205.02422.pdf>
- [70] W. Tong and P. Zhu (Eds.), *6G: The Next Horizon: From Connected People and Things to Connected Intelligence*. Cambridge, UK: Cambridge Univ. Press, 2021.
- [71] S. Russel and P. Norvig, *Artificial Intelligence: A Modern Approach*, 3rd ed. Englewood Cliffs, NJ, USA: Prentice Hall, 2018.
- [72] G. Marcus and E. Davis, *Rebooting AI: Building Artificial Intelligence We Can Trust*. USA: New York, NY, USA, Pantheon Books, 2019.
- [73] T. G. Dietterich, "Steps toward robust artificial intelligence," *AI Mag.*, vol. 38, pp. 3–24, 2017.
- [74] M. Jordan and T. Mitchell, "Machine learning: Trends, perspectives, and prospects," *Science*, vol. 349, pp. 255–60, Jul. 2015.
- [75] M. Chen, U. Challita, W. Saad, C. Yin, and M. Debbah, "Artificial neural networks-based machine learning for wireless networks: A tutorial," [Online]. Available: <https://arxiv.org/pdf/1710.02913.pdf>
- [76] Z. Ghahramani, "Probabilistic machine learning and artificial intelligence," *Nature*, vol. 521, pp. 452–459, 2015.
- [77] Y. LeCun, Y. Bengio, and G. Hinton, "Deep learning," *Nature*, vol. 521, no. 436, pp. 436–444, 2015.
- [78] T. J. Sejnowski, *The Deep Learning Revolution*. Cambridge, MA, USA: The MIT Press, 2018.
- [79] I. Goodfellow, Y. Bengio, and A. Courville, *Deep Learning*. MIT Press, 2016.
- [80] W. Scherer, *Mathematics of Quantum Computing: An Introduction*. Cham, Switzerland: Springer, 2019.
- [81] J. Preskill, "Quantum computing in the NISQ era and beyond," *Quantum*, vol. 2, p. 79, Aug. 2018.
- [82] N. Gisin and R. Thew, "Quantum communication," *Nat. Photon.*, vol. 1, no. 3, pp. 165–171, Mar. 2007.
- [83] S. Imre and L. Gyongyosi, *Advanced Quantum Communications: An Engineering Approach*. Hoboken, NJ, USA: Wiley-IEEE Press, 2012.
- [84] G. L. Cariolaro, *Quantum Communications*. Cham, Switzerland: Springer, 2015.
- [85] R. Bassoli, H. Boche, C. Deppe, R. Ferrara, F. H. P. Fitzek, G. Janssen, and S. Saedinaeeni, *Quantum Communication Networks*, Cham, Switzerland, 2021.
- [86] I. Djordjevic, *Quantum Communication, Quantum Networks, and Quantum Sensing*. Cambridge, MA, USA: Elsevier, Jan. 2022.
- [87] M. Dehghani, S. Gouws, O. Vinyals, J. Uszkoreit, and L. Kaiser, "Universal transformers," in *Proc. Int. Conf. Learn. Represent. (ICLR)*, 2019.
- [88] Z. Liu, Y. Lin, Y. Cao, H. Hu, Y. Wei, Z. Zhang, S. Lin, and B. Guo, "Swin transformer: Hierarchical vision transformer using shifted windows," in *Proc. ICCV*, 2021, pp. 9992–10002.
- [89] Y. Wang, Z. Gao, D. Zheng, S. Chen, D. Gündüz, and H. V. Poor, "Transformer-empowered 6G intelligent networks: From massive MIMO processing to semantic communication," 2022. [Online]. Available: <https://arxiv.org/pdf/2205.03770.pdf>
- [90] Q. Hu, G. Zhang, Z. Qin, Y. Cai, G. Yu, and G. Y. Li, "Robust semantic communications with masked VQ-VAE enabled codebook," 2022. [Online]. Available: <https://arxiv.org/pdf/2206.04011.pdf>
- [91] B. Güler, A. Yener, and A. Swami, "The semantic communication game," *IEEE Trans. Cogn. Commun. Netw.*, vol. 4, no. 4, pp. 787–802, 2018.

- [92] N. Farsad, M. Rao, and A. Goldsmith, "Deep learning for joint source-channel coding of text," in *Proc. IEEE ICASSP*, 2018, pp. 2326–2330.
- [93] H. Xie and Z. Qin, "A lite distributed semantic communication system for internet of things," *IEEE J. Sel. Areas Commun.*, vol. 39, no. 1, pp. 142–153, 2021.
- [94] X. Peng, Z. Qin, D. Huang, X. Tao, J. Lu, G. Liu, and C. Pan, "A robust deep learning enabled semantic communication system for text," 2022. [Online]. Available: <https://arxiv.org/abs/2206.02596>
- [95] S. Yao, K. Niu, S. Wang, and J. Dai, "Semantic coding for text transmission: An iterative design," *IEEE Trans. Cogn. Commun. Netw.*, pp. 1–1, 2022.
- [96] K. Lu, R. Li, X. Chen, Z. Zhao, and H. Zhang, "Reinforcement learning-powered semantic communication via semantic similarity," 2021. [Online]. Available: <https://arxiv.org/pdf/2108.12121.pdf>
- [97] X. Luo, Z. Chen, B. Xia, and J. Wang, "Autoencoder-based semantic communication systems with relay channels," 2021. [Online]. Available: <https://arxiv.org/pdf/2111.10083.pdf>
- [98] P. Jiang, C.-K. Wen, S. Jin, and G. Y. Li, "Deep source-channel coding for sentence semantic transmission with HARQ," *IEEE Trans. Commun.*, vol. 70, pp. 5225–5240, 2022.
- [99] Y. Liu, S. Jiang, Y. Zhang, K. Cao, L. Zhou, B.-C. Seet, H. Zhao, and J. Wei, "Extended context-based semantic communication system for text transmission," *Digit. Commun. Netw.*, Oct. 2022.
- [100] Z. Weng and Z. Qin, "Semantic communication systems for speech transmission," *IEEE J. Sel. Areas Commun.*, vol. 39, no. 8, pp. 2434–2444, 2021.
- [101] Z. Weng, Z. Qin, and G. Y. Li, "Semantic communications for speech signals," 2020. [Online]. Available: <https://arxiv.org/pdf/2012.05369.pdf>
- [102] Z. Weng, Z. Qin, and G. Y. Li, "Semantic communications for speech recognition," 2021. [Online]. Available: <https://arxiv.org/pdf/2107.11190.pdf>
- [103] T. Han, Q. Yang, Z. Shi, S. He, and Z. Zhang, "Semantic-aware speech to text transmission with redundancy removal," 2022. [Online]. Available: <https://arxiv.org/pdf/2202.03211.pdf>
- [104] Z. Weng, Z. Qin, X. Tao, C. Pan, G. Liu, and G. Y. Li, "Deep learning enabled semantic communications with speech recognition and synthesis," 2022. [Online]. Available: <https://arxiv.org/pdf/2205.04603.pdf>
- [105] E. Boursoulatz, D. Burth Kurka, and D. Gündüz, "Deep joint source-channel coding for wireless image transmission," *IEEE Trans. Cogn. Commun.*, vol. 5, no. 3, pp. 567–579, 2019.
- [106] D. B. Kurka and D. Gündüz, "DeepJSCC-f: Deep joint source-channel coding of images with feedback," *IEEE J. Sel. Areas Inf. Theory*, vol. 1, pp. 178–193, 2020.
- [107] D. B. Kurka and D. Gündüz, "Bandwidth-agile image transmission with deep joint source-channel coding," *IEEE Trans. Wirel. Commun.*, vol. 20, no. 12, pp. 8081–8095, 2021.
- [108] Z. Zhang, Q. Yang, S. He, M. Sun, and J. Chen, "Wireless transmission of images with the assistance of multi-level semantic information," 2022. [Online]. Available: <https://arxiv.org/pdf/2202.04754>
- [109] J. Xu, B. Ai, W. Chen, A. Yang, P. Sun, and M. Rodrigues, "Wireless image transmission using deep source channel coding with attention modules," *IEEE Trans. Circuits Syst. Video Technol.*, vol. 32, no. 4, pp. 2315–2328, 2022.
- [110] Q. Pan, H. Tong, J. Lv, T. Luo, Z. Zhang, C. Yin, and J. Li, "Image segmentation semantic communication over internet of vehicles," 2022. [Online]. Available: <https://arxiv.org/pdf/2210.05321.pdf>
- [111] K. Yang, S. Wang, J. Dai, K. Tan, K. Niu, and P. Zhang, "WITT: A wireless image transmission transformer for semantic communications," 2022. [Online]. Available: <https://arxiv.org/pdf/2211.00937.pdf>
- [112] J. Dai, S. Wang, K. Tan, Z. Si, X. Qin, K. Niu, and P. Zhang, "Nonlinear transform source-channel coding for semantic communications," *IEEE J. Sel. Areas Commun.*, vol. 40, no. 8, pp. 2300–2316, 2022.
- [113] C.-H. Lee, J.-W. Lin, P.-H. Chen, and Y.-C. Chang, "Deep learning-constructed joint transmission-recognition for internet of things," *IEEE Access*, vol. 7, pp. 76 547–76 561, 2019.
- [114] Q. Hu, G. Zhang, Guangyi, Z. Qin, Y. Cai, G. Yu, and G. Y. Li, "Robust semantic communications against semantic noise," 2022. [Online]. Available: <https://arxiv.org/pdf/2202.03338.pdf>
- [115] D. Huang, F. Gao, X. Tao, Q. Du, and J. Lu, "Toward semantic communications: Deep learning-based image semantic coding," *IEEE J. Sel. Areas Commun.*, vol. 41, no. 1, pp. 55–71, 2023.
- [116] P. Jiang, C.-K. Wen, S. Jin, and G. Y. Li, "Wireless semantic communications for video conferencing," 2022. [Online]. Available: <https://arxiv.org/pdf/2204.07790.pdf>
- [117] S. Wang, J. Dai, Z. Liang, K. Niu, Z. Si, C. Dong, X. Qin, and P. Zhang, "Wireless deep video semantic transmission," 2022. [Online]. Available: <https://arxiv.org/pdf/2205.13129.pdf>
- [118] T.-Y. Tung and D. Gündüz, "DeepWiVe: Deep-learning-aided wireless video transmission," 2021. [Online]. Available: <https://arxiv.org/pdf/2111.13034.pdf>
- [119] Y. Huang, B. Bai, Y. Zhu, X. Qiao, X. Su, and P. Zhang, "Iscom: Interest-aware semantic communication scheme for point cloud video streaming," 2022. [Online]. Available: <https://arxiv.org/pdf/2210.06808.pdf>
- [120] C. Wang, X. Yu, L. Xu, Z. Wang, and W. Wang, "Multimodal semantic communication accelerated bidirectional caching for 6G MEC," *Future Gener. Comput. Syst.*, vol. 140, pp. 225–237, 2023.
- [121] A. Li, X. Wei, D. Wu, and L. Zhou, "Cross-modal semantic communications," *IEEE Wirel. Commun.*, pp. 1–8, 2022.
- [122] F. Zhou, Y. Li, X. Zhang, Q. Wu, X. Lei, and R. Q. Hu, "Cognitive semantic communication systems driven by knowledge graph," 2022. [Online]. Available: <https://arxiv.org/abs/2202.11958>
- [123] Y. Xiao, Y. Li, G. Shi, and H. V. Poor, "Reasoning on the air: An implicit semantic communication architecture," 2022. [Online]. Available: <https://arxiv.org/pdf/2202.01950.pdf>
- [124] J. Dai, S. Wang, K. Yang, K. Tan, X. Qin, Z. Si, K. Niu, and P. Zhang, "Adaptive semantic communications: Overfitting the source and channel for profit," 2022. [Online]. Available: <https://arxiv.org/pdf/2211.04339.pdf>
- [125] Y. Zhang, H. Zhao, J. Wei, J. Zhang, M. F. Flanagan, and J. Xiong, "Context-based semantic communication via dynamic programming," *IEEE Trans. Cogn. Commun. Netw.*, pp. 1–1, 2022.
- [126] Y. Bo, Y. Duan, S. Shao, and M. Tao, "Learning based joint coding-modulation for digital semantic communication systems," 2022. [Online]. Available: <https://arxiv.org/pdf/2208.05704.pdf>
- [127] Q. Fu, H. Xie, Z. Qin, G. Slabaugh, and X. Tao, "Vector quantized semantic communication system," 2022. [Online]. Available: <https://arxiv.org/pdf/2209.11519.pdf>
- [128] D. Wheeler, E. E. Tripp, and B. Natarajan, "Semantic communication with conceptual spaces," 2022. [Online]. Available: <https://arxiv.org/pdf/2210.01629.pdf>
- [129] H. Du, J. Wang, D. Niyato, J. Kang, Z. Xiong, J. Zhang, Xuemin, and Shen, "Semantic communications for wireless sensing: RIS-aided encoding and self-supervised decoding," 2022. [Online]. Available: <https://arxiv.org/pdf/2211.12727.pdf>
- [130] H. Hu, X. Zhu, F. Zhou, W. Wu, R. Q. Hu, and H. Zhu, "One-to-many semantic communication systems: Design, implementation, performance evaluation," *IEEE Commun. Lett.*, vol. 26, no. 12, pp. 2959–2963, 2022.
- [131] W. Xu, Y. Zhang, F. Wang, Z. Qin, C. Liu, and P. Zhang, "Semantic communication for internet of vehicles: A multi-user cooperative approach," 2022. [Online]. Available: <https://arxiv.org/pdf/2212.03037.pdf>
- [132] Y. Xiao, X. Zhang, Y. Li, and G. Shi, "Rate-distortion theory for strategic semantic communication," 2022. [Online]. Available: <https://arxiv.org/pdf/2202.03711.pdf>
- [133] X. Luo, Z. Chen, M. Tao, and F. Yang, "Encrypted semantic communication using adversarial training for privacy preserving," 2022. [Online]. Available: <https://arxiv.org/pdf/2209.09008.pdf>
- [134] Q. Lan, D. Wen, Z. Zhang, Q. Zeng, X. Chen, P. Popovski, and K. Huang, "What is semantic communication? a view on conveying meaning in the era of machine intelligence," *J. Commun. Inf. Netw.*, vol. 6, no. 4, pp. 336–371, Dec. 2021.
- [135] W. Yang, Z. Q. Liew, W. Y. B. Lim, Z. Xiong, D. Niyato, X. Chi, X. Cao, and K. B. Letaief, "Semantic communication meets edge intelligence," 2022. [Online]. Available: <https://arxiv.org/pdf/2202.06471.pdf>
- [136] E. C. Strinati and S. Barbarossa, "6G networks: Beyond Shannon towards semantic and goal-oriented communications," 2020. [Online]. Available: <https://arxiv.org/pdf/2011.14844.pdf>
- [137] P. Zhang, W. Xu, H. Gao, K. Niu, X. Xu, X. Qin, C. Yuan, Z. Qin, H. Zhao, J. Wei, and F. Zhang, "Toward wisdom-evolutionary and primitive-concise 6G: A new paradigm of semantic communication networks," *Engineering*, vol. 8, Nov. 2021.
- [138] E. Beck, C. Bockelmann, and A. Dekorsy, "Semantic communication: An information bottleneck view," 2022. [Online]. Available: <https://arxiv.org/pdf/2204.13366.pdf>

- [139] P. Popovski, O. Simeone, F. Boccardi, D. Gunduz, and O. Sahin, "Semantic-effectiveness filtering and control for post-5G wireless connectivity," 2019. [Online]. Available: <https://arxiv.org/pdf/1907.02441.pdf>
- [140] G. Shi, D. Gao, X. Song, J. Chai, M. Yang, X. Xie, L. Li, and X. Li, "A new communication paradigm: from bit accuracy to semantic fidelity," 2021. [Online]. Available: <https://arxiv.org/pdf/2101.12649.pdf>
- [141] G. Shi, Y. Xiao, Y. Li, and X. Xie, "From semantic communication to semantic-aware networking: Model, architecture, and open problems," 2020. [Online]. Available: <https://arxiv.org/pdf/2012.15405.pdf>
- [142] J. Dai, P. Zhang, K. Niu, S. Wang, Z. Si, and X. Qin, "Communication beyond transmitting bits: Semantics-guided source and channel coding," 2022. [Online]. Available: <https://arxiv.org/pdf/2208.02481.pdf>
- [143] P. Dong, Q. Wu, X. Zhang, and G. Ding, "Edge semantic cognitive intelligence for 6G networks: Novel theoretical models, enabling framework, and typical applications," 2022. [Online]. Available: <https://arxiv.org/pdf/2205.12073v2.pdf>
- [144] Q. Zhao, M. Bennis, M. Debbah, and D. B. da Costa, "Semantic-native communication: A simplicial complex perspective," 2022. [Online]. Available: <https://arxiv.org/pdf/2210.16970.pdf>
- [145] S. Seo, J. Park, S.-W. Ko, J. Choi, M. Bennis, and S.-L. Kim, "Towards semantic communication protocols: A probabilistic logic perspective," 2022. [Online]. Available: <https://arxiv.org/pdf/2207.03920.pdf>
- [146] S. R. Pokhrel and J. Choi, "Understand-before-talk (UBT): A semantic communication approach to 6G networks," *IEEE Trans. Veh. Technol.*, pp. 1–13, 2022.
- [147] Z. Yu, H. Huang, L. Cheng, W. Zhang, Y. Mu, and K. Xu, "Semantic optical fiber communication system," 2022. [Online]. Available: <https://arxiv.org/pdf/2212.14739>
- [148] J. Biamonte, P. Wittek, N. Pancotti, P. Rebentrost, N. Wiebe, and S. Lloyd, "Quantum machine learning," *Nature*, vol. 549, no. 7671, pp. 195–202, Sep. 2017.
- [149] S. J. Nawaz, S. K. Sharma, S. Wyne, M. N. Patwary, and M. Asaduz-zaman, "Quantum machine learning for 6G communication networks: State-of-the-art and vision for the future," *IEEE Access*, vol. 7, pp. 46 317–46 350, Apr. 2019.
- [150] N. Wiebe, A. Kapoor, and K. M. Svore, "Quantum deep learning," 22 May 2015. [Online]. Available: <https://arxiv.org/pdf/1412.3489.pdf>
- [151] M. Schuld and N. Killoran, "Quantum machine learning in feature Hilbert spaces," *Phys. Rev. Lett.*, vol. 122, no. 4, Feb. 2019.
- [152] R. Raussendorf and H. J. Briegel, "A one-way quantum computer," *Phys. Rev. Lett.*, vol. 86, pp. 5188–5191, May 2001.
- [153] D. Aharonov, W. Van Dam, J. Kempe, Z. Landau, S. Lloyd, and O. Regev, "Adiabatic quantum computation is equivalent to standard quantum computation," *SIAM J. Comput.*, vol. 37, no. 1, pp. 166–194, 2007.
- [154] M. H. Freedman, M. Larsen, and Z. Wang, "A modular functor which is universal for quantum computation," *Commun. Math. Phys.*, vol. 227, pp. 605–622, 2002.
- [155] C. Chaccour, M. N. Soorki, W. Saad, M. Bennis, P. Popovski, and M. Debbah, "Seven defining features of terahertz (THz) wireless systems: A fellowship of communication and sensing," *IEEE Commun. Surv. Tutor.*, vol. 24, no. 2, pp. 967–993, 2022.
- [156] J.-W. Pan, C. Simon, Časlav Brukner, and A. Zeilinger, "Entanglement purification for quantum communication," *Nature*, vol. 410, no. 6832, pp. 1067–1070, Apr. 2001.
- [157] R. Kaewpuang, M. Xu, W. Y. B. Lim, D. Niyato, H. Yu, J. Kang, and X. S. Shen, "Cooperative resource management in quantum key distribution (QKD) networks for semantic communication," 2022. [Online]. Available: <https://arxiv.org/pdf/2209.11957.pdf>
- [158] Y. Cao, Y. Zhao, Q. Wang, J. Zhang, S. X. Ng, and L. Hanzo, "The evolution of quantum key distribution networks: On the road to the Qinternet," *IEEE Commun. Surv. Tutor.*, vol. 24, no. 2, pp. 839–894, 2022.
- [159] M. Kountouris and N. Pappas, "Semantics-empowered communication for networked intelligent systems," *IEEE Commun. Mag.*, vol. 59, pp. 96–102, 2021.
- [160] B. A. Juba and M. Sudan, "Universal semantic communication II: A theory of goal-oriented communication," *Electron. Colloquium Comput. Complex.*, vol. 15, 2008.
- [161] Y. Yang, C. Guo, F. Liu, C. Liu, L. Sun, Q. Sun, and J. Chen, "Semantic communications with AI tasks," 2021. [Online]. Available: <https://arxiv.org/pdf/2109.14170.pdf>
- [162] C. K. Thomas and W. Saad, "Neuro-symbolic artificial intelligence (AI) for intent based semantic communication," 2022. [Online]. Available: <https://arxiv.org/abs/2205.10768>
- [163] C. K. Thomas and W. Saad, "Neuro-symbolic causal reasoning meets signaling game for emergent semantic communications," 2022. [Online]. Available: <https://arxiv.org/pdf/2210.12040.pdf>
- [164] H. Xie, Z. Qin, X. Tao, and K. B. Letaief, "Task-oriented multi-user semantic communications," *IEEE J. Sel. Areas Commun.*, vol. 40, no. 9, pp. 2584–2597, 2022.
- [165] T.-Y. Tung, S. Kobus, J. P. Roig, and D. Gündüz, "Effective communications: A joint learning and communication framework for multi-agent reinforcement learning over noisy channels," *IEEE J. Sel. Areas Commun.*, vol. 39, no. 8, pp. 2590–2603, 2021.
- [166] E. G. Soyak and O. Ercetin, "Effective communications for 6G: Challenges and opportunities," 2022. [Online]. Available: <https://arxiv.org/pdf/2203.11695.pdf>
- [167] M. Sana and E. C. Strinati, "Learning semantics: An opportunity for effective 6G communications," 2021. [Online]. Available: <https://arxiv.org/pdf/2110.08049.pdf>
- [168] M. Goek, "Semantic and goal-oriented signal processing: semantic extraction," Master's thesis, Bilkent University, Turkey, Aug. 2022.
- [169] L. Yan, Z. Qin, R. Zhang, Y. Li, and G. Y. Li, "Resource allocation for text semantic communications," 2022. [Online]. Available: <https://arxiv.org/pdf/2201.06023.pdf>
- [170] M. E. Peters, M. Neumann, M. Iyyer, M. Gardner, C. Clark, K. Lee, and L. Zettlemoyer, "Deep contextualized word representations," in *Proc. North Amer. Chapter Assoc. Comput. Linguistics: Hum. Lang. Tech.*, New Orleans, LA, USA, 2018, pp. 2227–2237.
- [171] K. Papineni, S. Roukos, T. Ward, and W.-J. Zhu, "Bleu: a method for automatic evaluation of machine translation," in *Proc. Annu. Meeting Assoc. Comput. Linguistics*, Jul. 2002, pp. 311–318.
- [172] R. Vedantam, C. L. Zitnick, and D. Parikh, "CIDEr: Consensus-based image description evaluation," in *Proc. IEEE Conf. Comput. Vis. Pattern Recognit. (CVPR)*, 2015, pp. 4566–4575.
- [173] Wikipedia, "Cosine similarity," [Online]. Available: https://en.wikipedia.org/wiki/Cosine_similarity (accessed Oct. 2022).
- [174] S. Jiang, Y. Liu, Y. Zhang, P. Luo, K. Cao, J. Xiong, H. Zhao, and J. Wei, "Reliable semantic communication system enabled by knowledge graph," *Entropy*, vol. 24, no. 6, 2022.
- [175] T. M. Getu, W. Saad, G. Kaddoum, and M. Bennis, "Performance limits of a deep learning-enabled text semantic communication under interference," 2023. [Online]. Available: <https://arxiv.org/pdf/2302.14702.pdf>
- [176] T. Poggio, A. Banburski, and Q. Liao, "Theoretical issues in deep networks," *Proc. Natl. Acad. Sci. U.S.A.*, Jun. 2020.
- [177] F. Doshi-Velez and B. Kim, "Towards a rigorous science of interpretable machine learning," 2017. [Online]. Available: <https://arxiv.org/pdf/1702.08608.pdf>
- [178] B. Li, H. Zhou, J. He, M. Wang, Y. Yang, and L. Li, "On the sentence embeddings from pre-trained language models," in *Proc. Conf. on Empirical Methods in Natural Language Processing (EMNLP)*, Nov. 2020, pp. 9119–9130.
- [179] J.-H. Lee, D.-H. Lee, E. Sheen, T. Choi, J. Pujara, and J. Kim, "Seq2Seq-SC: End-to-end semantic communication systems with pre-trained language model," 2022. [Online]. Available: <https://arxiv.org/pdf/2210.15237.pdf>
- [180] N. Reimers and I. Gurevych, "Sentence-BERT: Sentence embeddings using Siamese BERT-networks," 2019. [Online]. Available: <https://arxiv.org/pdf/1908.10084.pdf>
- [181] S. Banerjee and A. Lavie, "METEOR: An automatic metric for MT evaluation with improved correlation with human judgments," in *Proceedings of the ACL Workshop on Intrinsic and Extrinsic Evaluation Measures for Machine Translation and/or Summarization*, Ann Arbor, Michigan, Jun. 2005, pp. 65–72.
- [182] C. D. Fellbaum, "WordNet: an electronic lexical database," *Language*, vol. 76, pp. 706–708, 2000.
- [183] M. Denkowski and A. Lavie, "Extending the METEOR machine translation evaluation metric to the phrase level," in *Proc. Annual Conf. the North American Chapter of the Association for Computational Linguistics*, 2010, pp. 250–253.
- [184] D. Chandrasekaran and V. Mago, "Evolution of semantic similarity—a survey," *ACM Comput. Surv.*, vol. 54, no. 2, pp. 1–37, 2022. [Online]. Available: <https://doi.org/10.1145/2F3440755>

- [185] G. Majumder, D. P. Pakray, A. Gelbukh, and D. Pinto, "Semantic textual similarity methods, tools, and applications: A survey," *Computacion y Sistemas*, vol. 20, pp. 647–665, Dec. 2016.
- [186] T. Han, Q. Yang, Z. Shi, S. He, and Z. Zhang, "Semantic-preserved communication system for highly efficient speech transmission," 2022. [Online]. Available: <https://arxiv.org/pdf/2205.12727.pdf>
- [187] E. Vincent, R. Gribonval, and C. Fevotte, "Performance measurement in blind audio source separation," *IEEE Trans. Audio, Speech, Language Process.*, vol. 14, no. 4, pp. 1462–1469, 2006.
- [188] A. Rix, J. Beerends, M. Hollier, and A. Hekstra, "Perceptual evaluation of speech quality (PESQ)-a new method for speech quality assessment of telephone networks and codecs," in *Proc. IEEE ICASSP*, vol. 2, 2001, pp. 749–752 vol.2.
- [189] ITU-T, "Perceptual evaluation of speech quality (PESQ): An objective method for end-to-end speech quality assessment of narrow-band telephone networks and speech codecs," ITU-T Recommendation P.862, Feb. 2001. [Online]. Available: <https://www.itu.int/rec/T-REC-P.862>
- [190] M. Bińkowski, J. Donahue, S. Dieleman, A. Clark, E. Elsen, N. Casagrande, L. C. Cobo, and K. Simonyan, "High fidelity speech synthesis with adversarial networks," 2019. [Online]. Available: <https://arxiv.org/pdf/1909.11646.pdf>
- [191] T.-J. Liu, J. Y.-c. Lin, W. Lin, and C.-C. J. Kuo, "Visual quality assessment: Recent developments, coding applications and future trends," *APSIPA Trans. Signal Inf. Process.*, vol. 2, Jan. 2013.
- [192] Z. Wang, A. Bovik, H. Sheikh, and E. Simoncelli, "Image quality assessment: from error visibility to structural similarity," *IEEE Trans. Image Process.*, vol. 13, no. 4, pp. 600–612, 2004.
- [193] C. Li and A. C. Bovik, "Three-component weighted structural similarity index," in *Proc. SPIE. Int. Soc. Opt. Eng.*, San Jose, CA, USA, 2009.
- [194] L. Zhang, L. Zhang, X. Mou, and D. Zhang, "FSIM: A feature similarity index for image quality assessment," *IEEE Trans. Image Process.*, vol. 20, no. 8, pp. 2378–2386, 2011.
- [195] Z. Wang, E. Simoncelli, and A. Bovik, "Multi-scale structural similarity for image quality assessment," in *Proc. IEEE Asilomar Conf. Signals, Syst. & Comput.*, vol. 2, 2003, pp. 1398–1402.
- [196] K. Ding, K. Ma, S. Wang, and E. P. Simoncelli, "Comparison of full-reference image quality models for optimization of image processing systems," *Int. J. Comput. Vis.*, vol. 129, no. 4, pp. 1258–1281, Jan. 2021. [Online]. Available: <https://doi.org/10.1007%2Fs11263-020-01419-7>
- [197] J. Wang, S. Wang, J. Dai, Z. Si, D. Zhou, and K. Niu, "Perceptual learned source-channel coding for high-fidelity image semantic transmission," 2022. [Online]. Available: <https://arxiv.org/pdf/2205.13120.pdf>
- [198] R. Zhang, P. Isola, A. A. Efros, E. Shechtman, and O. Wang, "The unreasonable effectiveness of deep features as a perceptual metric," 2018. [Online]. Available: <https://arxiv.org/pdf/1801.03924.pdf>
- [199] J. Engman and H. Nilsson, "A Novel Perceptual Metric in Deep Learning: A Comparison of Loss Functions for Image Denoising and Reconstruction," Master's thesis, Lund University, Lund, Sweden, 2020.
- [200] A. S. Kaplanyan, A. Sochenov, T. Leimkühler, M. Okunev, T. Goodall, and G. Rufo, "DeepFovea: Neural reconstruction for foveated rendering and video compression using learned statistics of natural videos," *ACM Trans. Graph.*, vol. 38, no. 6, Nov. 2019.
- [201] W. Zhang, Y. Wang, M. Chen, T. Luo, and D. Niyato, "Optimization of image transmission in a cooperative semantic communication networks," 2023. [Online]. Available: <https://arxiv.org/abs/2301.00433>
- [202] Z. Wang and E. Simoncelli, "Translation insensitive image similarity in complex wavelet domain," in *Proc. ICASSP*, vol. 2, 2005, pp. II/573–II/576.
- [203] M.-J. Chen and A. C. Bovik, "Fast structural similarity index algorithm," *J. Real-Time Image Process.*, vol. 6, no. 4, pp. 281–287, Dec. 2011.
- [204] Z. Wang and Q. Li, "Information content weighting for perceptual image quality assessment," *IEEE Trans. Image Process.*, vol. 20, no. 5, pp. 1185–1198, 2011.
- [205] H. Sheikh, A. Bovik, and G. de Veciana, "An information fidelity criterion for image quality assessment using natural scene statistics," *IEEE Trans. Image Process.*, vol. 14, no. 12, pp. 2117–2128, 2005.
- [206] H. Sheikh and A. Bovik, "Image information and visual quality," *IEEE Trans. Image Process.*, vol. 15, no. 2, pp. 430–444, 2006.
- [207] X. Gao, W. Lu, D. Tao, and X. Li, "Image quality assessment based on multiscale geometric analysis," *IEEE Trans. Image Process.*, vol. 18, no. 7, pp. 1409–1423, 2009.
- [208] S. Li, F. Zhang, L. Ma, and K. N. Ngan, "Image quality assessment by separately evaluating detail losses and additive impairments," *IEEE Trans. Multimed.*, vol. 13, no. 5, pp. 935–949, 2011.
- [209] T.-J. Liu, W. Lin, and C.-C. J. Kuo, "Image quality assessment using multi-method fusion," *IEEE Trans. Image Process.*, vol. 22, no. 5, pp. 1793–1807, 2013.
- [210] E. Larson and D. Chandler, "Most apparent distortion: Full-reference image quality assessment and the role of strategy," *J. Electron. Imaging*, vol. 19, pp. 011 006–1 – 011 006–21, Jan. 2010.
- [211] N. Ponomarenko, F. Silvestri, K. Egiazarian, M. Carli, J. Astola, and V. Lukin, "On between-coefficient contrast masking of DCT basis functions," in *Proc. Int. Workshop on Video Processing and Quality Metrics for Consumer Electronics*, Scottsdale, AZ, USA, 2007.
- [212] N. Damara-Venkata, T. Kite, W. Geisler, B. Evans, and A. Bovik, "Image quality assessment based on a degradation model," *IEEE Trans. Image Process.*, vol. 9, no. 4, pp. 636–650, 2000.
- [213] D. M. Chandler and S. S. Hemami, "VSNR: A wavelet-based visual signal-to-noise ratio for natural images," *IEEE Trans. Image Process.*, vol. 16, no. 9, pp. 2284–2298, 2007.
- [214] I. Goodfellow et al., "Generative adversarial nets," in *Proc. NIPS*, 2014, pp. 2672–2680.
- [215] A. Creswell et al., "Generative adversarial networks: An overview," *IEEE Signal Process. Mag.*, vol. 35, no. 1, pp. 53–65, 2018.
- [216] Z. Wang et al., "Generative adversarial networks in computer vision: A survey and taxonomy," [Online]. Available: <https://arxiv.org/pdf/1906.01529.pdf>
- [217] T. Salimans, I. Goodfellow, W. Zaremba, V. Cheung, A. Radford, and X. Chen, "Improved techniques for training GANs," 2016. [Online]. Available: <https://arxiv.org/pdf/1606.03498.pdf>
- [218] M. Heusel, H. Ramsauer, T. Unterthiner, B. Nessler, and S. Hochreiter, "GANs trained by a two time-scale update rule converge to a local Nash equilibrium," 2017. [Online]. Available: <https://arxiv.org/pdf/1706.08500.pdf>
- [219] M. Bińkowski, D. J. Sutherland, M. Arbel, and A. Gretton, "Demystifying MMD GANs," 2018. [Online]. Available: <https://arxiv.org/pdf/1801.01401.pdf>
- [220] Z. Wang and A. C. Bovik, "Mean squared error: Love it or leave it? A new look at signal fidelity measures," *IEEE Signal Process. Mag.*, vol. 26, no. 1, pp. 98–117, 2009.
- [221] K. Seshadrinathan and A. C. Bovik, "Motion tuned spatio-temporal quality assessment of natural videos," *IEEE Trans. Image Process.*, vol. 19, no. 2, pp. 335–350, 2010.
- [222] J. Y. Lin, T.-J. Liu, E. C.-H. Wu, and C.-C. J. Kuo, "A fusion-based video quality assessment (FVQA) index," in *Proc. APSIPA Annual Summit and Conf.*, 2014, pp. 1–5.
- [223] M. Pinson and S. Wolf, "A new standardized method for objectively measuring video quality," *IEEE Trans. Broadcast.*, vol. 50, no. 3, pp. 312–322, 2004.
- [224] S. Wolf and M. H. Pinson, "Video quality model for variable frame delay (VQM_VFD)," U.S. Dept. Commer., Nat. Telecommun. Inf. Admin. (NTIA) Tech. Memo. TM-11-482, Boulder, CO, USA, 2011. [Online]. Available: <https://its.ntia.gov/umbraco/surface/download/publication?reportNumber=11-482.pdf>
- [225] R. Rassool, "VMAF reproducibility: Validating a perceptual practical video quality metric," in *Proc. IEEE Int. Symposium on Broadband Multimedia Systems and Broadcasting*, 2017, pp. 1–2.
- [226] Z. Li, A. Aaron, I. Katsavounidis, A. Moorthy, and M. Manohara, "Toward a practical perceptual video quality metric," Netflix Technology Blog, Jun. 2016. [Online]. Available: <https://netflixtechblog.com/toward-a-practical-perceptual-video-quality-metric-653f208b9652>
- [227] ITU-T, "Subjective video quality assessment methods for multimedia applications," ITU-T Recommendation P.910, Sep. 1999. [Online]. Available: <https://handle.itu.int/11.1002/1000/4751>
- [228] J. Y.-c. Lin, R. Song, C.-H. Wu, T.-J. Liu, H. Wang, and C.-C. J. Kuo, "MCL-V: A streaming video quality assessment database," *J. Vis. Commun. Image Represent.*, vol. 30, pp. 1–9, Jul. 2015.
- [229] Z. Wang and Q. Li, "Video quality assessment using a statistical model of human visual speed perception," *J. Opt. Soc. Am. A*, vol. 24, no. 12, pp. B61–B69, Dec. 2007.
- [230] A. B. Watson, J. Hu, and J. F. McGowan, "Digital video quality metric based on human vision," *J. Electron. Imaging*, vol. 10, pp. 20–29, 2001.
- [231] Y. Kawayoke and Y. Horita, "NR objective continuous video quality assessment model based on frame quality measure," in *Proc. ICIP*, 2008, pp. 385–388.
- [232] M. Barkowsky, J. Bialkowski, B. Eskofier, R. Bitto, and A. Kaup, "Temporal trajectory aware video quality measure," *IEEE J. Sel. Top. Signal Process.*, vol. 3, pp. 266–279, May 2009.

- [233] S. Winkler and P. Mohandas, "The evolution of video quality measurement: From PSNR to hybrid metrics," *IEEE Trans. Broadcast.*, vol. 54, no. 3, pp. 660–668, 2008.
- [234] S. A. Amirshahi and M.-C. Larabi, "Spatial-temporal video quality metric based on an estimation of QoE," in *Int. Workshop on Quality of Multimedia Experience*, 2011, pp. 84–89.
- [235] P. V. Vu, C. T. Vu, and D. M. Chandler, "A spatiotemporal most-apparent-distortion model for video quality assessment," in *Proc. ICIP*, 2011, pp. 2505–2508.
- [236] C. Ionescu, D. Papava, V. Olaru, and C. Sminchisescu, "Human3.6M: Large scale datasets and predictive methods for 3D human sensing in natural environments," *IEEE Trans. Pattern Anal. Mach. Intell.*, vol. 36, no. 7, pp. 1325–1339, 2014.
- [237] B. Zhang, Z. Qin, Y. Guo, and G. Y. Li, "Semantic sensing and communications for ultimate extended reality," 2022. [Online]. Available: <https://arxiv.org/pdf/2212.08533.pdf>
- [238] A. Kosta, N. Pappas, and V. Angelakis, "Age of information: A new concept, metric, and tool," *Found. Trends Netw.*, vol. 12, no. 3, pp. 162–259, 2017.
- [239] R. D. Yates, Y. Sun, D. R. Brown, S. K. Kaul, E. H. Modiano, and S. Ulukus, "Age of information: An introduction and survey," *IEEE J. Sel. Areas Commun.*, vol. 39, pp. 1183–1210, 2021.
- [240] E. Uysal, O. Kaya, S. Baghaee, and H. B. Beytur, "Age of information in practice," 2021. [Online]. Available: <https://arxiv.org/pdf/2106.02491.pdf>
- [241] A. Maatouk, M. Assaad, and A. Ephremides, "The age of incorrect information: an enabler of semantics-empowered communication," 2020. [Online]. Available: <https://arxiv.org/pdf/2012.13214.pdf>
- [242] A. Maatouk, "Optimization of Wireless Networks: Freshness in Communications," Ph.D. dissertation, Université Paris-Saclay, Nov. 2020. [Online]. Available: <https://tel.archives-ouvertes.fr/tel-03028195>
- [243] J. Holm, A. E. Kalør, F. Chiariotti, B. Soret, S. K. Jensen, T. B. Pedersen, and P. Popovski, "Freshness on demand: Optimizing age of information for the query process," 2020. [Online]. Available: <https://arxiv.org/abs/2011.00917>
- [244] S. Kaul, R. Yates, and M. Gruteser, "Real-time status: How often should one update?" in *Proc. IEEE INFOCOM*, 2012, pp. 2731–2735.
- [245] I. Kadota and E. Modiano, "Minimizing the age of information in wireless networks with stochastic arrivals," *IEEE Trans. Mob. Comput.*, vol. 20, no. 3, pp. 1173–1185, 2021.
- [246] P. Popovski, F. Chiariotti, K. Huang, A. E. Kalør, M. Kountouris, N. Pappas, and B. Soret, "A perspective on time toward wireless 6G," *Proc. IEEE*, vol. 110, no. 8, pp. 1116–1146, 2022.
- [247] Y. Sun, I. Kadota, R. Talak, and E. Modiano, *Age of Information: A New Metric for Information Freshness*. San Rafael, CA, USA: Morgan & Claypool Publishers, 2019.
- [248] M. Costa, M. Codreanu, and A. Ephremides, "Age of information with packet management," in *Proc. IEEE ISIT*, 2014, pp. 1583–1587.
- [249] M. Costa, M. Codreanu, and A. Ephremides, "On the age of information in status update systems with packet management," *IEEE Trans. Inf. Theory*, vol. 62, no. 4, pp. 1897–1910, 2016.
- [250] P. Zou, O. Ozel, and S. Subramaniam, "Relative age of information: A new metric for status update systems," in *Proc. ITW*, 2019, pp. 1–5.
- [251] A. Maatouk, S. Kriouile, M. Assaad, and A. Ephremides, "The age of incorrect information: A new performance metric for status updates," *IEEE/ACM Trans. Netw.*, vol. 28, no. 5, p. 2215–2228, Oct. 2020.
- [252] Y. Sun, Y. Polyanskiy, and E. Uysal, "Sampling of the wiener process for remote estimation over a channel with random delay," *IEEE Trans. Inf. Theory*, vol. 66, no. 2, pp. 1118–1135, 2020.
- [253] T. Soleymani, "Value of information analysis in feedback control," Ph.D. dissertation, Technical University of Munich, Germany, 2019.
- [254] R. A. Howard, "Information value theory," *IEEE Trans. Syst. Sci. Cybern.*, vol. 2, pp. 22–26, 1966.
- [255] O. Ayan, M. Vilgelm, M. Klügel, S. Hirche, and W. Kellerer, "Age-of-information vs. value-of-information scheduling for cellular networked control systems," in *Proc. ACM/IEEE Int. Conf. Cyber-Physical Systems*, New York, NY, USA, 2019, p. 109–117.
- [256] A. Molin, H. Esen, and K. H. Johansson, "Scheduling networked state estimators based on value of information," *Automatica*, vol. 110, no. C, Dec. 2019.
- [257] Y. Wang, M. Chen, W. Saad, T. Luo, S. Cui, and H. V. Poor, "Performance optimization for semantic communications: An attention-based learning approach," in *Proc. IEEE GLOBECOM*, 2021, pp. 1–6.
- [258] Y. Wang, M. Chen, T. Luo, W. Saad, D. Niyato, H. V. Poor, and S. Cui, "Performance optimization for semantic communications: An attention-based reinforcement learning approach," *IEEE J. Sel. Areas Commun.*, vol. 40, no. 9, pp. 2598–2613, 2022.
- [259] L. Yan, Z. Qin, R. Zhang, Y. Li, and G. Y. Li, "QoE-aware resource allocation for semantic communication networks," 2022. [Online]. Available: <https://arxiv.org/pdf/2205.14530.pdf>
- [260] L. Xia, Y. Sun, X. Li, G. Feng, and M. A. Imran, "Wireless resource management in intelligent semantic communication networks," 2022. [Online]. Available: <https://arxiv.org/pdf/2202.07632.pdf>
- [261] C. Dong, H. Liang, X. Xu, S. Han, B. Wang, and P. Zhang, "Innovative semantic communication system," 2022. [Online]. Available: <https://arxiv.org/pdf/2202.09595.pdf>
- [262] J. Kang, H. Du, Z. Li, Z. Xiong, S. Ma, D. Niyato, and Y. Li, "Personalized saliency in task-oriented semantic communications: Image transmission and performance analysis," *IEEE J. Sel. Areas Commun.*, vol. 41, no. 1, pp. 186–201, 2023.
- [263] J. Zhang, W. Zeng, X. Li, Q. Sun, and K. P. Peppas, "New results on the fluctuating two-ray model with arbitrary fading parameters and its applications," *IEEE Trans. Veh. Technol.*, vol. 67, no. 3, pp. 2766–2770, 2018.
- [264] Q. Sun, C. Guo, Y. Yang, J. Chen, and X. Xue, "Semantic-assisted image compression," 2022. [Online]. Available: <https://arxiv.org/pdf/2201.12599.pdf>
- [265] P. Cheng, W. Hao, S. Dai, J. Liu, Z. Gan, and L. Carin, "CLUB: A contrastive log-ratio upper bound of mutual information," 2020. [Online]. Available: <https://arxiv.org/pdf/2006.12013.pdf>
- [266] J. Watrous, *The Theory of Quantum Information*. Cambridge, UK: Cambridge Univ. Press, 2018.
- [267] M. M. Wilde, "From classical to quantum shannon theory," 2019. [Online]. Available: <https://arxiv.org/pdf/1106.1445.pdf>
- [268] A. Fonseca, "High-dimensional quantum teleportation under noisy environments," *Phys. Rev. A*, vol. 100, no. 6, Dec. 2019.
- [269] N. Pappas and M. Kountouris, "Goal-oriented communication for real-time tracking in autonomous systems," in *Proc. IEEE Int. Conf. Autonomous Systems*, 2021, pp. 1–5.
- [270] J. Shao, X. Zhang, and J. Zhang, "Task-oriented communication for edge video analytics," 2022. [Online]. Available: <https://arxiv.org/pdf/2211.14049.pdf>
- [271] R. Kasturi, D. Goldgof, P. Soundararajan, V. Manohar, J. Garofolo, R. Bowers, M. Boonstra, V. Korzhova, and J. Zhang, "Framework for performance evaluation of face, text, and vehicle detection and tracking in video: Data, metrics, and protocol," *IEEE Trans. Pattern Anal. Mach. Intell.*, vol. 31, no. 2, pp. 319–336, 2009.



TILAHUN M. GETU (M'19) earned the Ph.D. degree (with highest honor) in electrical engineering from the École de Technologie Supérieure (ÉTS), Montreal, QC, Canada in 2019. He is currently a Guest Researcher with the National Institute of Standards and Technology (NIST), Gaithersburg, MD, USA and a Post-doctoral Fellow with the ÉTS, Montreal, QC, Canada. His specialist and generalist fundamental research interests span the numerous fields of classical and quantum **STEM** (Science, Technology, Engineering, and Mathematics) at the nexus of communications, signal processing, and networking (all types); intelligence (both artificial and natural); robotics; computing; security; optimization; high-dimensional statistics; and high-dimensional causal inference.

Dr. Getu has received several awards, including the 2019 ÉTS Board of Director's Doctoral Excellence Award in recognition of his Ph.D. dissertation selected as the 2019 ÉTS all-university best Ph.D. dissertation.



GEORGES KADDOUM (M'11–SM'20) is a professor and Tier 2 Canada Research Chair with the École de Technologie Supérieure (ÉTS), Université du Québec, Montréal, Canada. He is also a Faculty Fellow in the Cyber Security Systems and Applied AI Research Center at Lebanese American University. His recent research activities cover 5G/6G networks, tactical communications, resource allocations, and security. Dr. Kaddoum has received many prestigious national and international awards in recognition of his outstanding research outcomes. Currently, Prof. Kaddoum serves as an Area Editor for the IEEE Transactions on Machine Learning in Communications and Networking and an Associate Editor for IEEE Transactions on Information Forensics and Security, and IEEE Transactions on Communications.



MEHDI BENNIS (F'20) is a full tenured Professor at the Centre for Wireless Communications, University of Oulu, Finland and head of the Intelligent Connectivity and Networks/Systems Group (ICON). His main research interests are in radio resource management, game theory and distributed AI in 5G/6G networks. He has published more than 200 research papers in international conferences, journals and book chapters. He has been the recipient of several prestigious awards. Dr. Bennis is an editor of IEEE TCOM and Specialty Chief Editor for Data Science for Communications in the Frontiers in Communications and Networks journal.

...